Lecture 8
CFD for Ramjets/Scramjets and Rockets

- High compressibility in the flow
  - Shock-vortex-turbulence-flame interactions
- Challenge
  - Shock capturing schemes are too dissipative and can overwhelm turbulent features
  - Turbulent features must show compressibility effects
- Some strategies
  - Hybrid solvers (WENO-central; MUSCL-central etc)
  - Artificial dissipation, high order PPM etc
- What will work for practical applications?

Challenges for Supersonic Combustion LES

- Algorithms for shock-turbulence-flame interactions
  - Shock capturing without dissipating turbulence or affecting combustion or flame within LES framework
- Subgrid closure for compressible turbulent flows
  - Shock interactions with {un}resolved turbulence
- Subgrid closure for compressible mixing and combustion
  - Interaction of compressible waves with flames
- Molecular mixing and chemical kinetics within subgrid
  - Detailed kinetics within LES framework

Compressible LES Governing Equations

- Favre-averaged filtered conservation equations

Mass $$\frac{\partial \bar{\rho}}{\partial t} + \frac{\partial \bar{\rho}\tilde{u}_i}{\partial x_i} = 0$$

Moment. $$\frac{\partial \bar{\rho}\tilde{u}_i}{\partial t} + \frac{\partial}{\partial x_j}\left(\bar{\rho}\tilde{u}_i\tilde{u}_j + \bar{p}\delta_{ij} - \bar{\tau}_{ij} + \boxed{\tau_{ij}^{sgs}}\right) = 0$$

Energy $$\frac{\partial \bar{\rho}\tilde{E}}{\partial t} + \frac{\partial}{\partial x_i}\left[\tilde{u}_i(\bar{\rho}\tilde{E} + \bar{p}) - \bar{\tau}_{ij}\tilde{u}_j + \bar{q}_i + \boxed{H_i^{sgs} + \sigma_i^{sgs}}\right] = 0$$

E.O.S $$\bar{p} = \bar{\rho}\tilde{R}\tilde{T} + \boxed{\bar{\rho}T^{sgs}}$$

$$\bar{q}_i = -\bar{\kappa}\frac{\partial \tilde{T}}{\partial x_i} + \bar{\rho}\sum_{k=1}^{N_s}\tilde{h}_k\tilde{V}_{i,k}\tilde{Y}_k + \sum_{k=1}^{N_s}\boxed{q_{i,k}^{sgs}} \qquad k = 1, N_s$$

- Species solved using LEMLES

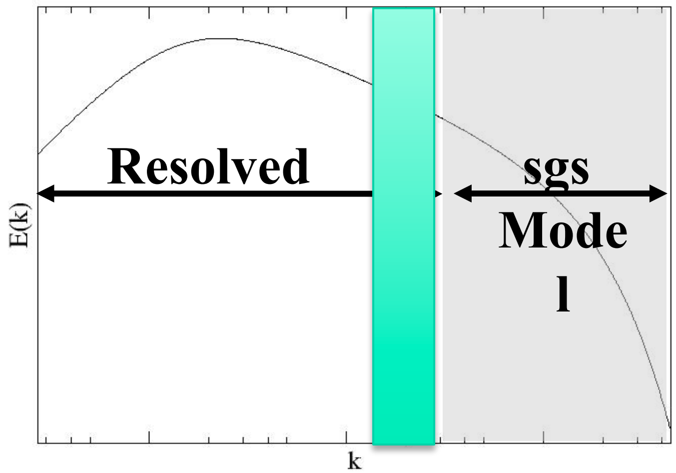

Hybrid Algorithm for Shock-Turbulence-Flame

- Locally adaptive hybrid strategy switches from shock capturing solver to a smooth-flow (O(4)) solver dynamically in 3D
- Piecewise Parabolized Method (PPM – FLASH3D type)*
  - Extended to viscous flows, multi-domain, stretched grids
- MUSCL reconstruction with a Hybrid HLL Riemann Solver**
  - Non-contact preserving in shock transverse directions (Einfeldt, 1988, 1991)
  - Contact preserving Riemann solver (HLLC, Toro, 1997)
- Local shock detection using multiple sensors
- Algorithm validated for many canonical and complex test cases: Sod, Noh, Richtmyer-Meshkov, Shock-turbulence etc.**

*** Phys Scripta 08, ** ICDERS 05, AIAA J (2010), Comp. Fluids (2010), J. of Turb. (2010), Shock Wave (2010)**

VLES-LES *k-kl* Model

- Hybrid RANS-LES for compressible flows using an additive filter (J. Comp. Phys. Vol. 228, 2009)
  - Hybrid terms need to be modeled – still under work
- Solve for the single point and two-point velocity correlations *(k, kl)* for near-wall treatment – model is still under development
  - $l_{sgs} > \Delta$, the grid size is the length scale
  - $l_{sgs} < \Delta$, the modeled length scale is used
- Distance from wall is used currently in the isolator (K-DES)

$$\frac{\partial\left(\bar{\rho}k_{sgs}\right)}{\partial t}+\frac{\partial\left(\bar{\rho}\tilde{u}_i k_{sgs}\right)}{\partial x_j}=\tau_{ij}\frac{\partial \tilde{u}_i}{\partial x_j}-D_{sgs}+\frac{\partial}{\partial x_i}\left[\bar{\rho}\left(\frac{\nu}{\Pr_t}+\frac{\nu_t}{\sigma_k}\right)\frac{\partial k_{sgs}}{\partial x_i}\right]$$

$$\frac{\partial\left(\bar{\rho}\left(k\ell\right)_{sgs}\right)}{\partial t}+\frac{\partial\left(\bar{\rho}\tilde{u}_i\left(k\ell\right)_{sgs}\right)}{\partial x_j}=C_{L1}\ell_{sgs}\tau_{ij}\frac{\partial \tilde{u}_i}{\partial x_j}-C_{L2}\bar{\rho}k_{sgs}^{3/2}+\frac{\partial}{\partial x_i}\left[\bar{\rho}\left(\frac{\nu}{\Pr_t}+\frac{\nu_t}{\sigma_{k\ell}}\right)\frac{\partial\left(k\ell\right)_{sgs}}{\partial x_i}\right]$$

Fang and Menon (2006) Rocha and Menon, 2009

General Realizability Constraints

- Constraints on subgrid models (Vreman, *et al.*, 1994; Nelson and Menon, 1998, Fang and Menon, 2006) :

$$\tau^{sgs}_{\alpha\alpha} \geq 0 \qquad \left(\tau^{sgs}_{\alpha\beta}\right)^2 \leq \tau^{sgs}_{\alpha\alpha}\tau^{sgs}_{\beta\beta} \quad \text{for} \quad \alpha \neq \beta \qquad \det\left(\tau^{sgs}_{\alpha\beta}\right) \geq 0$$

$$k^{sgs} \geq \frac{\sqrt{3}}{C_\alpha}\nu_t\sqrt{2\tilde{S}_{ij}\tilde{S}_{ji} - \frac{2}{3}\tilde{S}^2_{kk}} \quad \text{with} \quad \tilde{S}_{ij}\tilde{S}_{ji} = \sum_{i=1}^{3}\sum_{j=1}^{3}\tilde{S}_{ij}\tilde{S}_{ji}$$

$$C_\nu = \mathbf{min}(C_\nu, C_{\nu,\mathbf{lim}}) \qquad C_{\nu,\mathbf{lim}} = \frac{1}{\sqrt{6}s}$$

$$s = \frac{l^{sgs}}{\sqrt{k^{sgs}}}\sqrt{\tilde{S}_{ij}\tilde{S}_{ji} - \frac{1}{3}\tilde{S}^2_{kk}}$$

$$l^{sgs} = \mathbf{min}(l^{sgs}, l^{sgs}_{\mathbf{lim}}) \quad l^{sgs}_{\mathrm{lim}} = \frac{1}{\sqrt{6}}\frac{\sqrt{k^{sgs}}}{C_\nu}\left(\tilde{S}_{ij}\tilde{S}_{ji} - \frac{1}{3}\tilde{S}^2_{kk}\right)^{-0.5}$$

K-KL Rearward Facing Step

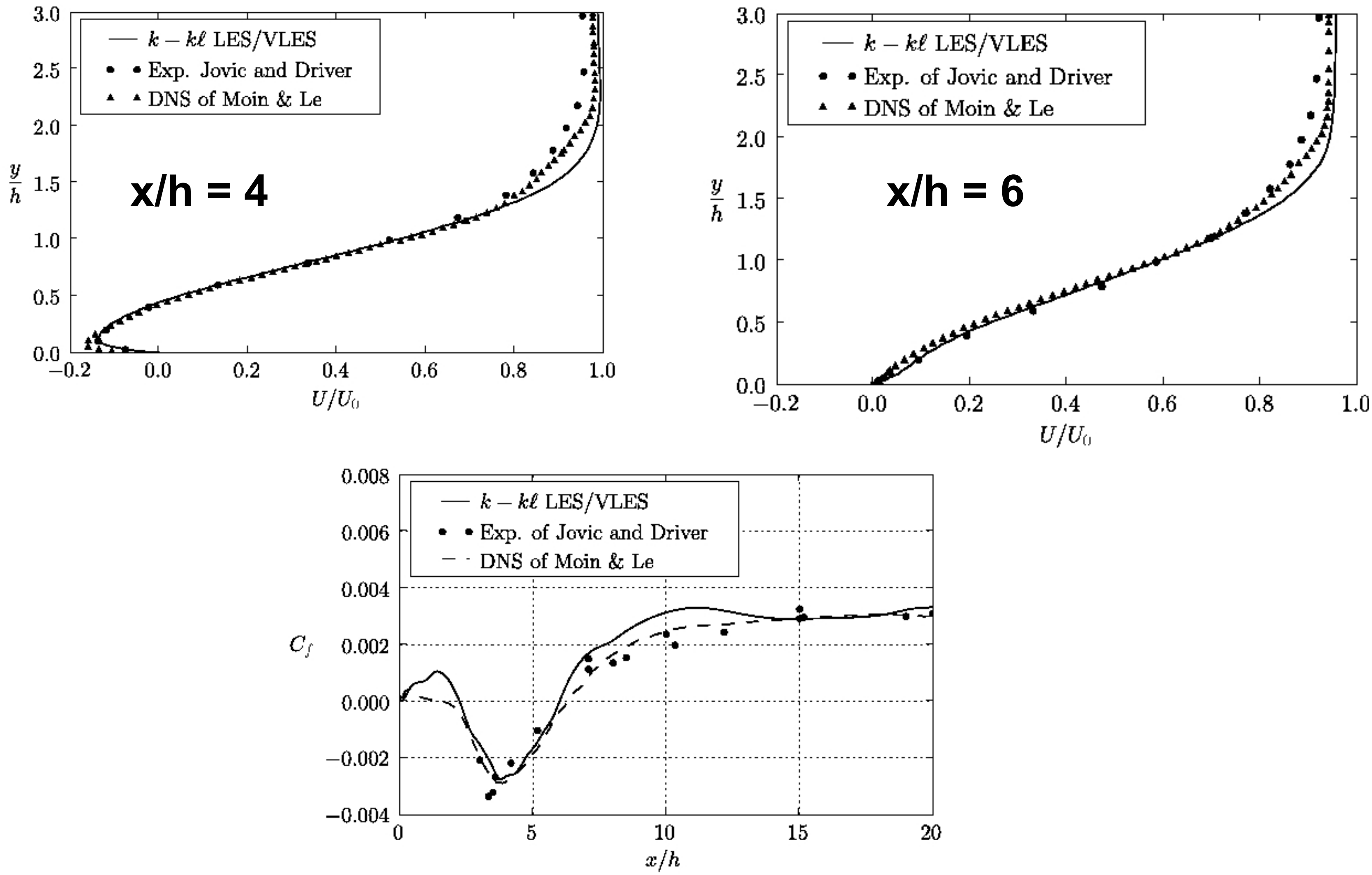

Scalar Fluctuation Modeling

- Used in typical RANS, URANS codes (e.g. CRAFTTech)
- Specify turbulent Prandtl and Schmidt numbers
  - First order effect impacts combustion efficiency
  - Use local estimates of turbulent Pr and Sc
    - **Adjust to the flow rather than set a priori**
    - **Obtained from the turbulent closure**
      - **Used in URANS and in conventional LES**
- **Dynamic subgrid closures avoid this explicit relations but also capture variable and local turbulent Pr and Sc.**

SCALAR FLUCTUATION MODEL (SFM)

Transport equations solved for scalar variance and its dissipation rate

$$\frac{\partial(\bar{\rho}k_e)}{\partial t} + \frac{\partial(\bar{\rho}\tilde{u}_j k_e)}{\partial x_j} = \frac{\partial}{\partial x_j}\left[\bar{\rho}\left(\alpha + \frac{\alpha_t}{\sigma_{k,e}}\right)\frac{\partial k_e}{\partial x_j}\right] + 2\bar{\rho}\alpha_t\left(\frac{\partial \tilde{e}}{\partial x_j}\right)^2 - 2\bar{\rho}\varepsilon_e$$

$$\frac{\partial(\bar{\rho}\varepsilon_e)}{\partial t} + \frac{\partial(\bar{\rho}\tilde{u}_j \varepsilon_e)}{\partial x_j} = \frac{\partial}{\partial x_j}\left[\bar{\rho}\left(\alpha + \frac{\alpha_t}{\sigma_{\varepsilon,e}}\right)\frac{\partial \varepsilon_e}{\partial x_j}\right] + \bar{\rho}\alpha_t\left(C_{d1}\frac{\varepsilon_e}{k_e} + C_{d2}\frac{\varepsilon}{k}\right)\left(\frac{\partial \tilde{e}}{\partial x_j}\right)^2$$

$$+ C_{d3}\hat{P}_k\frac{\varepsilon_e}{k} - \left(C_{d4}\frac{\varepsilon_e}{k_e} + C_{d5}\frac{\varepsilon}{k}\right)\bar{\rho}\varepsilon_e + \xi_{\varepsilon T}$$

Near-wall damping

Compressibility Correction $\longrightarrow$ $\hat{P}_k = P_k - \alpha_1 \hat{M}_T^2 P_k - \alpha_2 \hat{M}_T^2 \bar{\rho}\varepsilon$

Turbulent Prandtl Number	Turbulent Schmidt Number
$Pr_t = \frac{C_\mu f_\mu}{C_\lambda f_\lambda}\sqrt{\frac{k}{\varepsilon}\frac{\varepsilon_e}{k_e}}$	$Sc_t = \frac{C_\mu f_\mu}{C_\lambda f_\lambda}\sqrt{\frac{k}{\varepsilon}\frac{\varepsilon_f}{k_f}}$
• Energy Variance $k_e = \widetilde{e''e''}$ • Dissipation Rate ε_e	• Mixture Fraction Variance $k_f = \widetilde{f''f''}$ • Dissipation Rate ε_f

$C_{d1} = 2.0$	$C_{d2} = 0.0$	$C_{d3} = 0.72$	$C_{d4} = 2.2$	$C_{d5} = 0.8$	$\sigma_{k,e} = 1.0$	$\sigma_{\varepsilon,e} = 1.0$

Hot (800K) Supersonic Jet - SFM vs LES

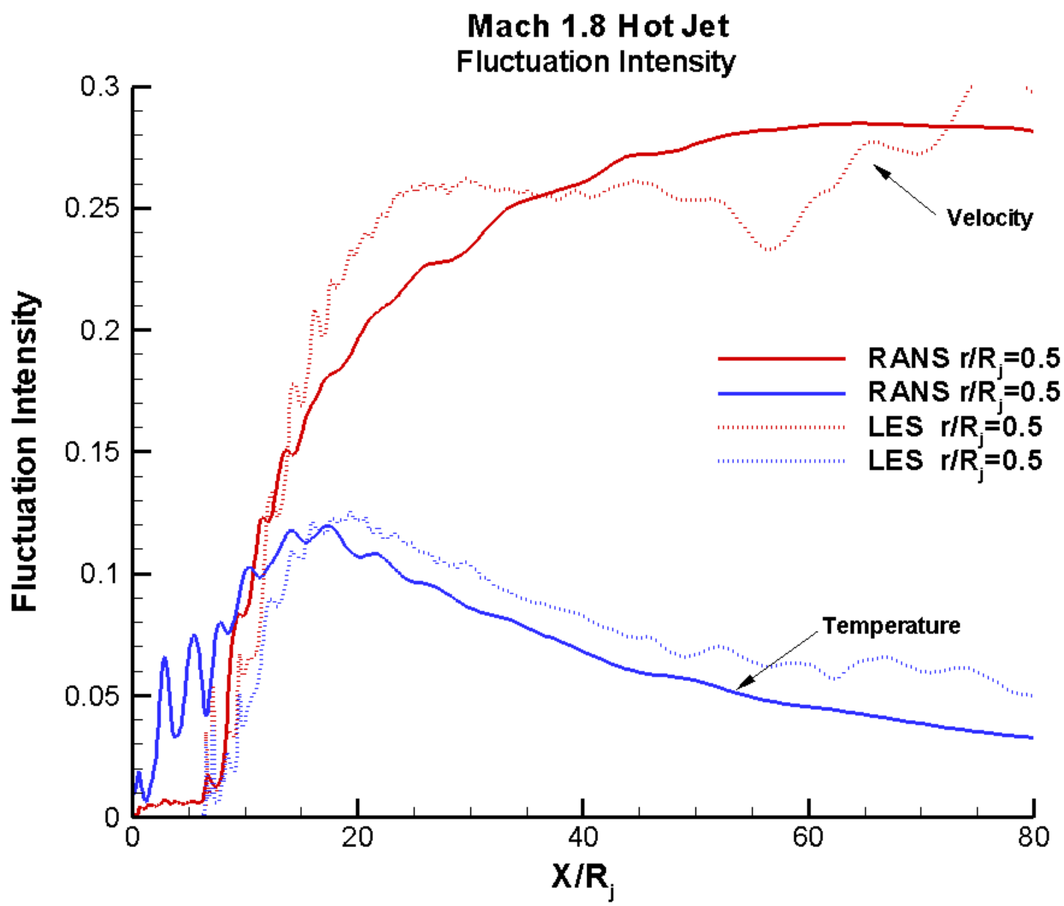

SCHOLAR COMBUSTION EXPERIMENT

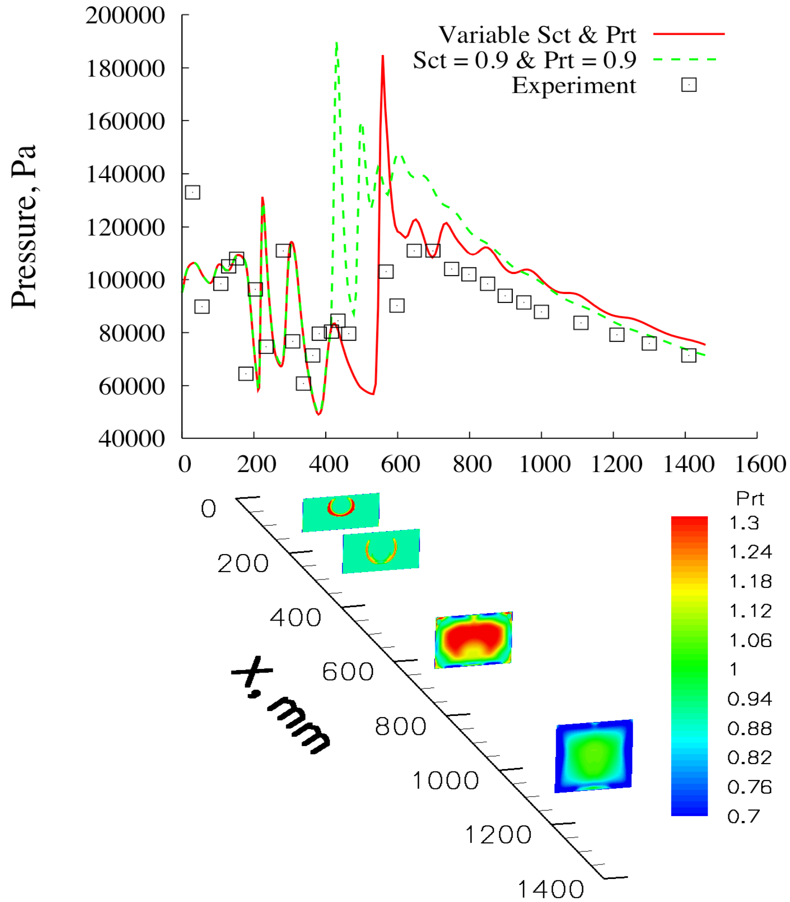

Turbulent Prandtl Number

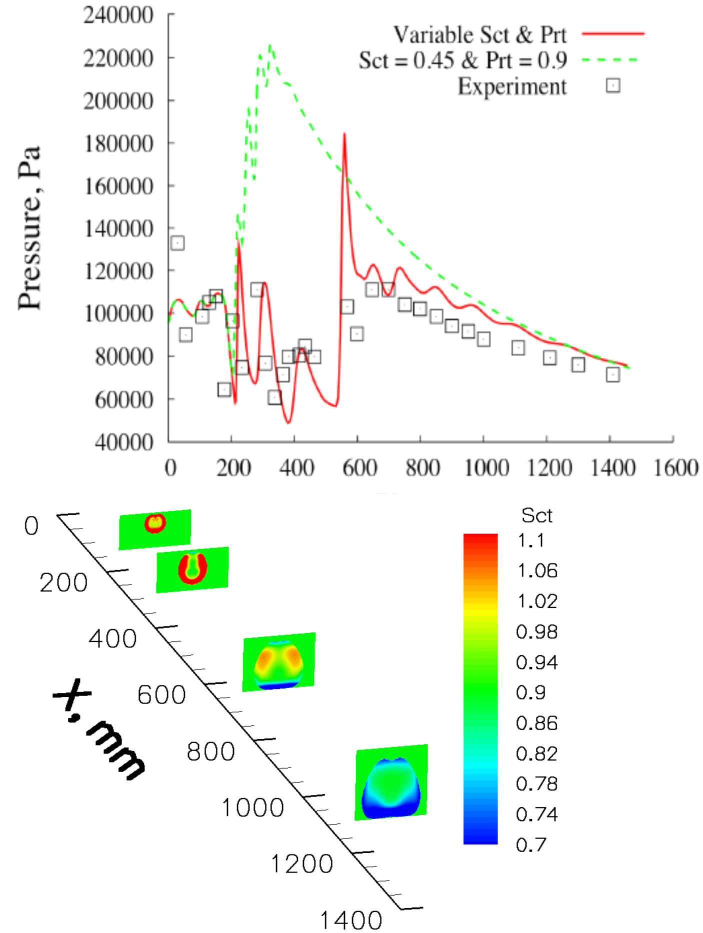

Turbulent Schmidt Number

Compressible Subgrid Kinetic Energy Closure

- Transport of the subgrid kinetic energy

$$\frac{\partial}{\partial t}\overline{\rho}\,k^{sgs} + \frac{\partial}{\partial x_i}\left(\overline{\rho}\,\widetilde{u}_i k^{sgs}\right) = \mathcal{T}_{k^{sgs}} + pd_{k^{sgs}} + P_{k^{sgs}} - D_{k^{sgs}}$$

  - Production

$$P_{k^{sgs}} = -\tau_{ij}^{sgs}\frac{\partial \widetilde{u}_j}{\partial x_i} \qquad \tau_{ij}^{sgs} = -2\overline{\rho}\nu_t\left(\tilde{S}_{ij} - \frac{1}{3}\tilde{S}_{kk}\delta_{ij}\right) + \frac{2}{3}\overline{\rho}k^{sgs}\delta_{ij}$$

  - Dissipation

$$\boxed{D_{k^{sgs}} = \left(\overline{\tau_{ij}\frac{\partial u_i}{\partial x_j}} - \overline{\tau_{ij}}\frac{\partial \widetilde{u}_i}{\partial x_j}\right)}$$

  - Diffusion/Tran

  - Pressure-Dilatation Correlation

$$\mathcal{T}_{k^{sgs}} = -\frac{\partial}{\partial x_i}\left(\left(\overline{\rho}\widetilde{K u_i} - \overline{\rho}\,\widetilde{K}\widetilde{u}_i - \widetilde{u}_j\tau_{ij}^{sgs}\right) + \boxed{\left(\overline{u_i P} - \widetilde{u}_i\overline{P}\right)} - \left(\overline{u_j\tau_{ij}} - \widetilde{u}_j\,\overline{\tau_{ij}}\right)\right)$$

$$\boxed{pd_{k^{sgs}} = \overline{P\frac{\partial u_i}{\partial x_i}} - \overline{P}\frac{\partial \widetilde{u}_i}{\partial x_i}}$$

Genin and Menon (AIAA-2009, Comp. Fl., 2010; J. Turb., 2010)

Closure for Compressible Flows

- Diffusion of k^{sgs} due to pressure fluctuations transfers acoustic energy from shock front corrugation to subgrid kinetic energy

$$\overline{u_i P} - \widetilde{u}_i \overline{P} = \overline{\rho}\widetilde{R}(\widetilde{u_i T} - \widetilde{u}_i \widetilde{T}) = -\frac{\overline{\rho}\nu_t \widetilde{R}}{Pr_t}\frac{\partial \widetilde{T}}{\partial x_i}$$

- Subgrid pressure – dilatation correlation

$$pd_{k^{sgs}} = \alpha_{pd} M_t^{sgs\,2} \left(\frac{\overline{\rho}\widetilde{S} k^{sgs}}{D_{k^{sgs}}} \right)^2 (P_{k^{sgs}} - D_{k^{sgs}})$$

- Energy Equation closure (turbulent Prandtl number)

$$H_i^{sgs} + \sigma_i^{sgs} = -(\overline{\rho}\nu_t + \mu)\frac{\partial k^{sgs}}{\partial x_i} - \frac{\overline{\rho}\nu_t}{\mathrm{Pr}_t}\frac{\partial \tilde{T}}{\partial x_i} + \tilde{u}_j \tau_{ij}^{sgs}$$

Genin and Menon (Comp. Fl., 2010; J. Turb., 2010)

Localized Dynamic Evaluation

- Extension of LDKM (Kim and Menon, 1995, 1991) for low-speed flows to compressible flows
  - Genin and Menon, Comp. Fl (2010), JoT (2010)
- SGS closure model constants obtained from shock-turbulence DNS/LES comparison (Comp. Fl., 2010)
- Dynamic closure using scale similarity at the test filter level
  - Numerically robust and stable in complex flows
- Localized dynamic evaluation of Pr_t can be used to close
  - Subgrid energy diffusion in the energy equation
  - Diffusion of k^{sgs} due to pressure fluctuations
- Localized dynamic evaluation of Sc_t (if not using LEM)
- NO model parameters that are adjusted to match test case

LEMLES: Grid-Within-Grid Approach

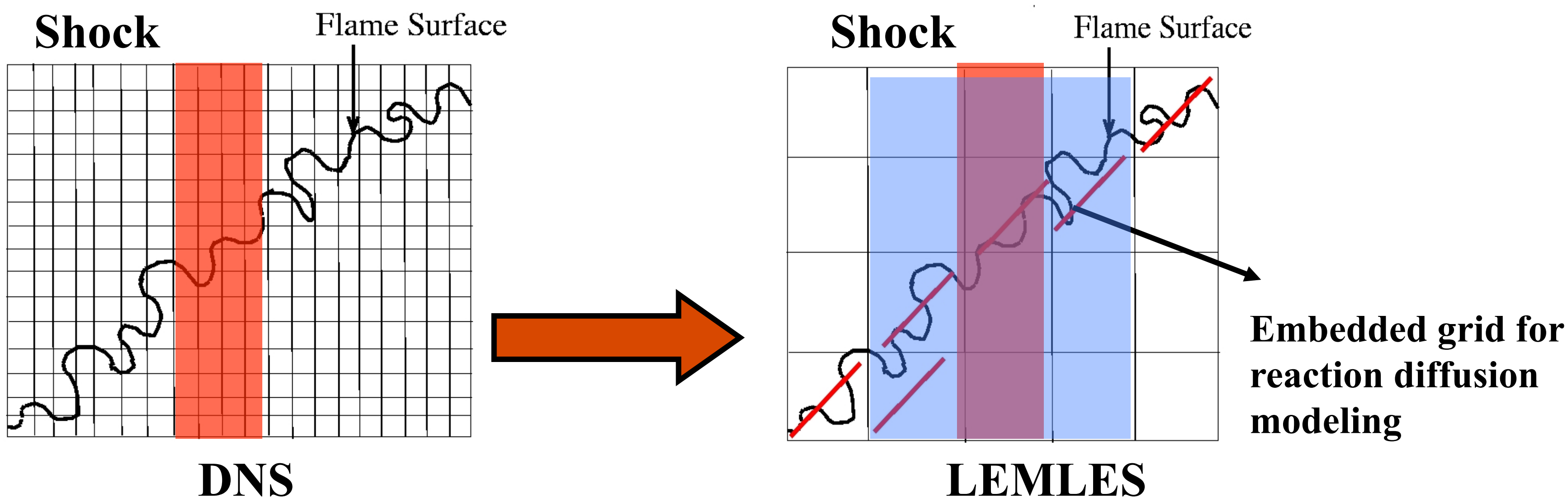

- **Multi-scale (space and time) approach (LEMLES)**
- **Application to subsonic turbulent reacting flows since 2000**
  - **No ad hoc model constant adjustments**
- **Extension to shock-turbulence-flame interaction problems**
  - **LEM updated to allow for subgrid pressure variation**
    - **subgrid compression and expansion**
  - **Explicit presence of shock in subgrid not yet included**

Hybrid Numerical Algorithm

- Locally adaptive hybrid strategy switches from shock capturing solver to a smooth-flow (O(4)) solver locally and dynamically
- Piecewise Parabolized Method (PPM – FLASH3D)
  - Extended to viscous flows, multi-domain, stretched grids
- MUSCL reconstruction with Hybrid HLL Riemann Solver
  - Non-contact preserving in shock transverse directions (HLLE, Einfeldt, 1988, 1991)
  - Contact preserving Riemann solver (HLLC, Toro, 1997)
- The current hybrid solver is identified as 4th/HLLC/E
  - Smoothness local sensors to switch between O(4) & HLL
  - Local shock detection to switch from HLLC to HLLE

Numerical scheme and accuracy

- Illustration for Scramjet flowfield: Supersonic airflow (M=2) over a 6 degrees wedge – vortex street and turbulence

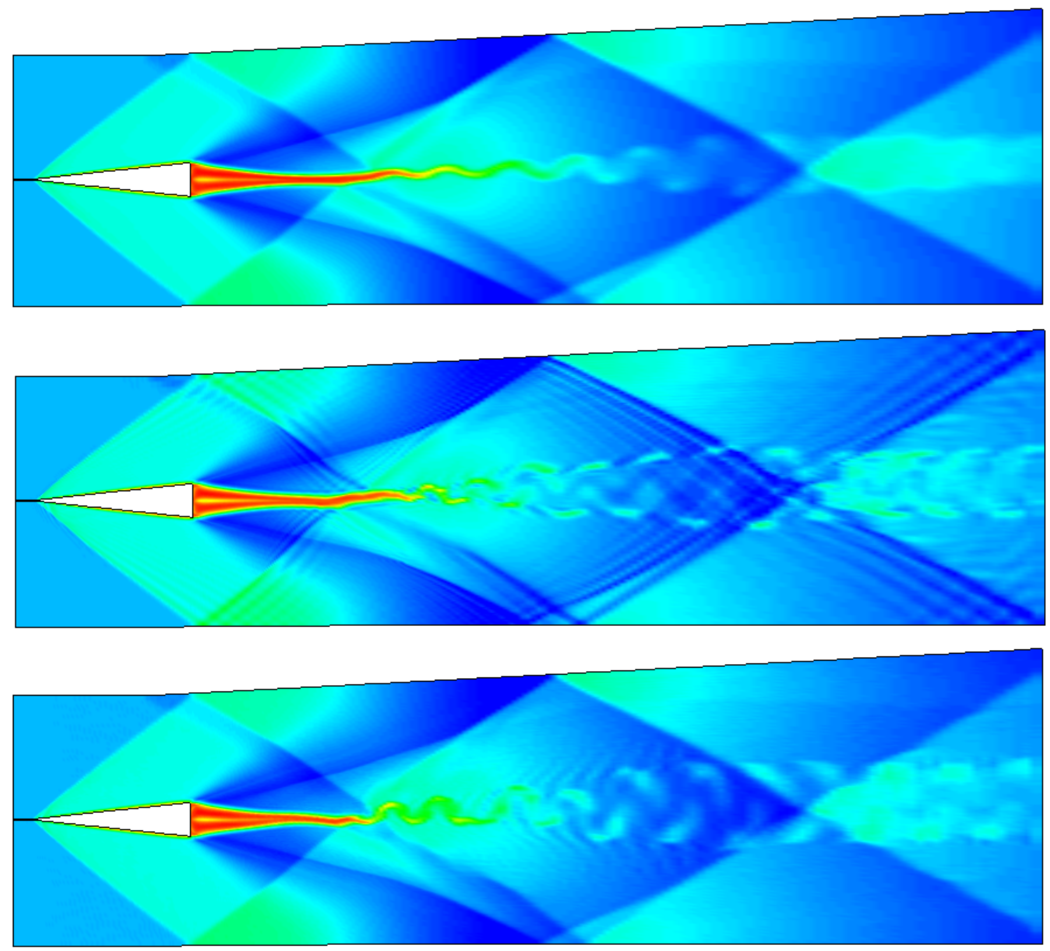

(1) Pure upwind is dissipative

(2) Central with artificial dissipation is dispersive

(3) Hybrid method to switch between numerical schemes

Riemann Solvers Instabilities and Remedy

- Odd-Even decoupling and Carbuncle phenomenon arise in numerical resolution of shock waves
  - neighboring mesh points along a shock front decouple
  - strongly deform shock fronts and creates parasitic oscillations in the post-shock region

➔Design of a hybrid Riemann solver – Extension of Quirk's cure to Riemann solvers: use of a non-contact preserving Riemann solver in the directions transverse to the shock normal

- Flattening (reduce reconstruction order close to strong shocks) to prevent post-shock oscillations

Carbuncle Test Case

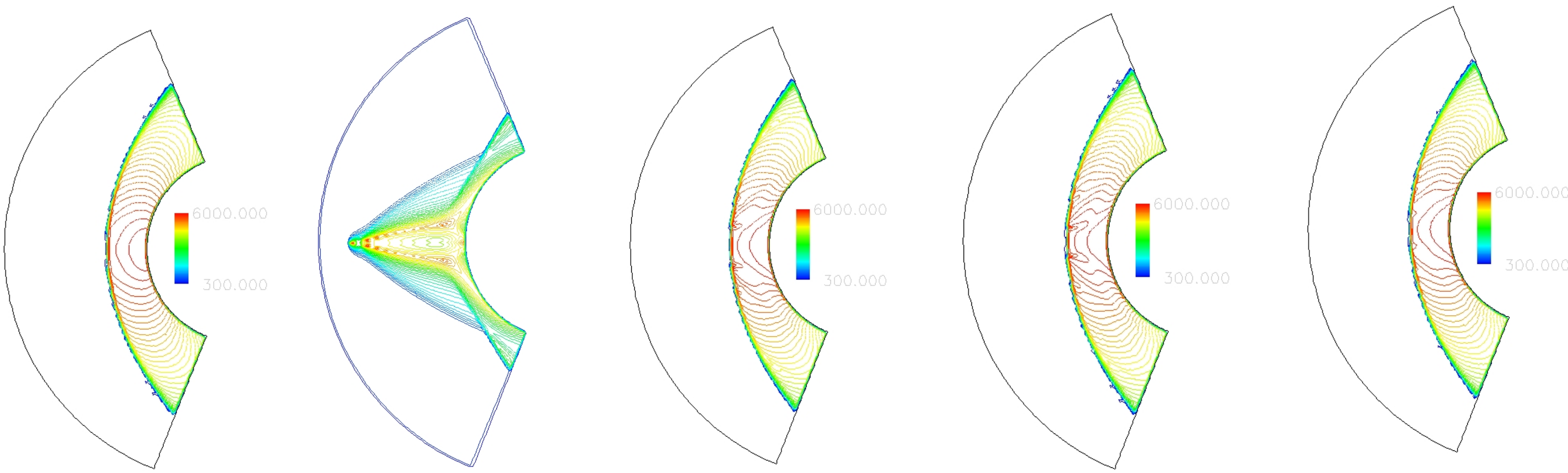

HLLE **Roe** **TSRS** **HLLC** **HLLC/E**

- M=10 air flow onto a cylindrical body
- Appearance of singular points for contact-preserving solvers
  - not seen for HLLE
- Even more reduced effect with HLLC/E

Normal Shock-Turbulence Interaction

- DNS (231x81x81) and LES (106x32x32)
- Isotropic turbulence (243x81x81) superposed on supersonic inflow:

M_{inflow}	1.29	2	3
Re_{λ}	19.1	19.0	19.7
M_t	0.140	0.108	0.110

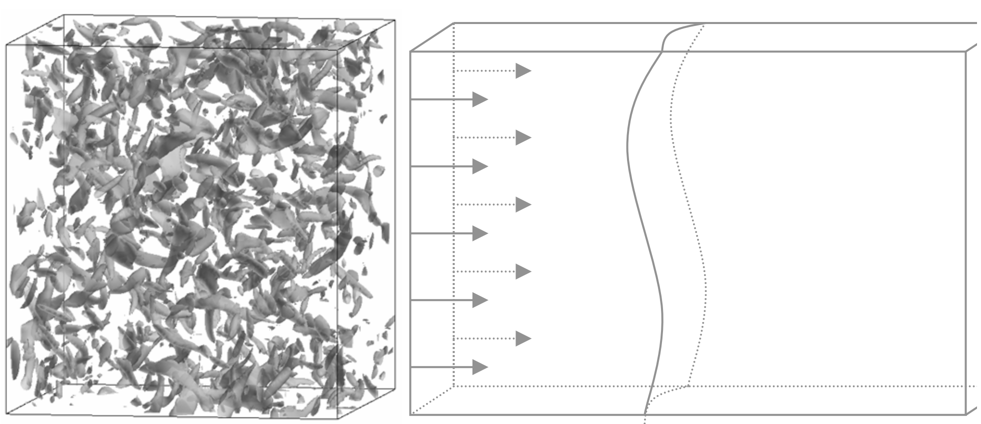

- Variations of local Mach number ➔ Shock corrugation
- Post-shock pressure fluctuations, acoustic wave
- Exchange between acoustic energy & turbulent kinetic energy

Shock-Turbulence Interaction

- DNS (231x81x81) LES (106x32x32)
- Dynamic LES closure captures turbulence across shock

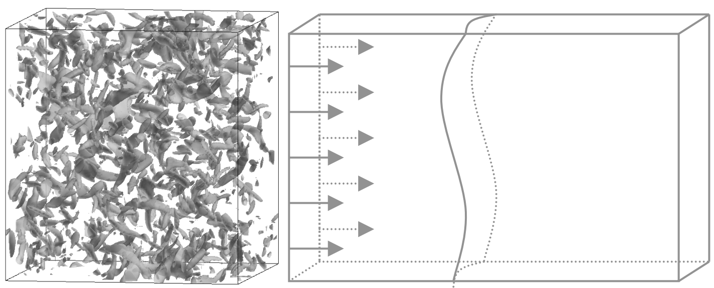

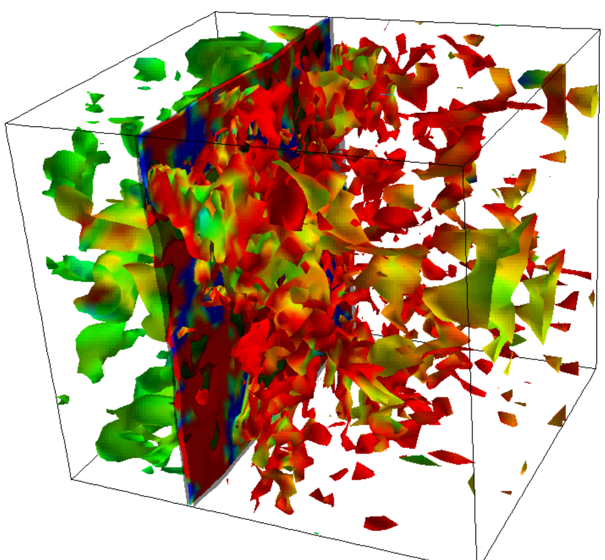

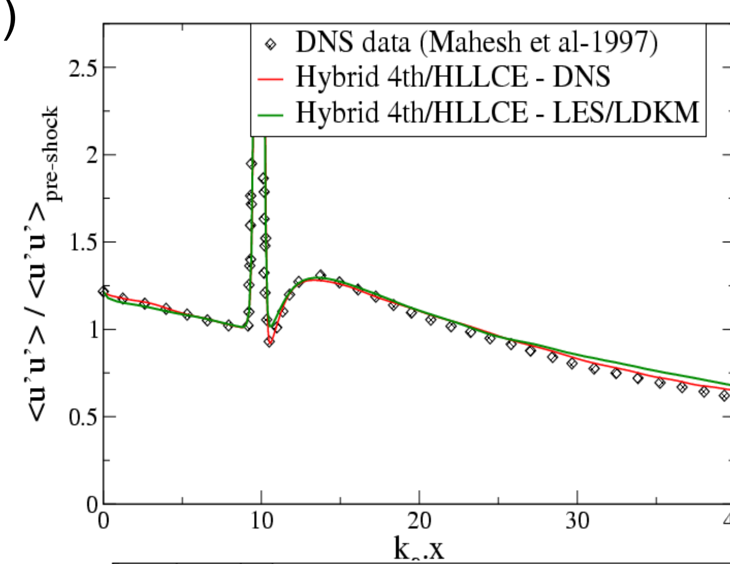

M = 1.29

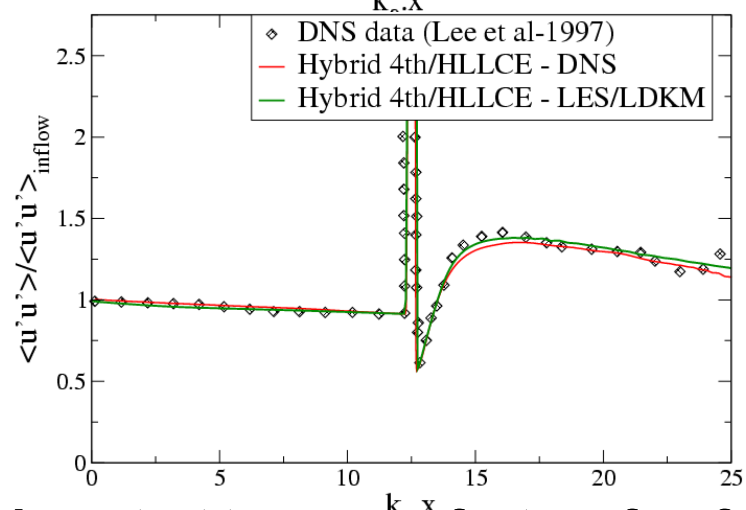

M = 3.0

- **Compressibility correction is important to account for transfer of acoustic energy from shock corrugations to sub-grid kinetic energy**

Normal Shock / Turbulence Interaction

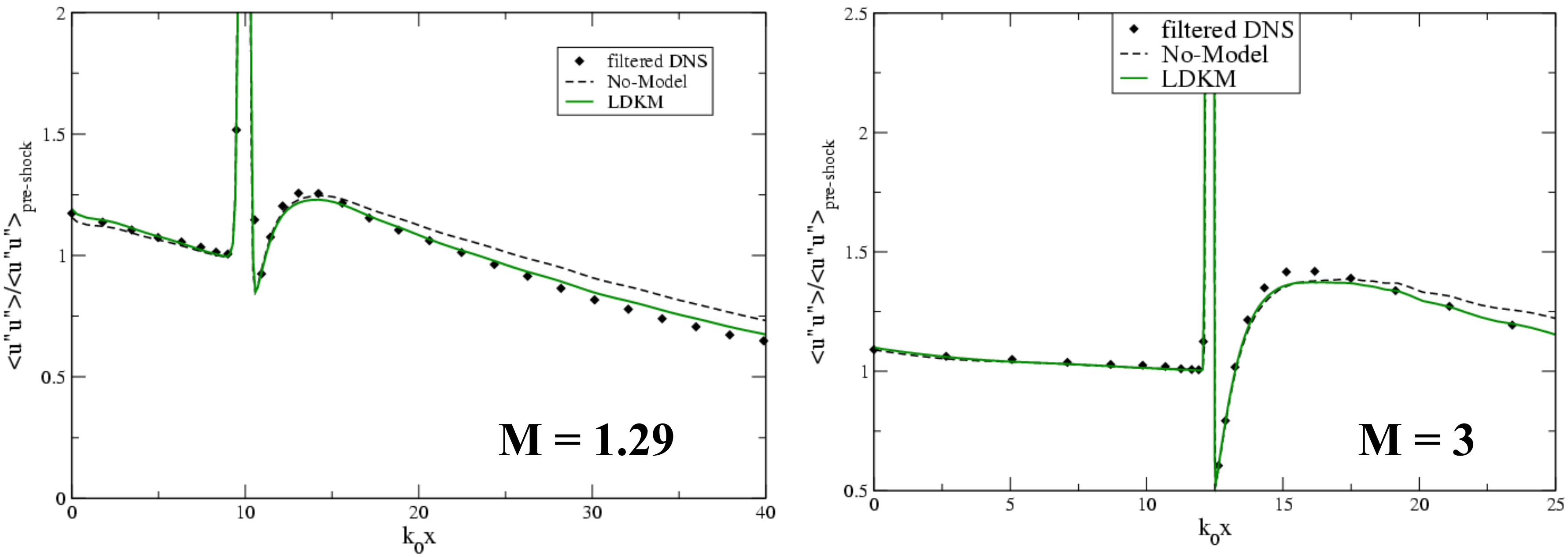

- LES captures most of the DNS features
- Dynamic model shows stable predictions for all simulated M
- Compressibility corrections appears to work well

Numerical scheme and accuracy

- Proper capture of the flow discontinuities with upwind scheme and resolution of the instability and turbulence

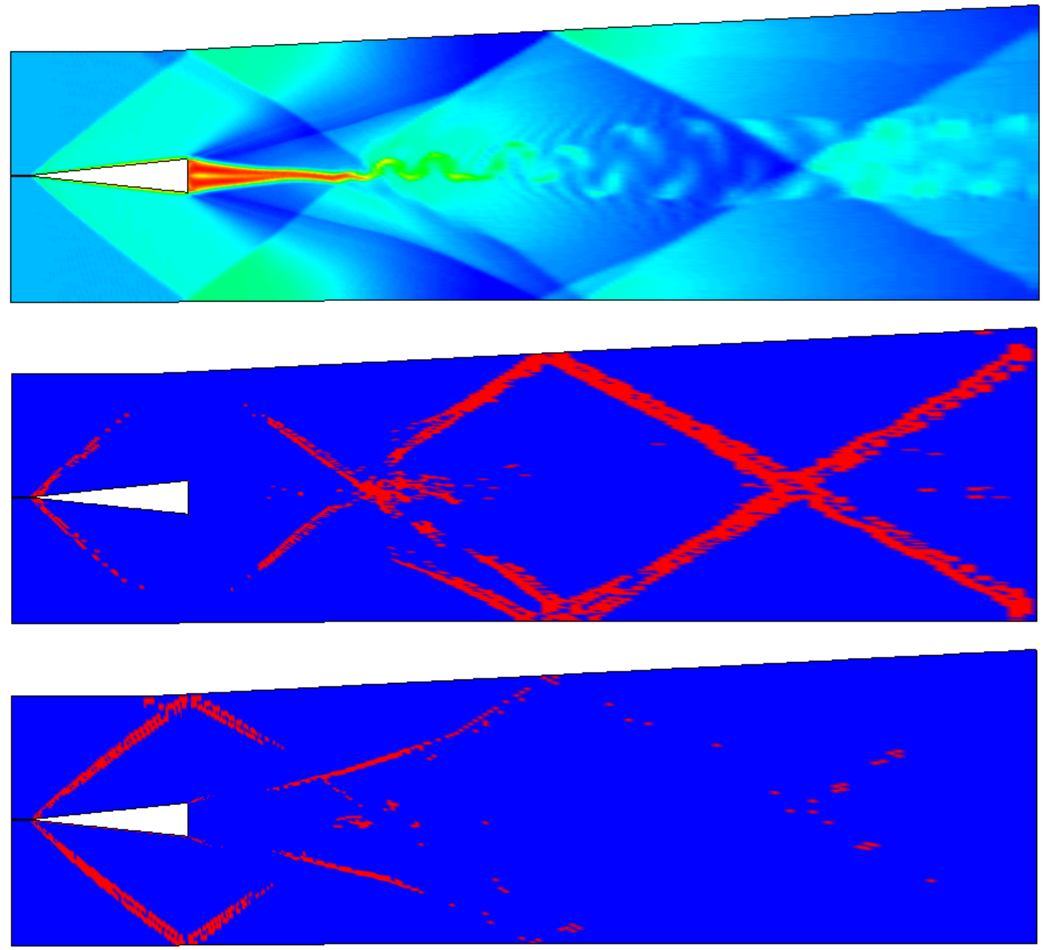

(1) Temperature field

(2) Use of upwinding in the I-direction

(3) Use of upwinding in the J-direction

Numerical scheme and accuracy

- With reaction, more sharp fronts
- Sonic injection of H_2 at the base of the wedge

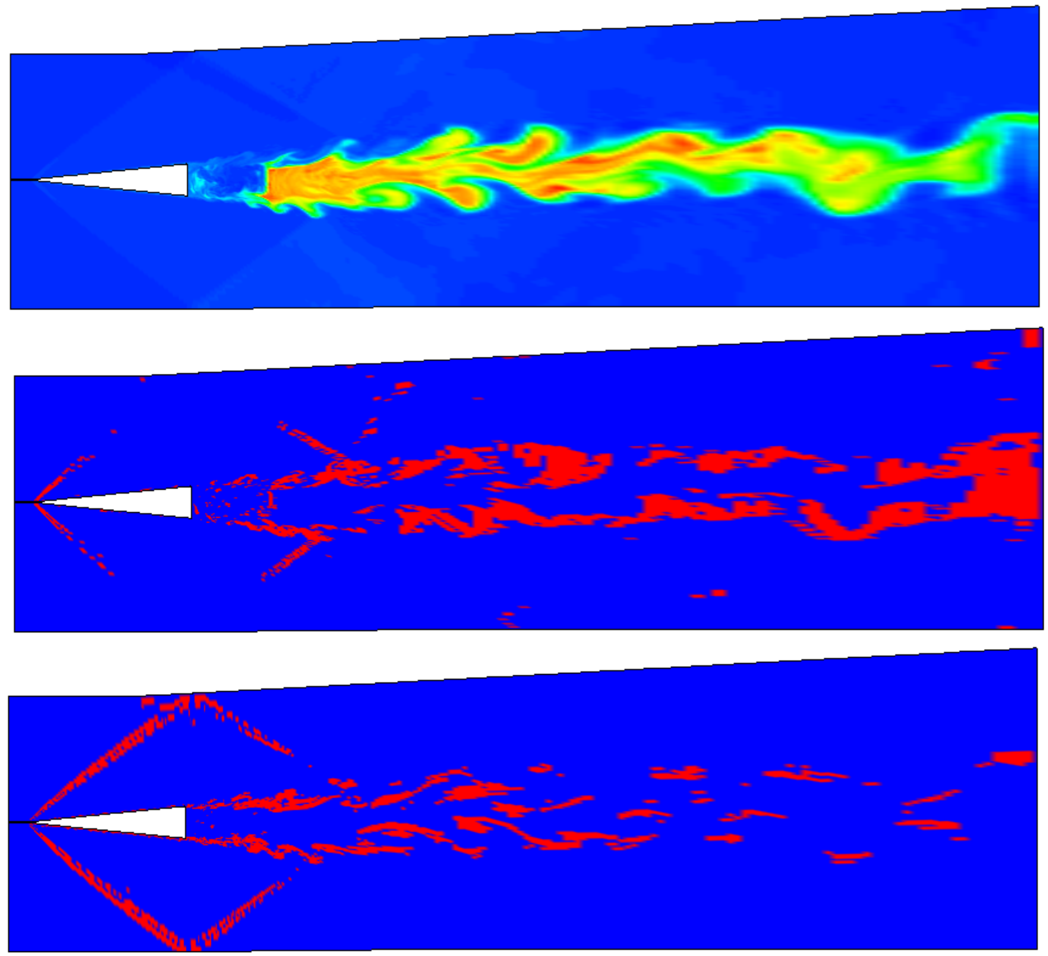

(1)Temperature field

(2)Use of upwinding in the I-direction

(3)Use of upwinding in the J-direction

Non-Reacting and Reacting DLR Test Case

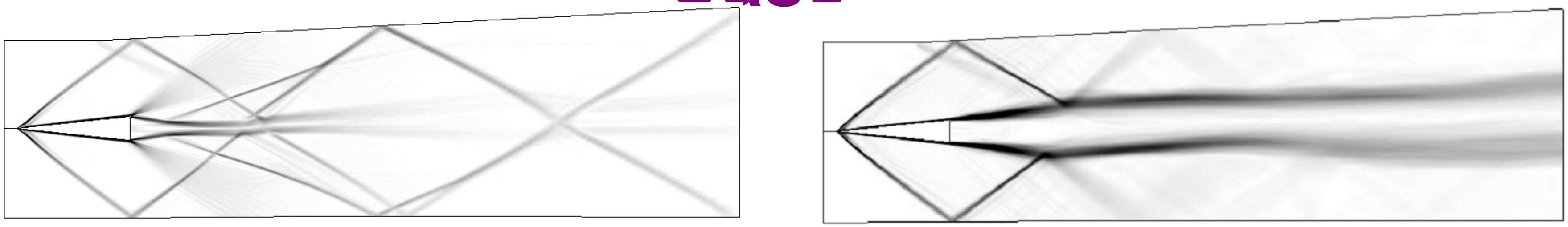

Time-averaged density gradient

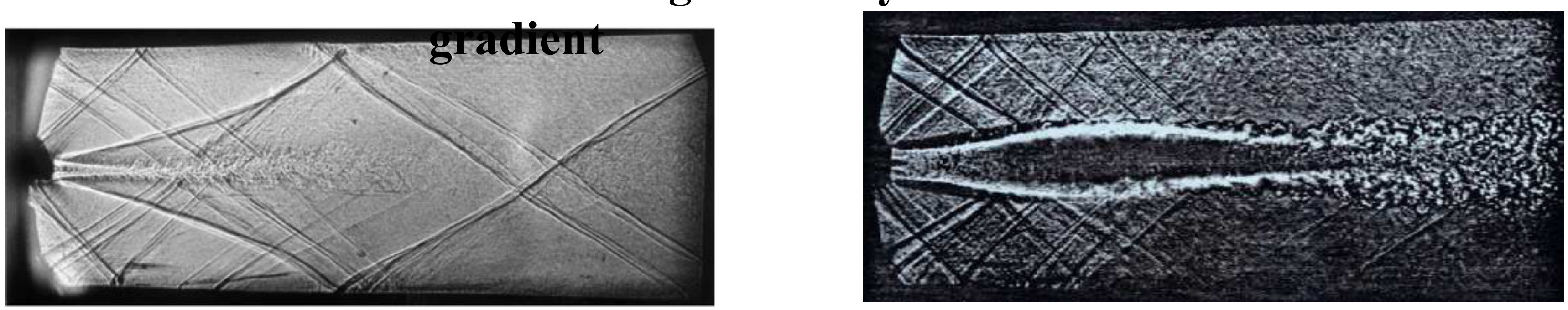

Experimental Schlieren

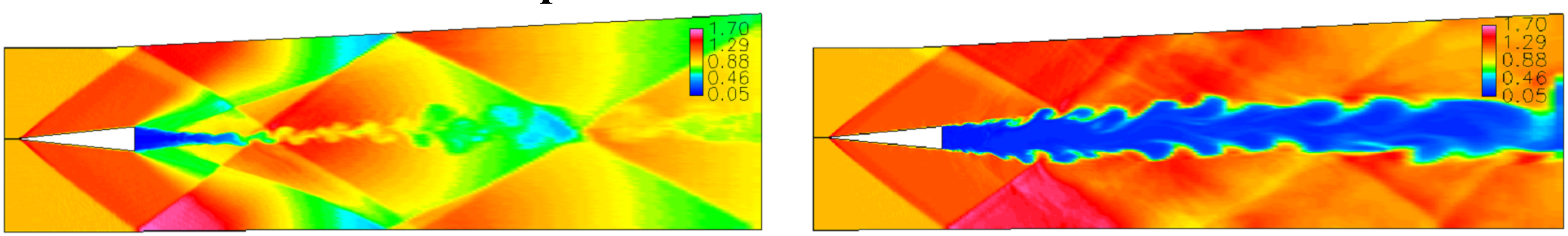

COLD Instantaneous density HOT

Genin and Menon, AIAAJ (2010)

Comparisons with DLR Data

U Velocity

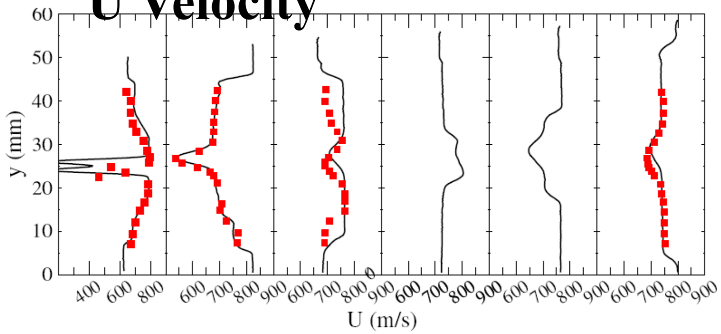

Experimental

OH-PLIF

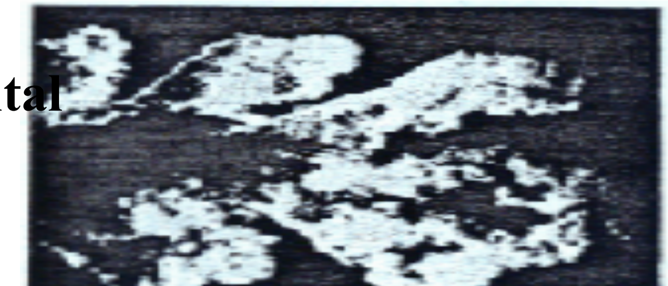

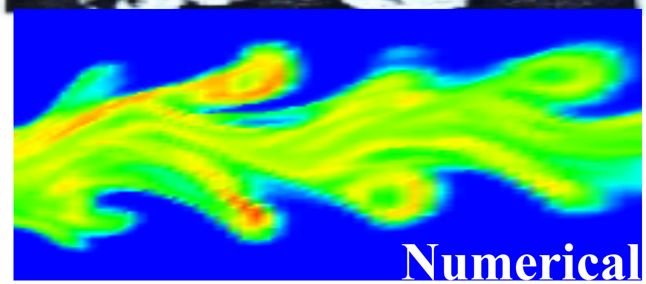

- Flame anchors by re-circulation of hot products with intermittent reverse flows
- Partially premixed ignition
- Diffusion flame along the shear layer

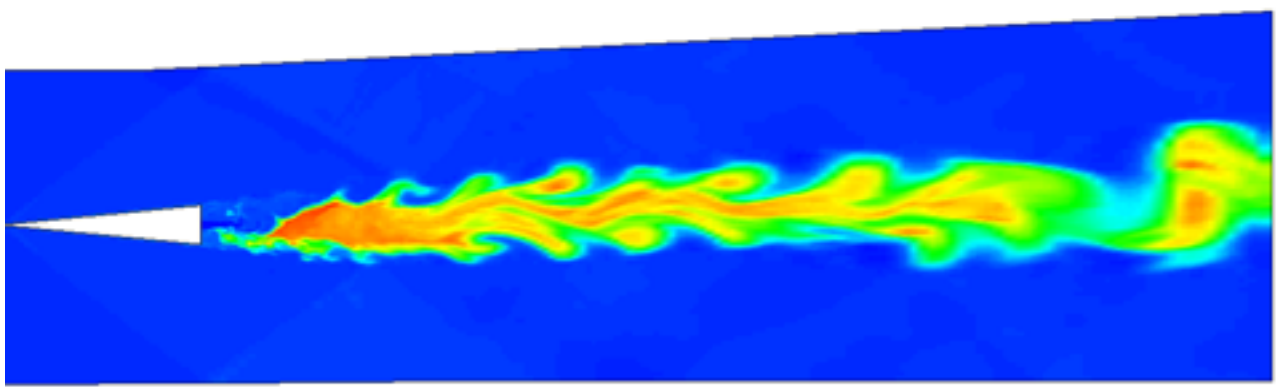

Genin and Menon, AIAA-2009-0132, AIAA Journal, 2010

Sonic Jet in M=1.6 Cross-Flow

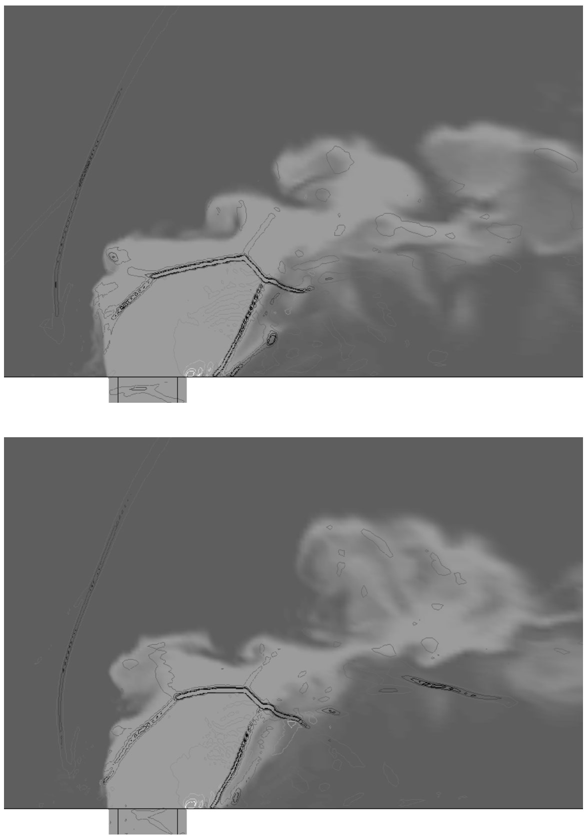

Current LES

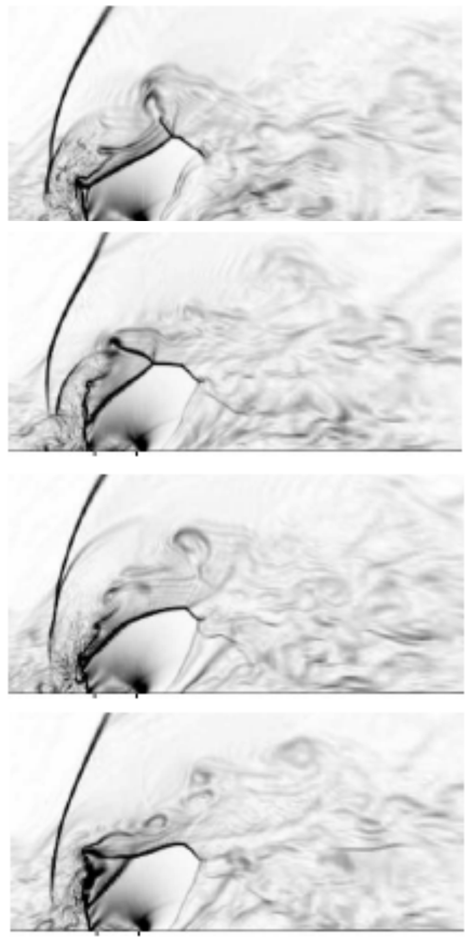

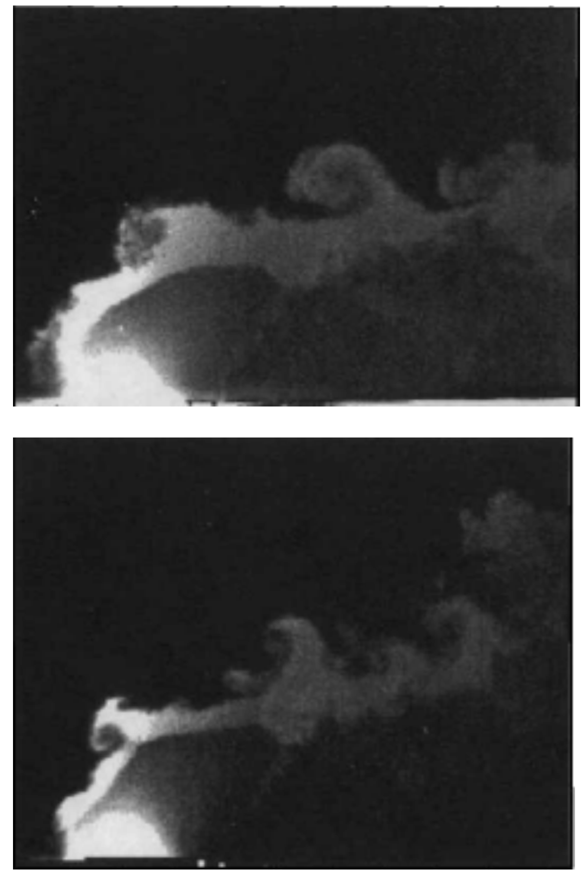

Flow Vis (vanLarberghe, 2000)

Comparison with Experiments

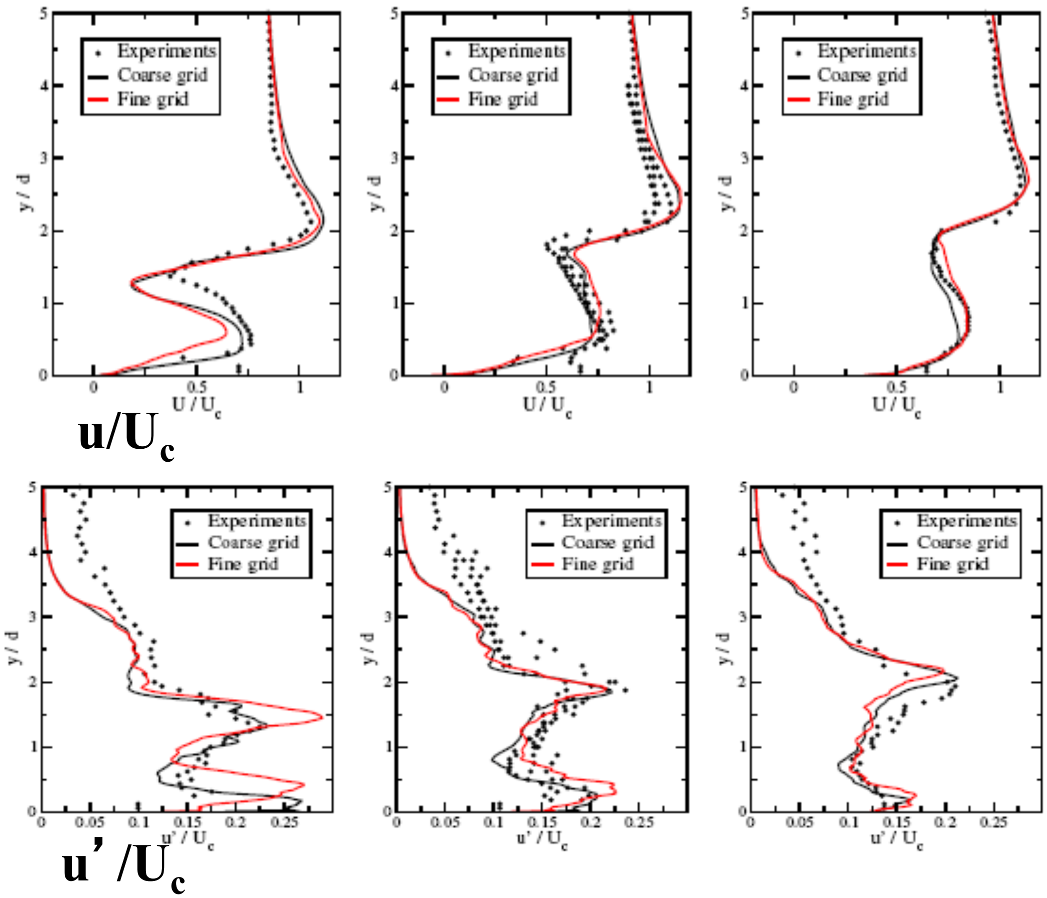

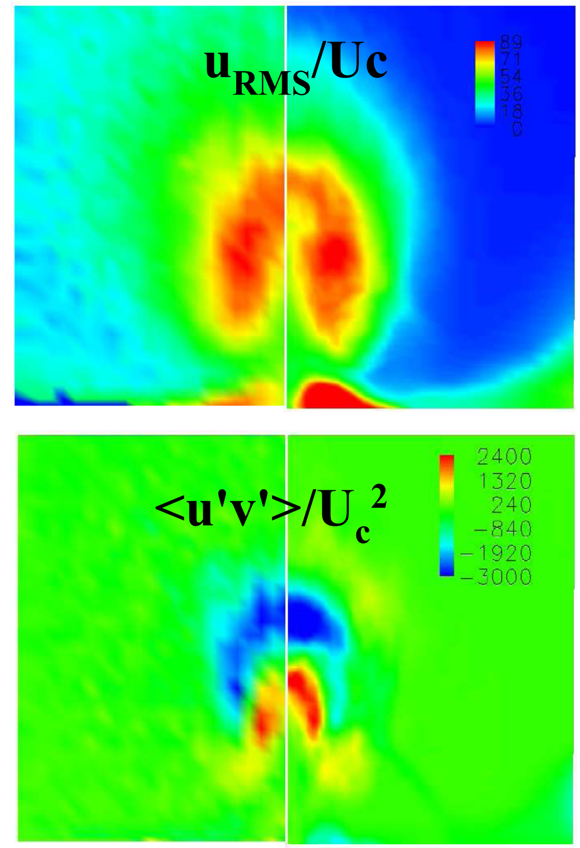

Expt. (x/d=5) LES

Santiago and Dutton (JPP, 1997)

Supersonic JICF

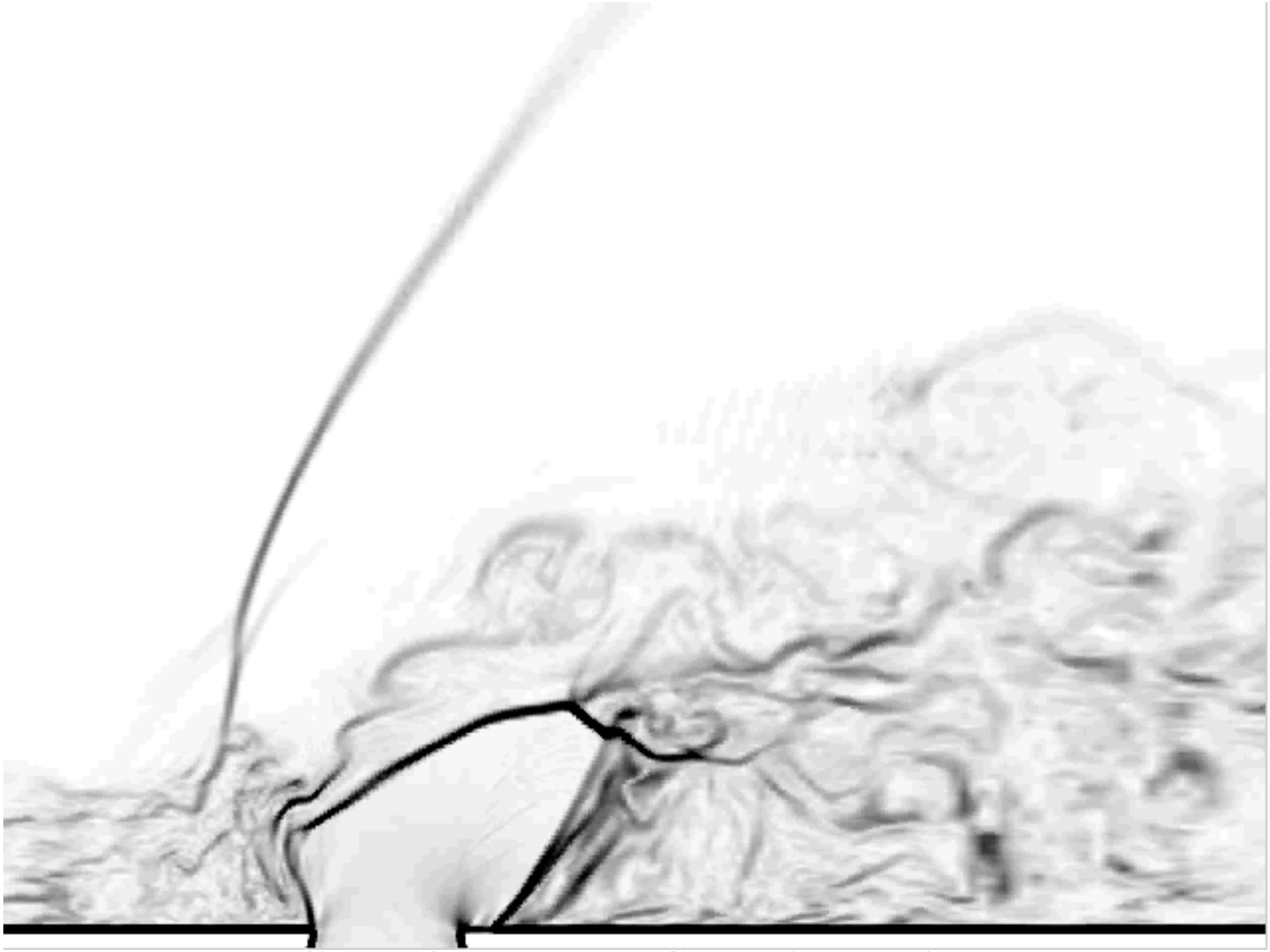

Adaptive Refined Level Set in LESLIE

- Application to moving shocks, flames and bodies
- ~ AMR for shocks and flames
- Interface tracking and cut-cell for moving bodies

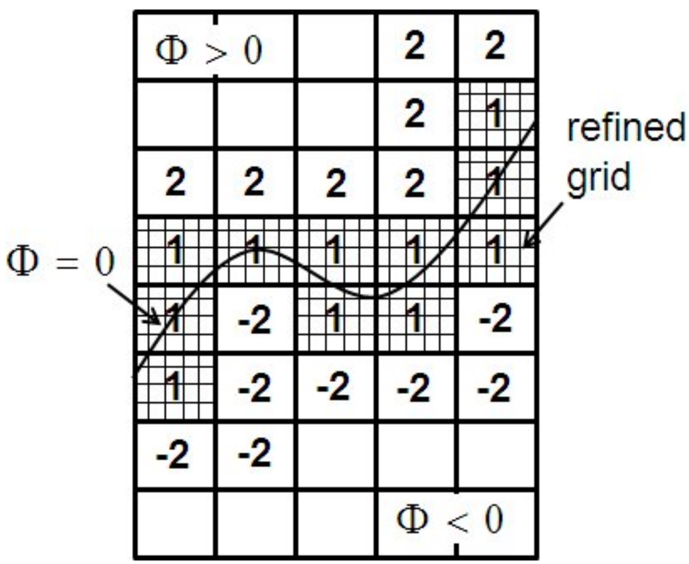

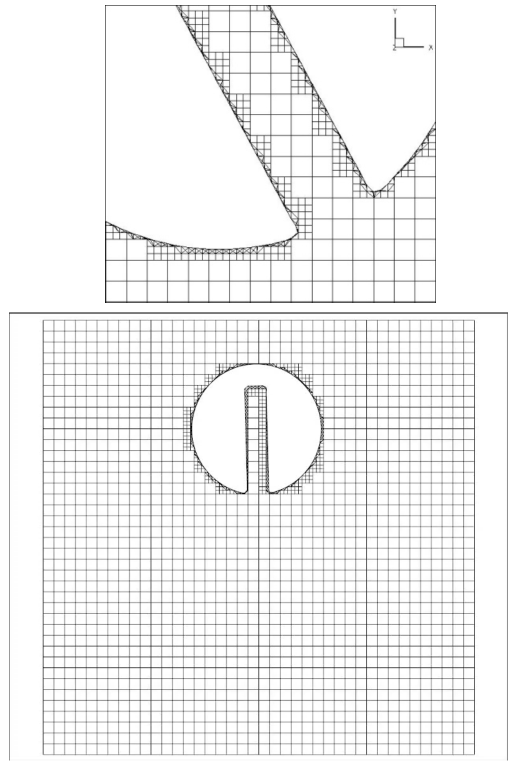

Zaleski Disk

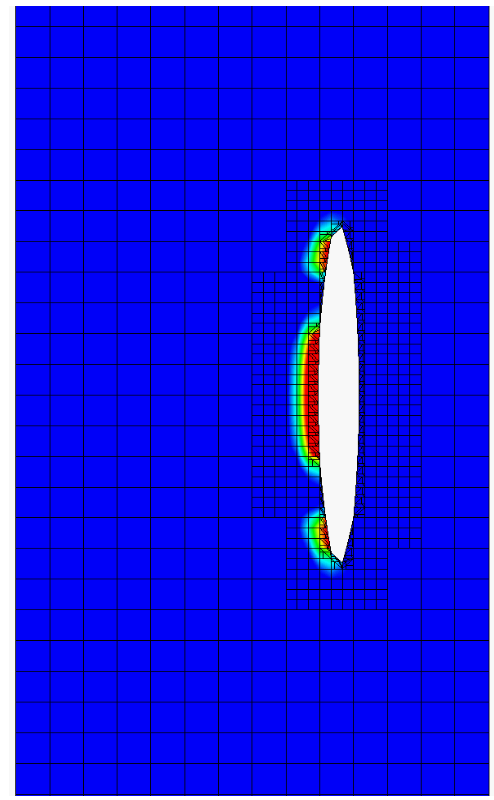

Deforming Ellipsoid in M = 6

- **Osher and Fedkiw, Level Set Methods and Dynamic Implicit Surfaces, 2002**
- **Choi and Menon, AIAA-2010-414, 2011-417**

Strategies in DIGGIT

- Compressible 5-equation two-fluid model included
- Time integration with TVD-RK O(3) or SDC (for higher order)
- AMR based on detecting inter-element discontinuity
- For smooth flows: Up to O(7) in space and O(5) in time
- Trouble cell detector to apply moment limiter for shocks

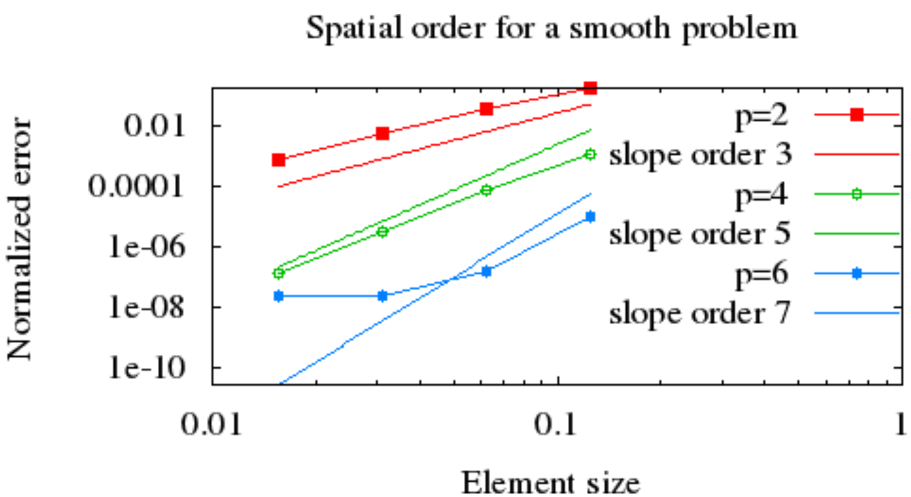

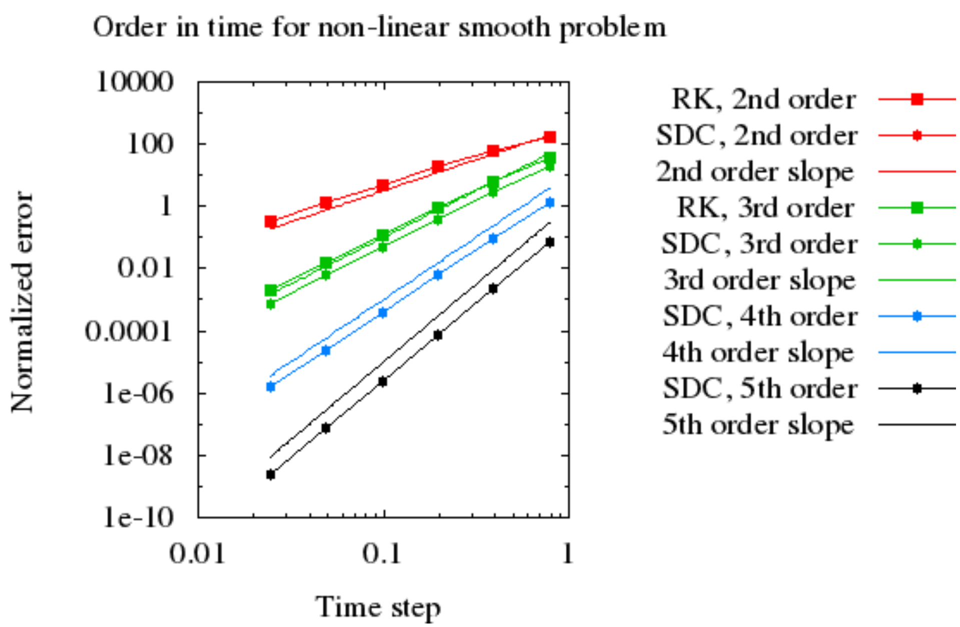

Gryngarten et al., 2011, Gryngarten and Menon, AIAA-2011-294

LDG: Shock – Gas Bubble in Air

- M=1.22 He-air 2D cylindrical bubble with 4-level AMR (right)
- M=1.7 Kr-air spherical bubble
- Layes and Le Metayer, (Phys. Fl., 2007)

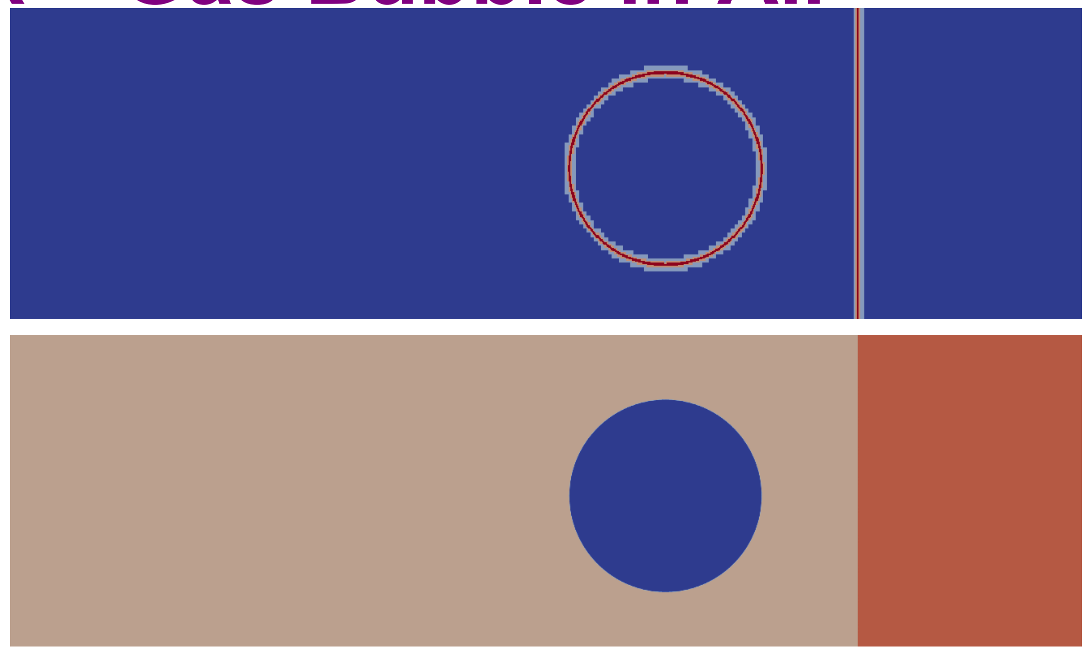

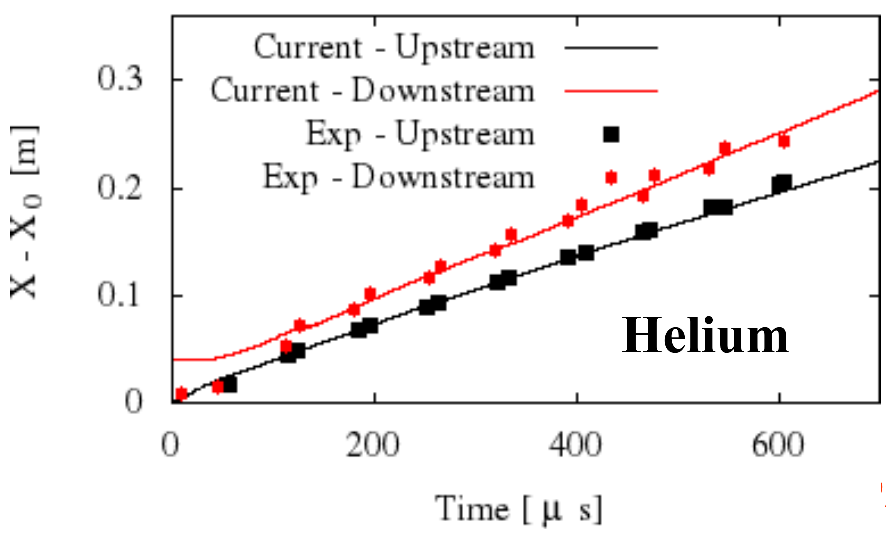

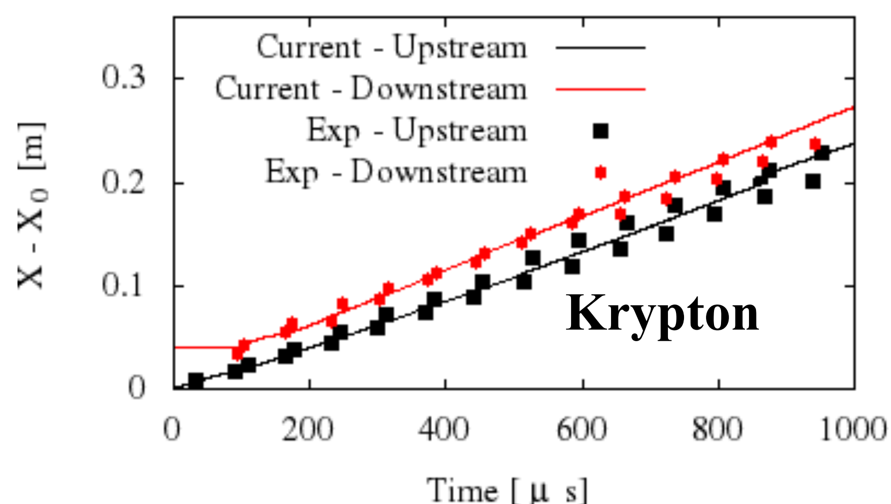

LDG: Shock – Air 3D Bubble in Water

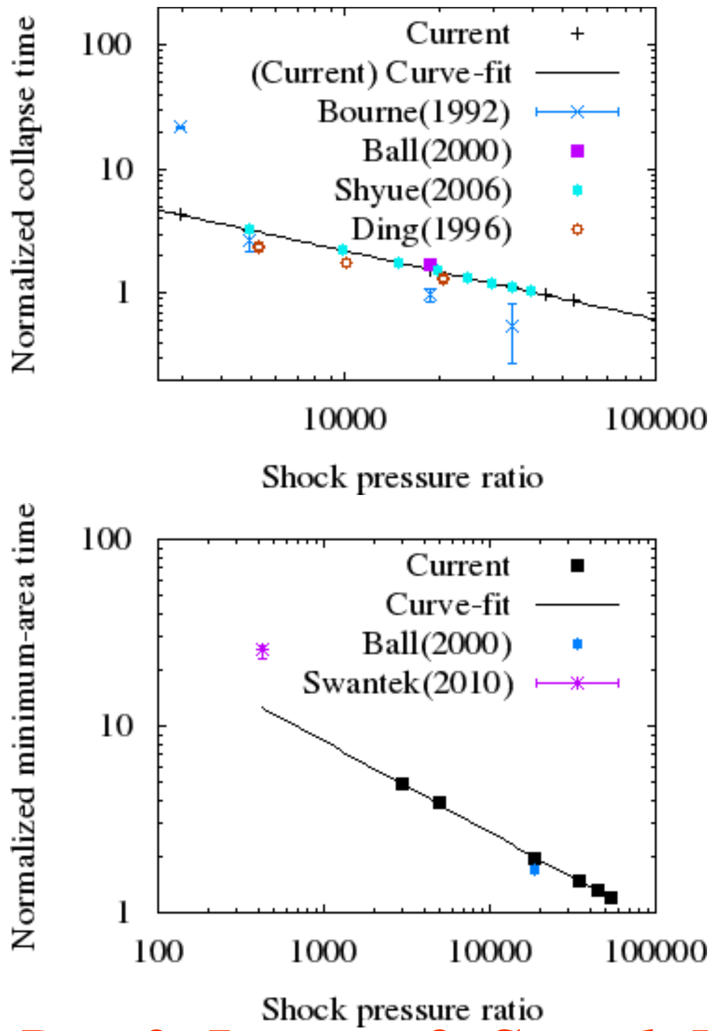

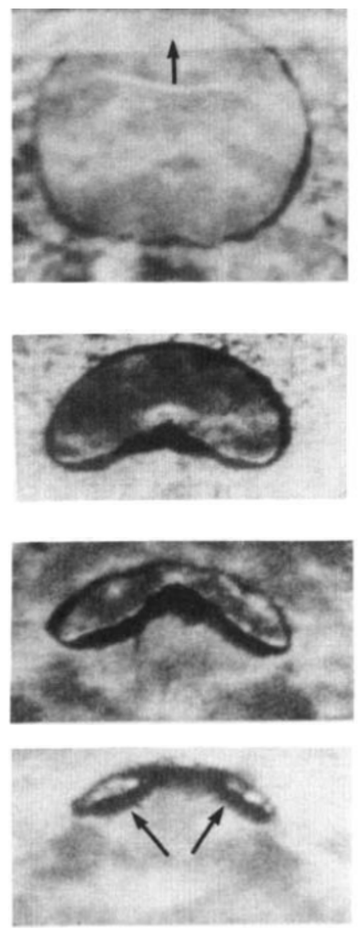

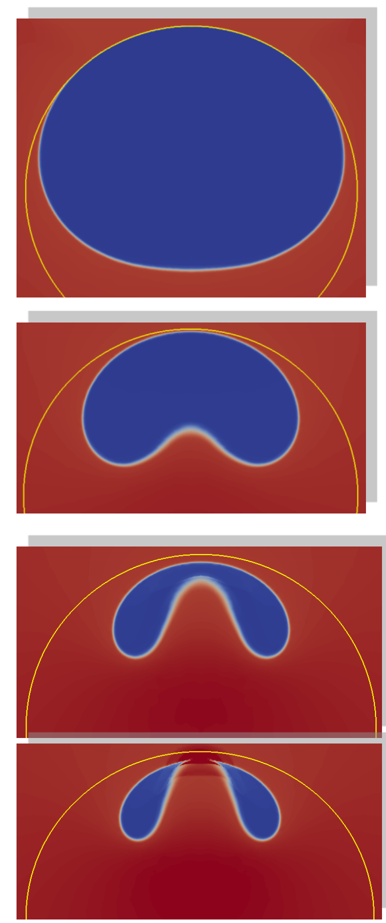

Gryngarten and Menon, 2011

Compressible Spatial Shear Layer

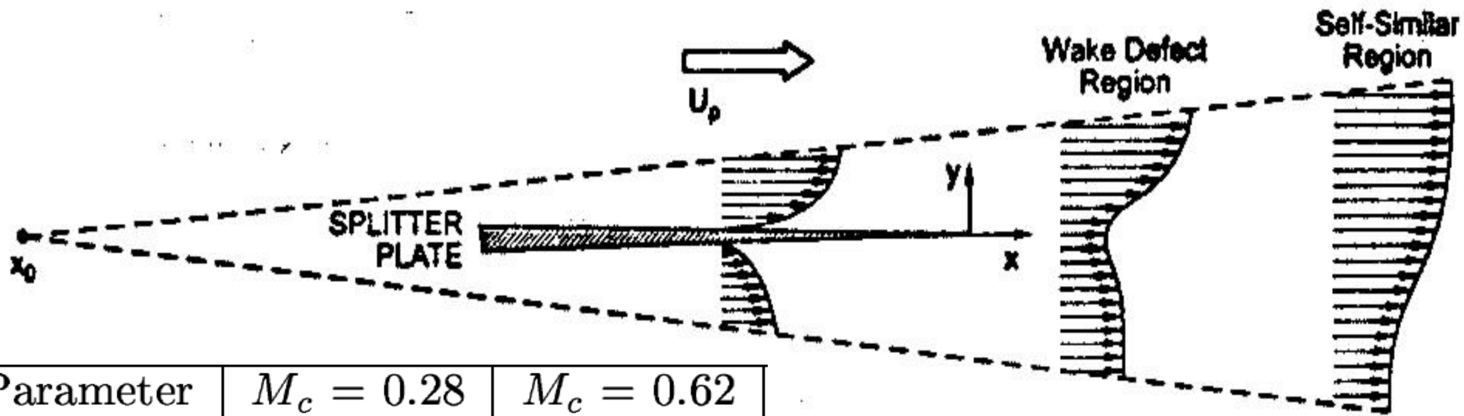

Parameter	$M_c = 0.28$	$M_c = 0.62$
M_1	1.64	2.0
M_2	0.91	0.4
$U_1(m/s)$	430	480
$U_2(m/s)$	275	130
$T_1(K)$	172	150
$T_2(K)$	223	252
$P_{O_1}(Kpa)$	302	495
$P_{O_2}(Kpa)$	115	75
ρ_2/ρ_1	0.77	0.59
U_2/U_1	0.63	0.27
λ_B μm	1.7	0.8
Resolution	$2-7\ \lambda_B$	$5-14\ \lambda_B$

- *LEMLES resolution same as experiment deliberately*

* *Passive scalar mixing*

182 x 150 x 5 - Quasi-3D

182 x 150 x 100 - Full 3D

y+ = 15 @ splitter plate

Uniform grid in Z direction

Profiles of Axial Velocity, Mc = 0.62

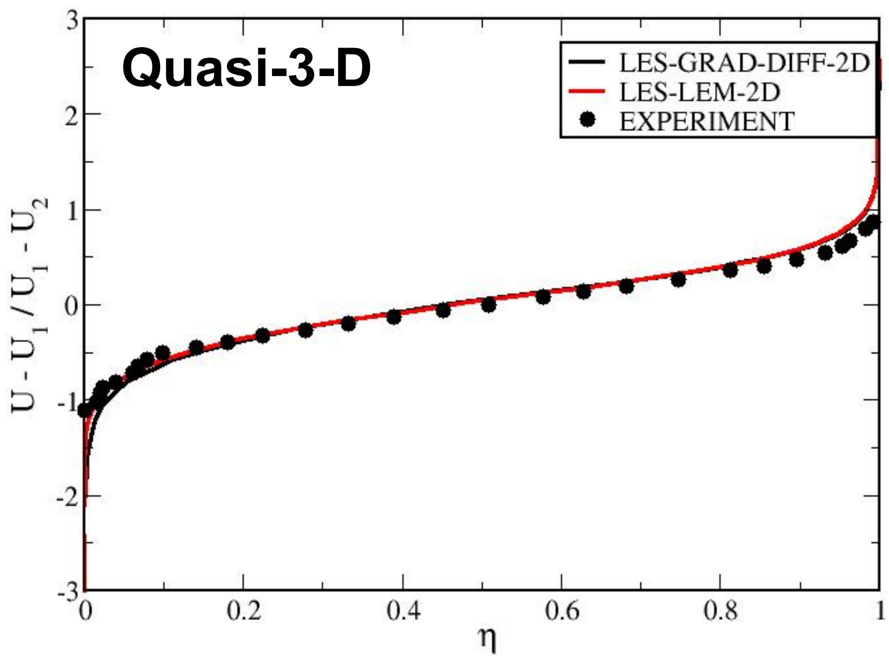

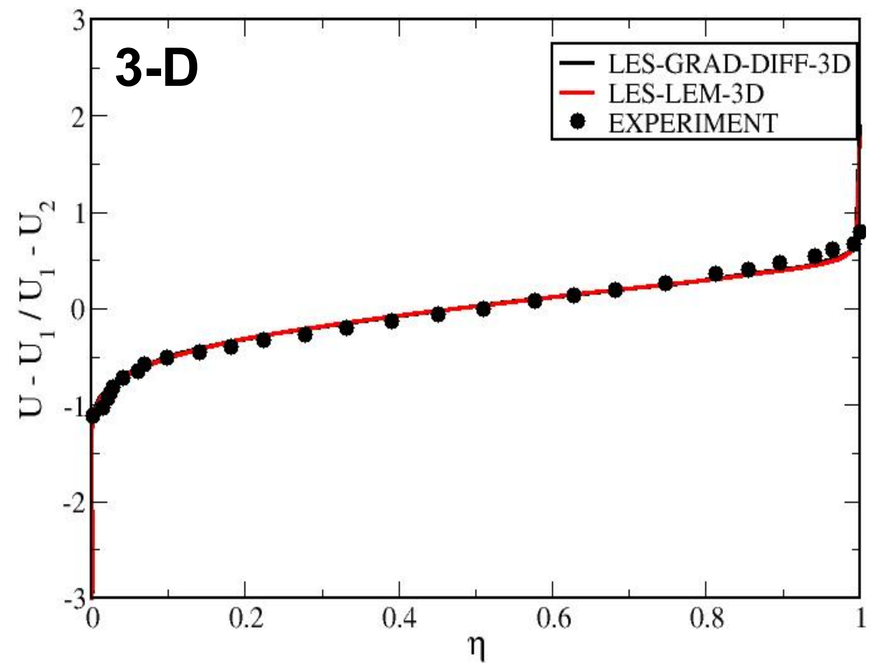

- **GRAD-DIFF and LEMLES employs same k-sgs closure**
- **Both methods agree well with the experiments**

RMS Axial Velocity, Mc = 0.62

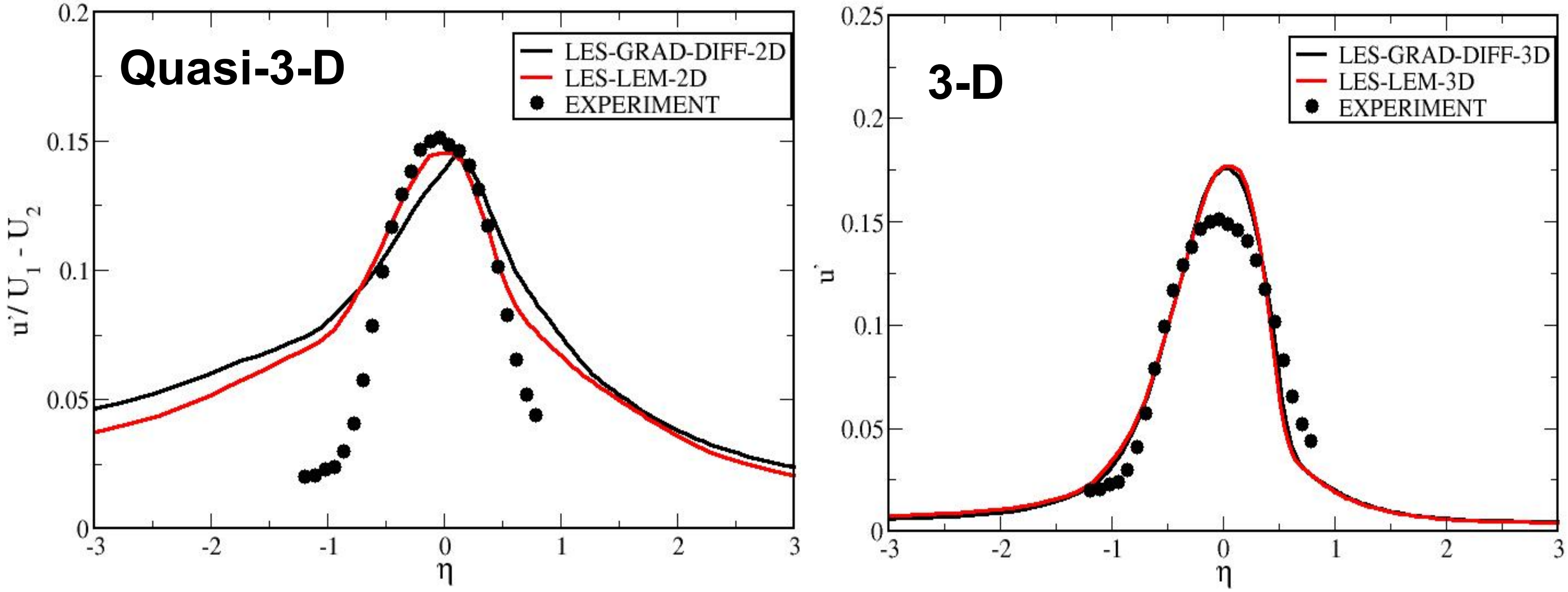

- 3D captures the shear layer spread correctly

RMS Transverse Velocity, Mc = 0.62

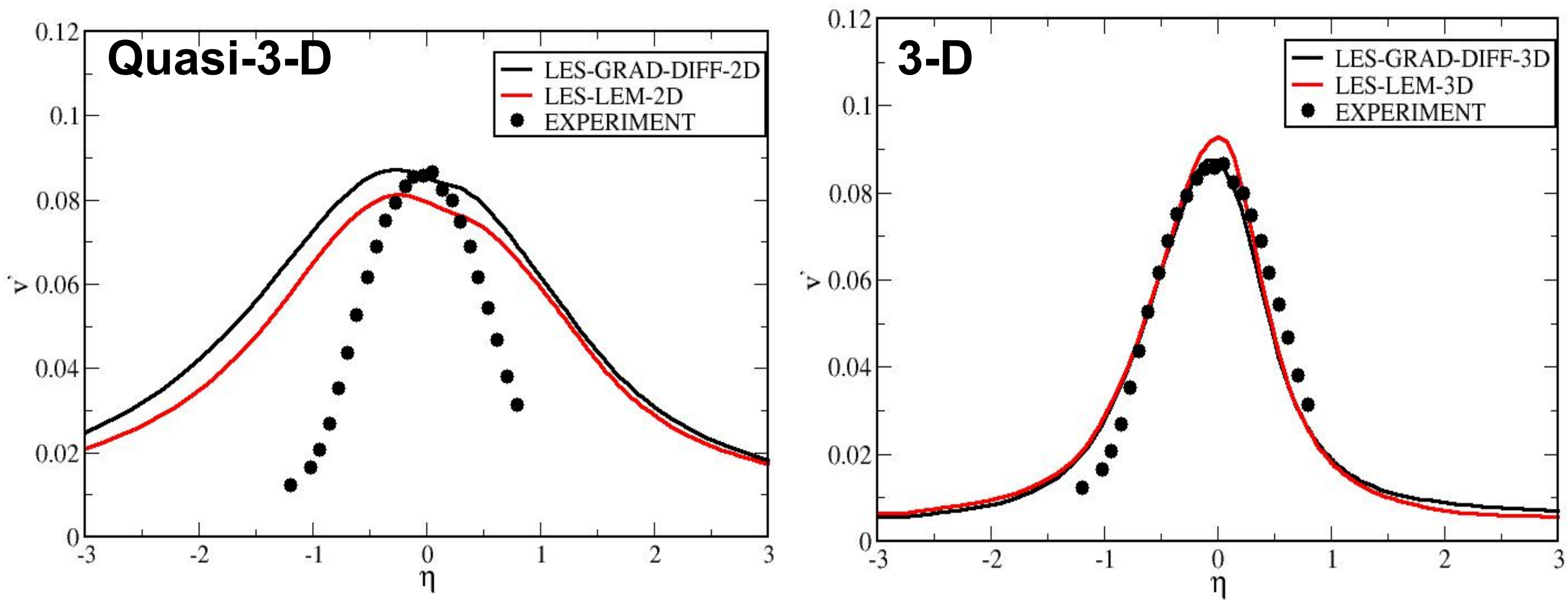

- **GRAD-DIFF and LEMLES over-predicts the peak by < 6%**
- **Good agreement in the shear layer region**

Normalized Growth Rate

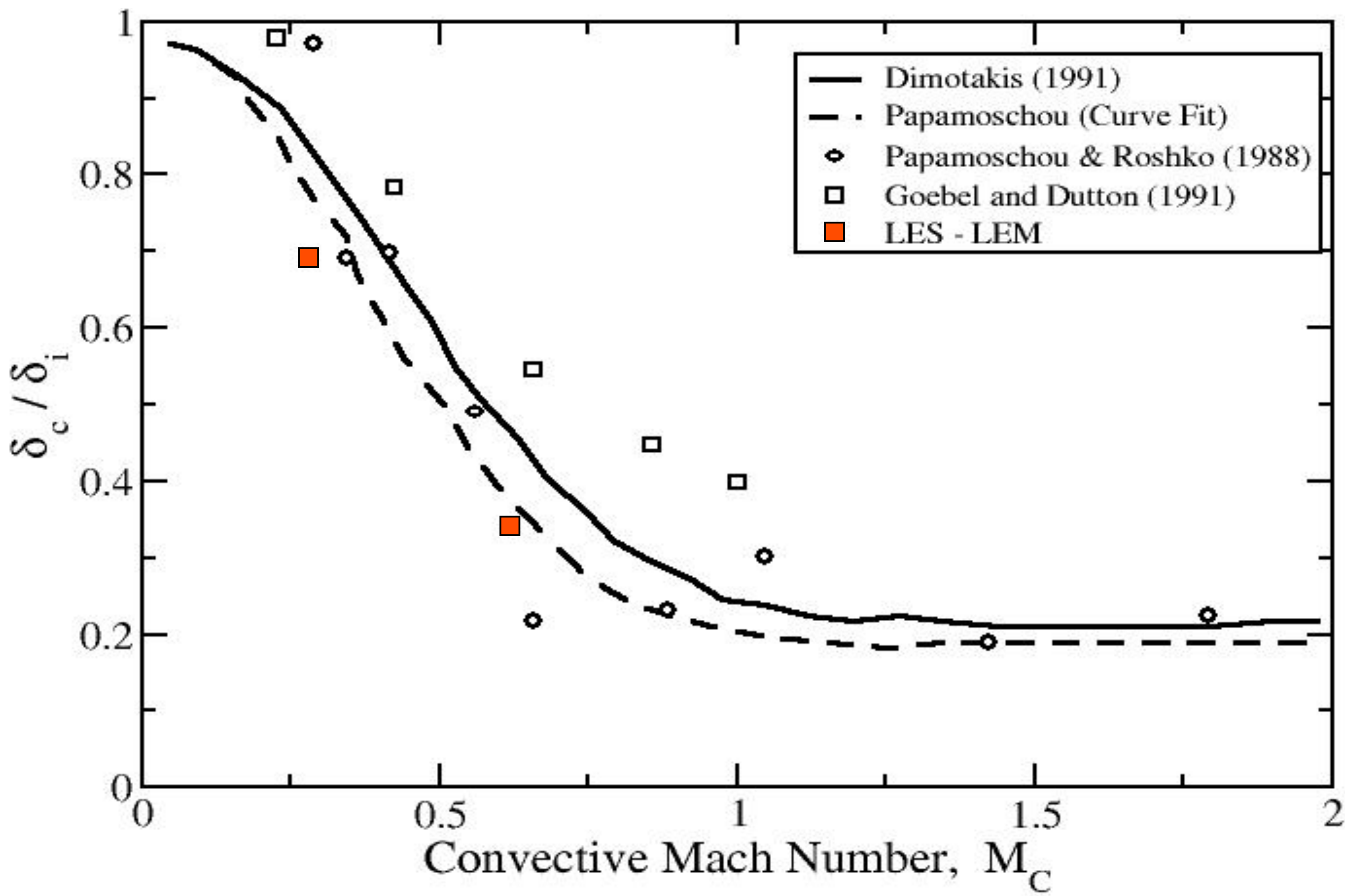

Mean Mixture Fraction, Mc = 0.62

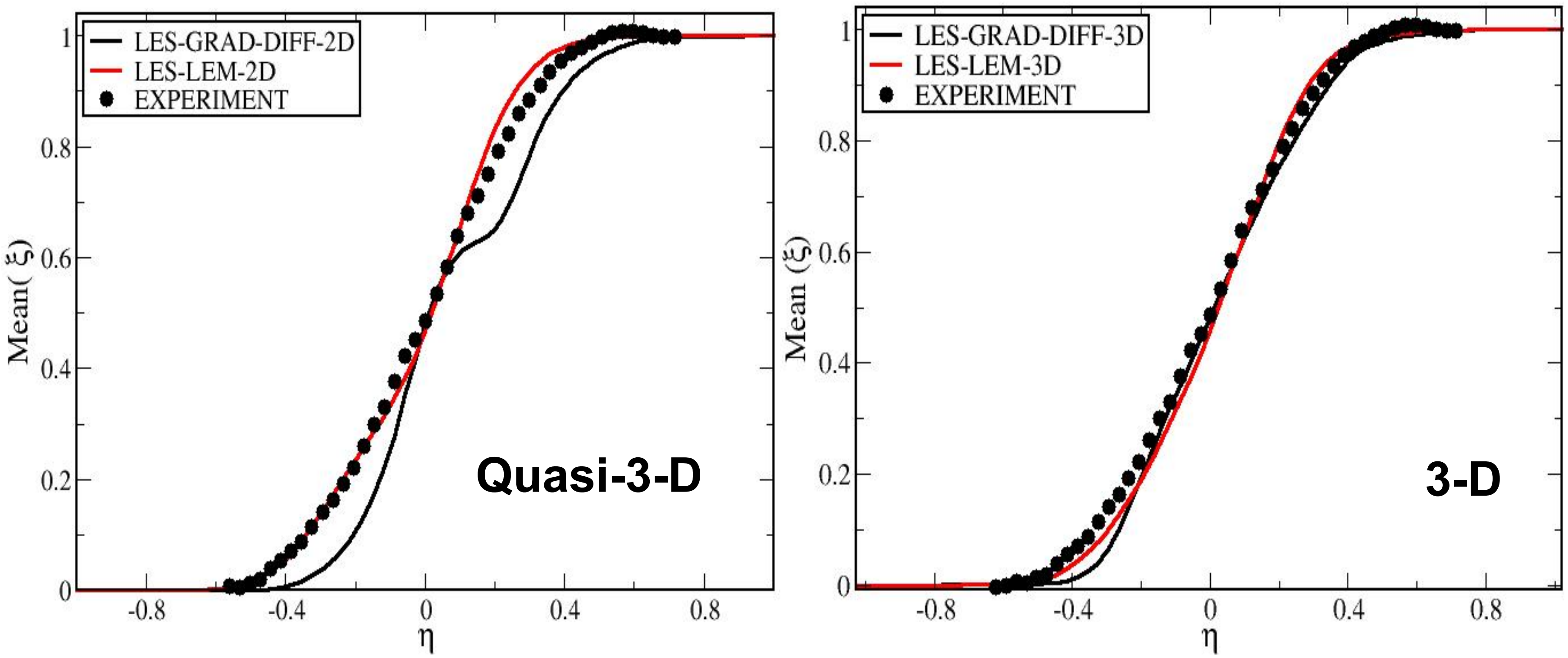

- Improvement in mean mixture fraction prediction for GRAD-DIFF
- LEMLES results are closer to the experiment near the edges

RMS of the Mixture Fraction, Mc = 0.62

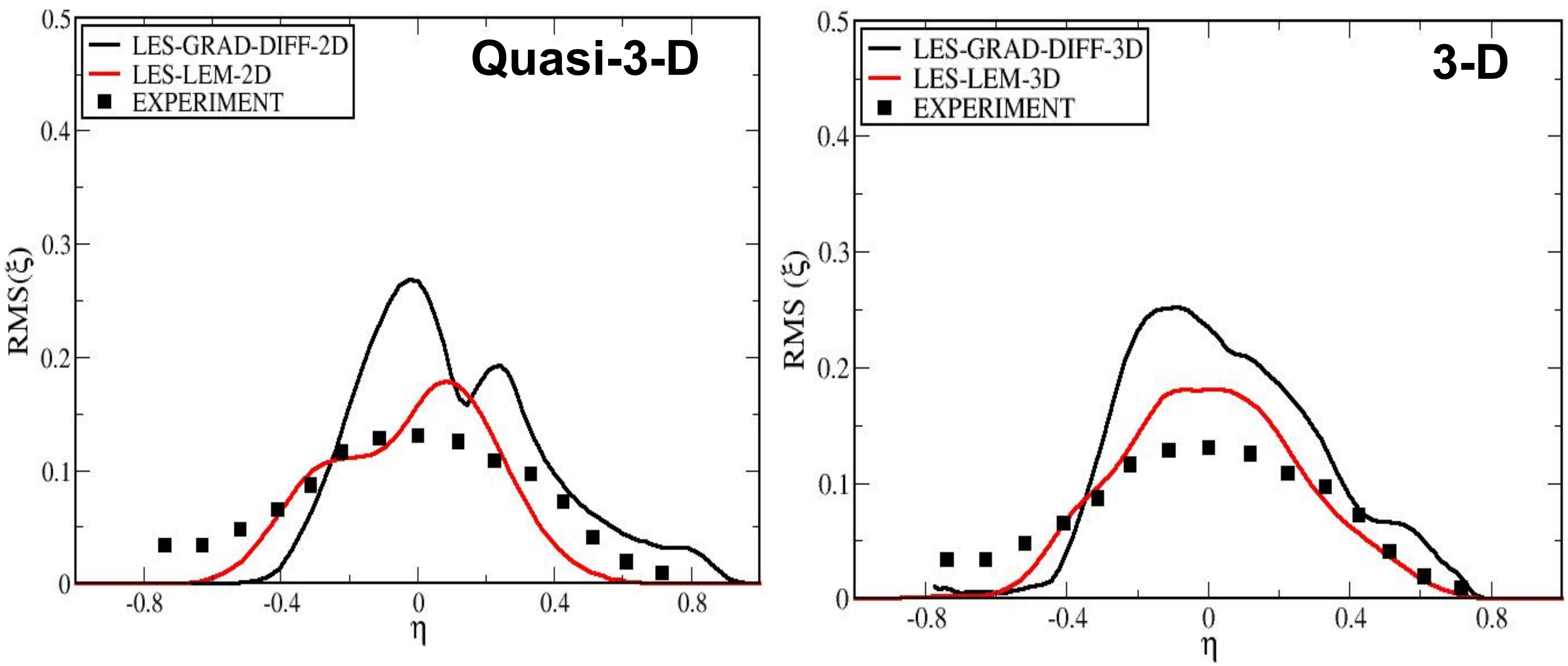

- GRAD-DIFF predicts a higher RMS compared to LEMLES

PDF of Mixture Fraction

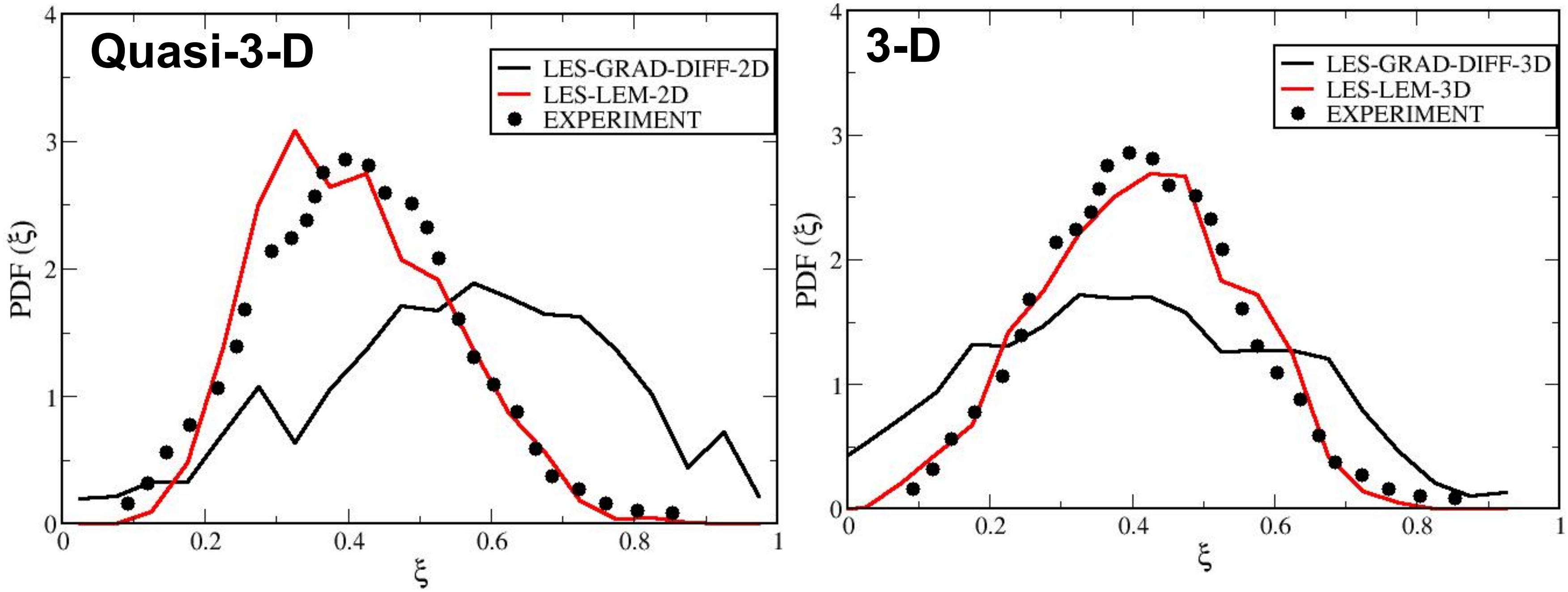

- LEMLES correctly predicts the shape and width of the PDF
- Gradient diffusion LES fails to predict both these features
- Note: given PDF all scalar moments can be predicted

Numerical Studies of WPAFB TC19

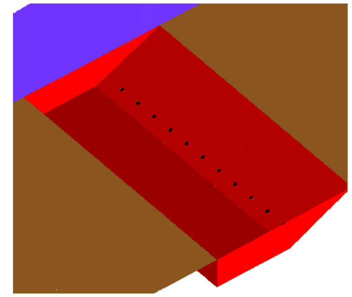

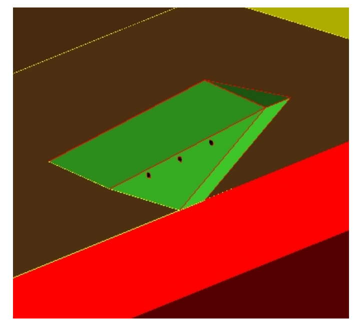

- Full test facility is numerically simulated
- Hybrid VLES-LES in the isolator
- Two configurations studied
  - Cavity with 11 injectors on aft ramp
  - Strut upstream of cavity with 6 injectors
- 8+ million cells, 12/18 LEM cells per LES cell
  - Smallest mesh size ~ 0.01 mm
  - 30+ points in wall boundary layer

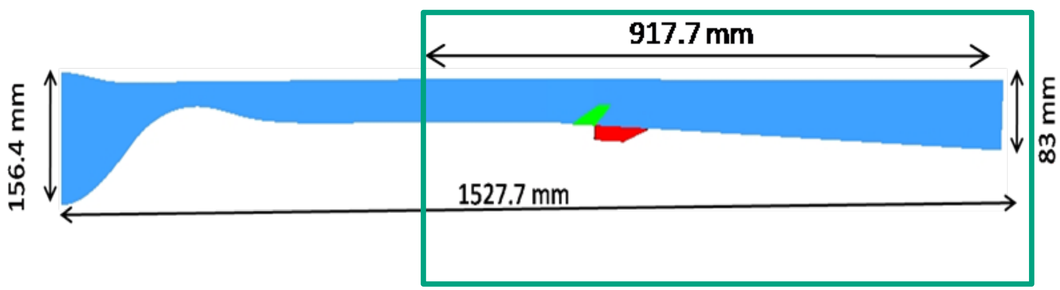

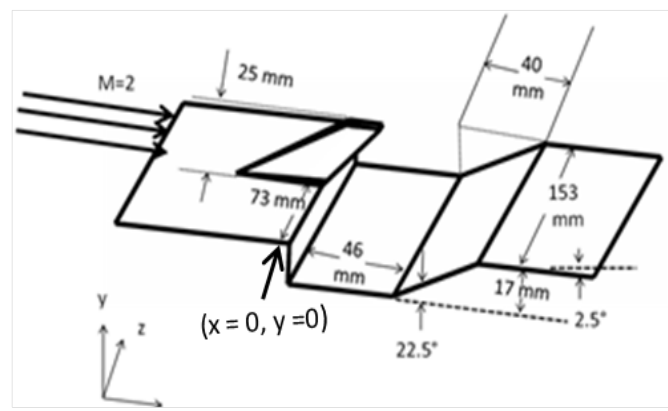

Mach 2 Flow Conditions

Test Configuration	Stagnation Conditions		Isentropic Conditions at Isolator					
	P0 (kPa)	T0 (K)			$\dot{m}_{air}$ (kg/s)	$\dot{m}_{water}$ (kg/s)	Relative Humidity (%)	Fuel Rate (SLPM)
No-Strut	414	589	53	327	3.2	25	4	225
Strut (Reacting)	207 (449)	564 (600)	26	313	1.6	25	9	270

P_inj (KPa)	T_inj (K)
690	300

- $CH_4 - H_2$ blended fuel (70% - 30%)
- Reduced 4-step, 8 species mechanisms*
- Local Reynolds number, $Re_x \sim 42e6\ m^{-1}$
- Stagnation conditions for strut reacting case are changed (shown in red)

$$CH_4 + 2H + H_2O \rightarrow 4H_2 + CO \quad H_2O + CO \rightarrow H_2 + CO_2$$

$$2H + M \rightarrow H_2 + M \qquad 3H_2 + O_2 \rightarrow 2H + 2H_2O$$

* Klassen, Menon et al., 2009, AFRL-FA8650-06-C-2659, AFRL Final Report

Energy Spectrum

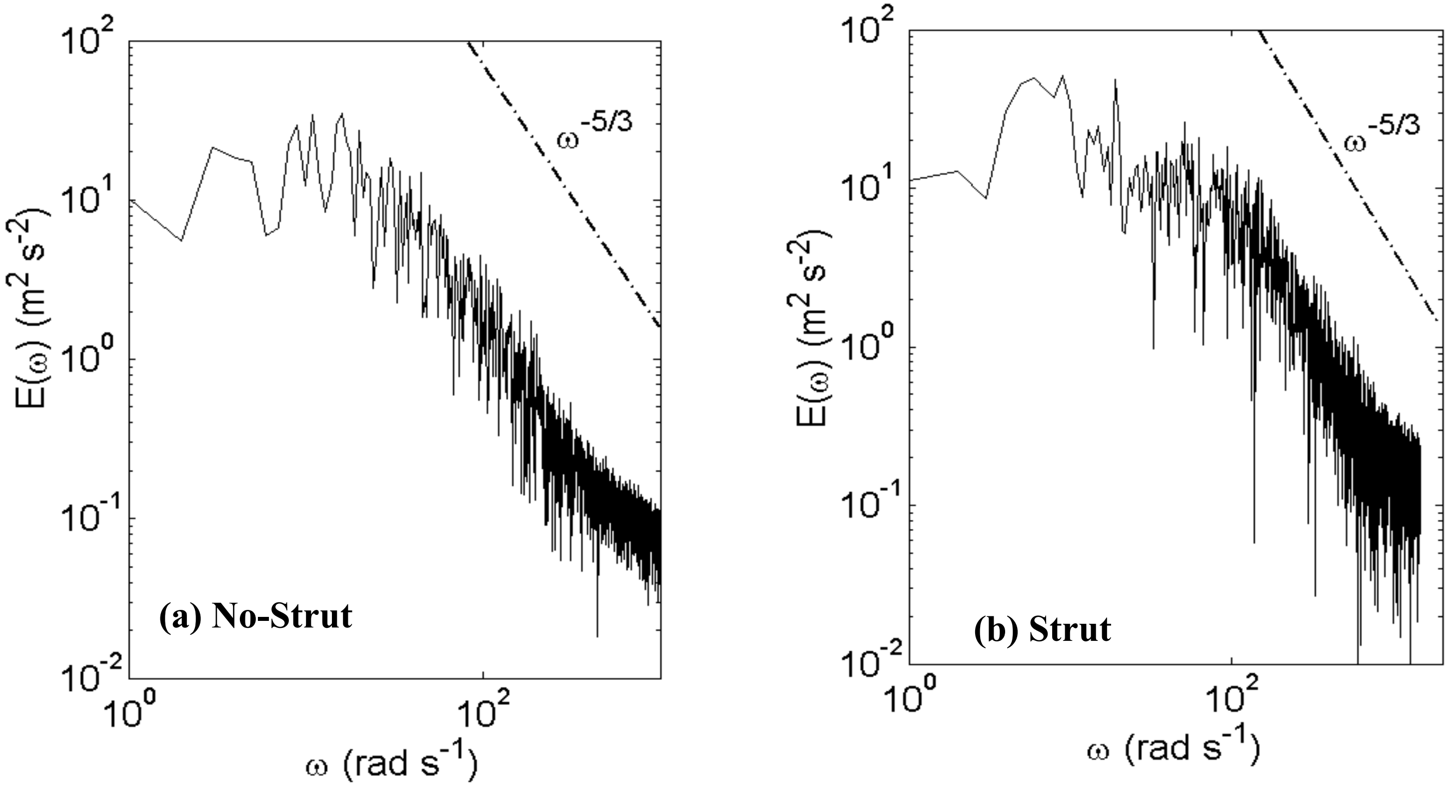

(a) No-Strut: X = 53.8 mm within the shear layer and (b) Strut: X = 33.8 mm in the strut wake

Recover $k^{-5/3}$ law in shear layer and strut wake

Non-reacting Flow: Cavity without Strut

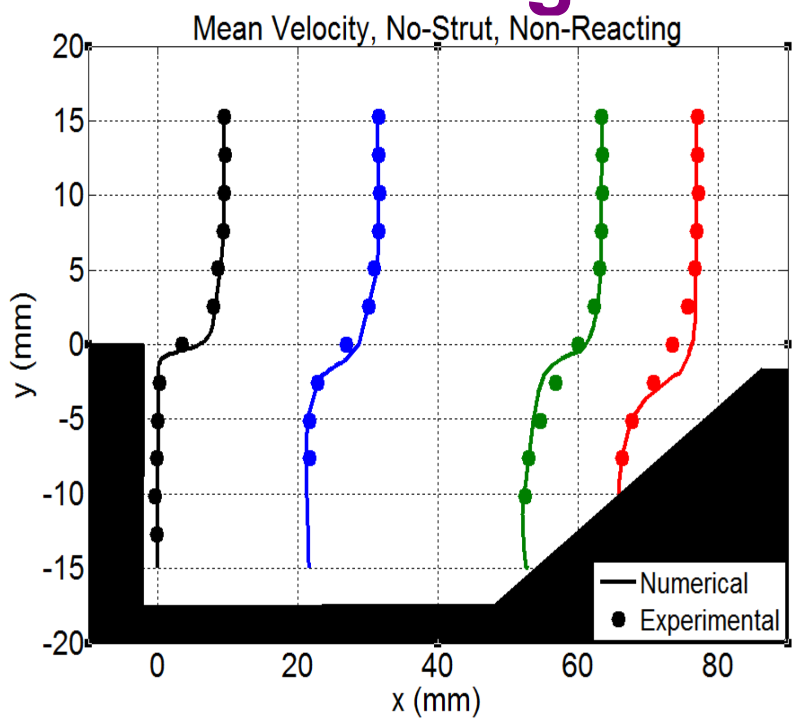

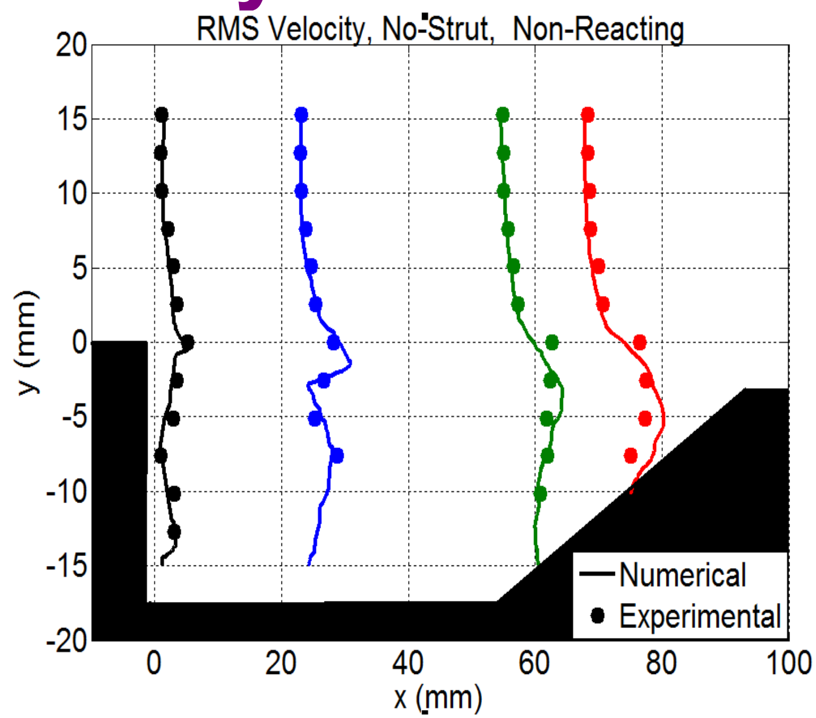

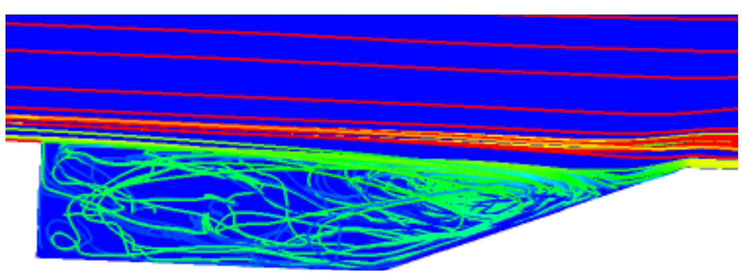

Time averaged mean velocity streamlines

- Large vortical flow inside cavity
- Good agreement with data

Wall Pressure

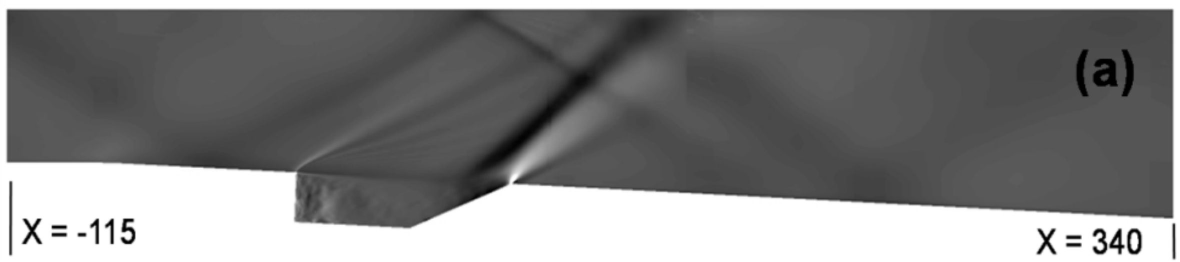

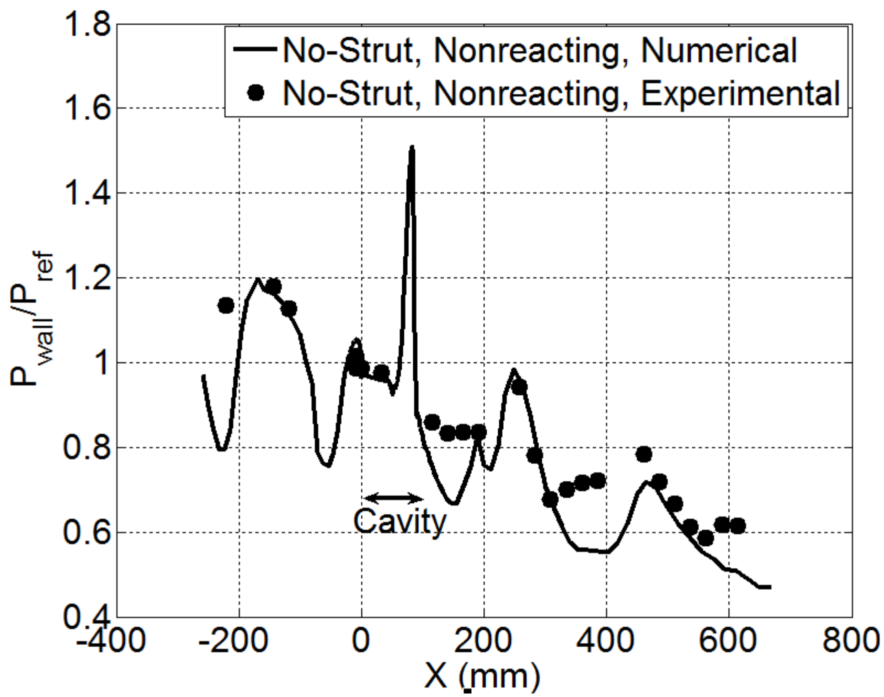

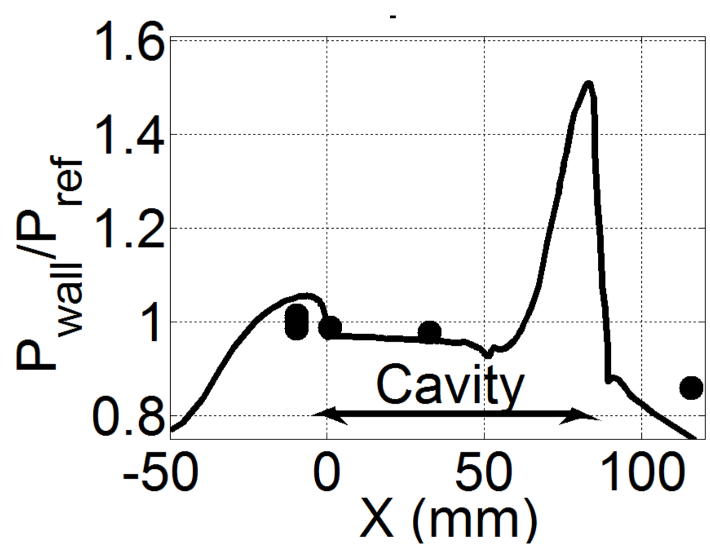

Wall Pressure

* Grady, N.R., et.al., 2010, AIAA-2010-1405

Velocity Comparisons: Non-Reacting, Strut

- Multiple shear layers in the wake of strut
- The overall spreading of wall-bounded cavity shear layer and velocity fluctuations are captured reasonably well

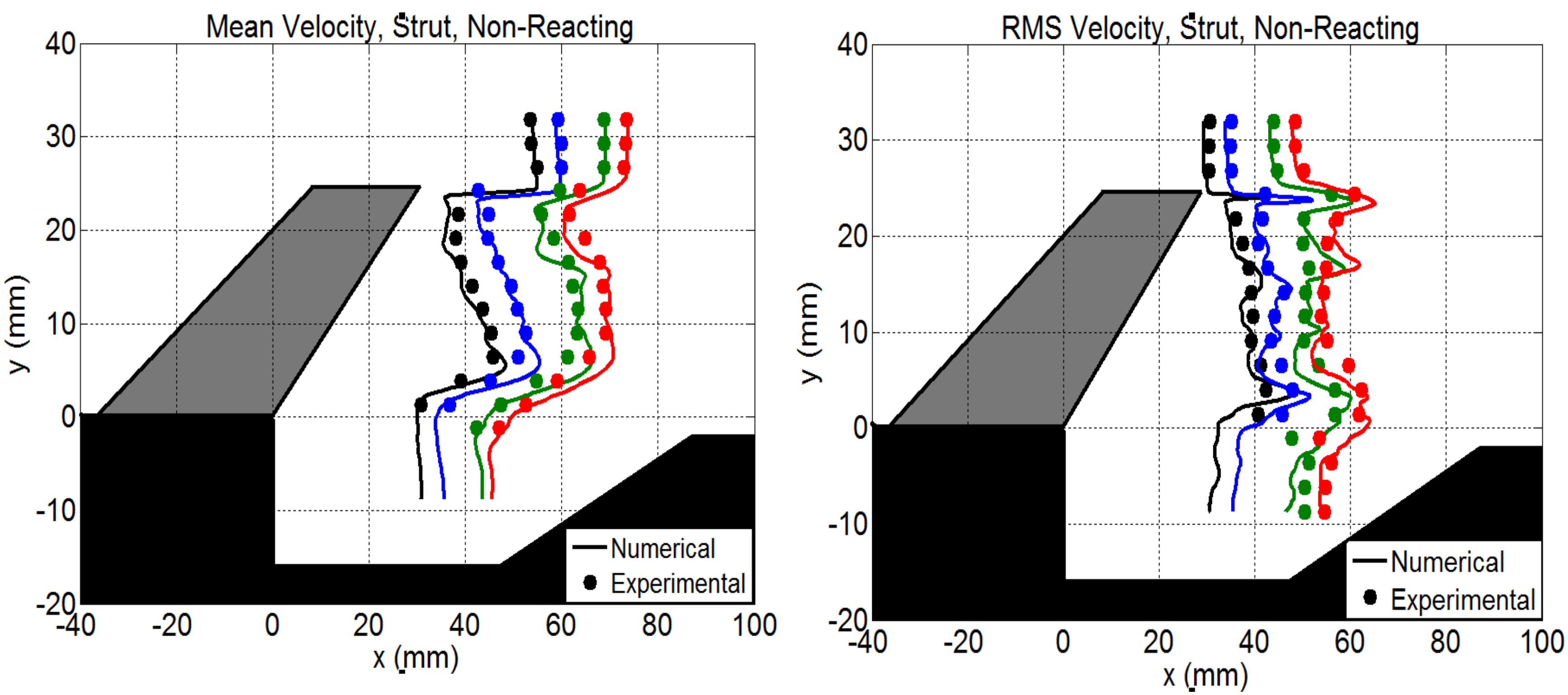

* Grady, N.R., et.al., 2010, AIAA-2010-1405

Wall Pressure Strut

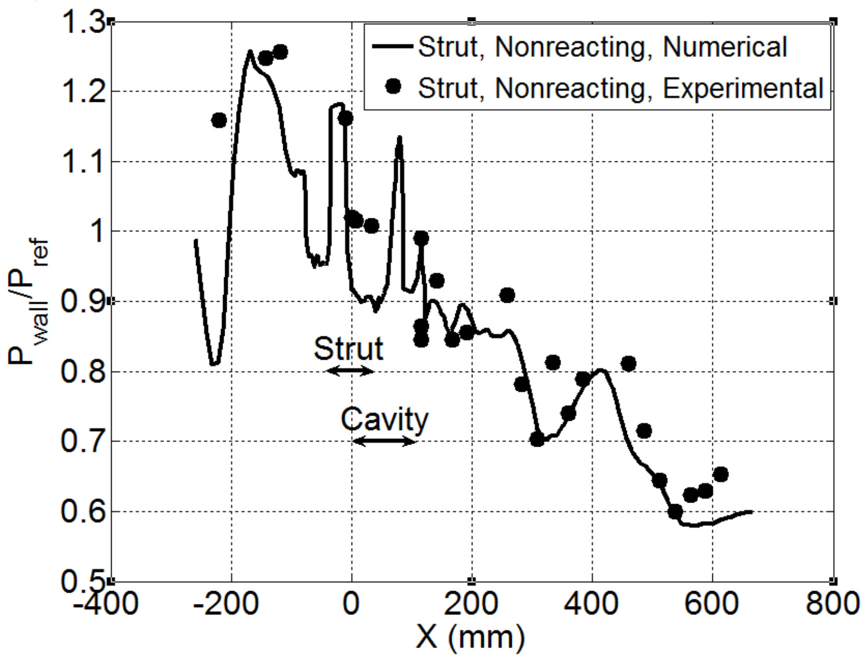

- Shock off strut LE (X= -30 mm)
- re-compression shock at aft ramp portion (X ~ 86 mm)
- Expansion at the cavity leading edge
- Expansion-compression around strut top edge

Wall Pressure

*Grady, N.R., et.al., 2010, AIAA-2010-1405

Reacting Case: Temperature Field No-Strut

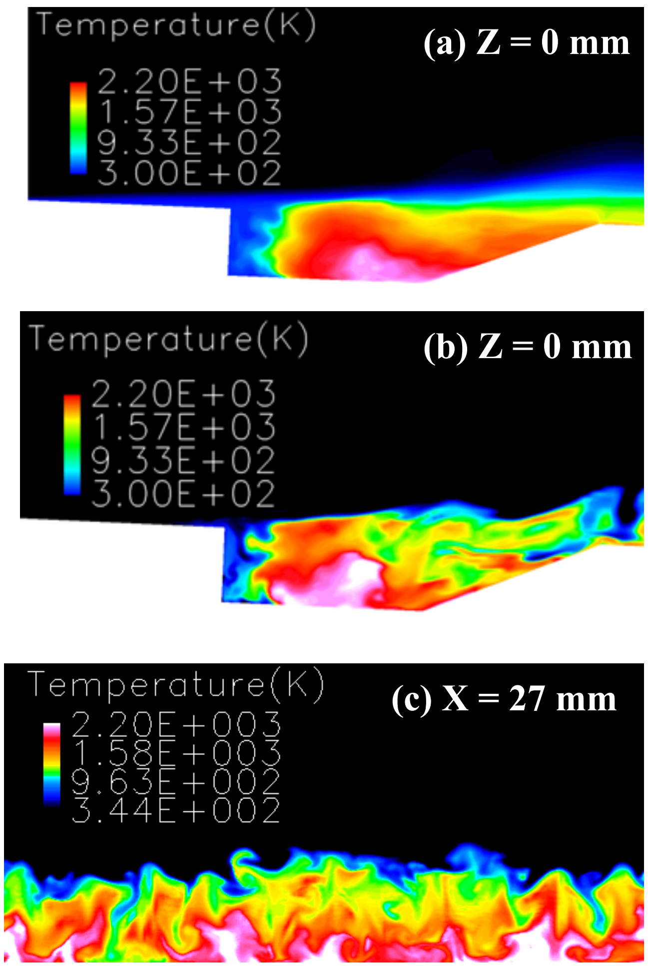

- Mean <T> shows that the cavity is full of products
  - Lifts shear layer for oxidizer entrainment into the cavity
- Instantaneous Temperature shows more variation in the cavity
- T at span-wise location (X = 27 mm) shows significant 3D structures
- High level of turbulence generated by aft wall fuelling

Flame Structure and Reaction Rate: No-Strut

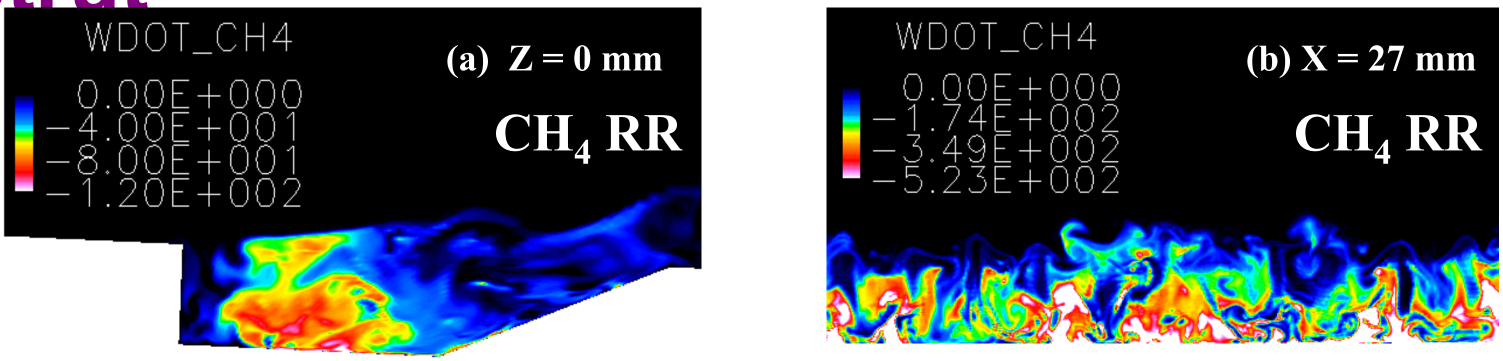

Reaction rate of CH4 at (a) Z = 0 plane and (b) X = 27 mm span-wise plane

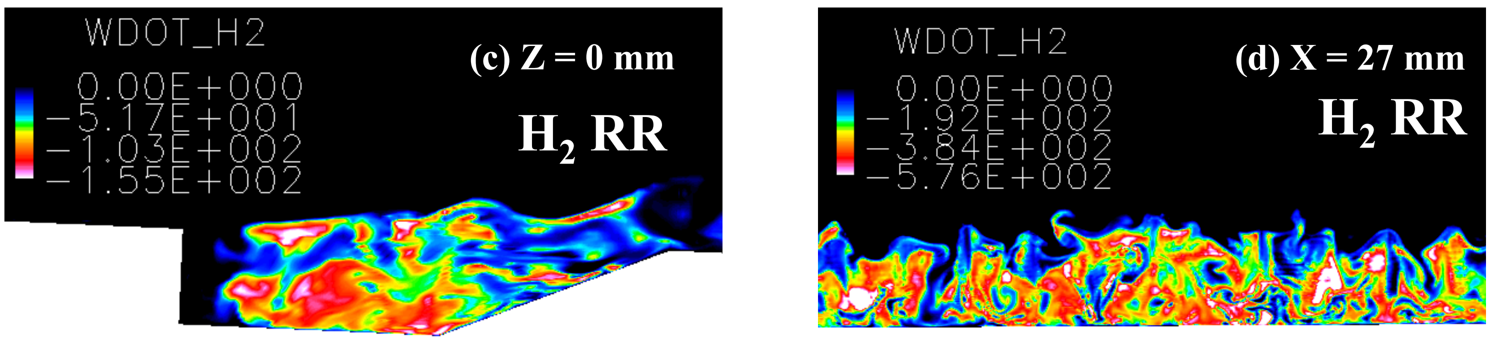

Reaction rate of H2 at (c) Z = 0 plane and (d) X = 27 mm span-wise plane

Methane and Hydrogen flame structures

Reacting Case: with and without Strut

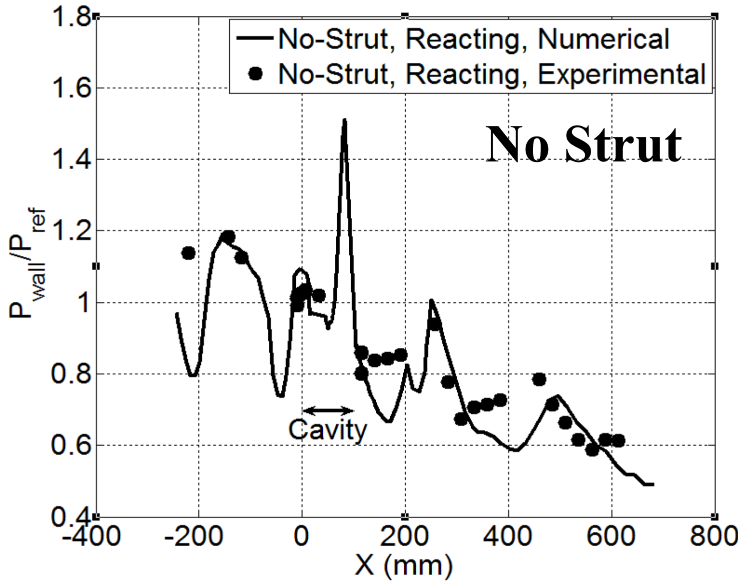

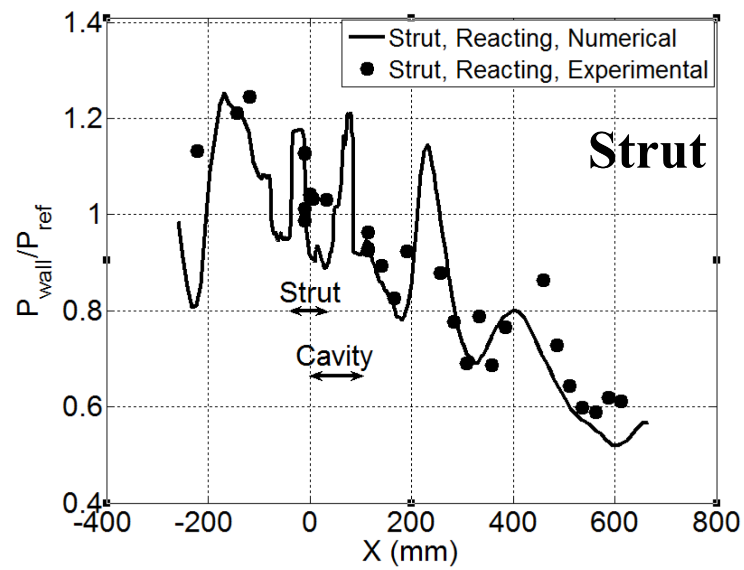

- Pressure comparison shows some reasonable agreement
- Peaks observed at locations where there are no pressure data locations of secondary shocks

Instantaneous Contours of Products: Strut

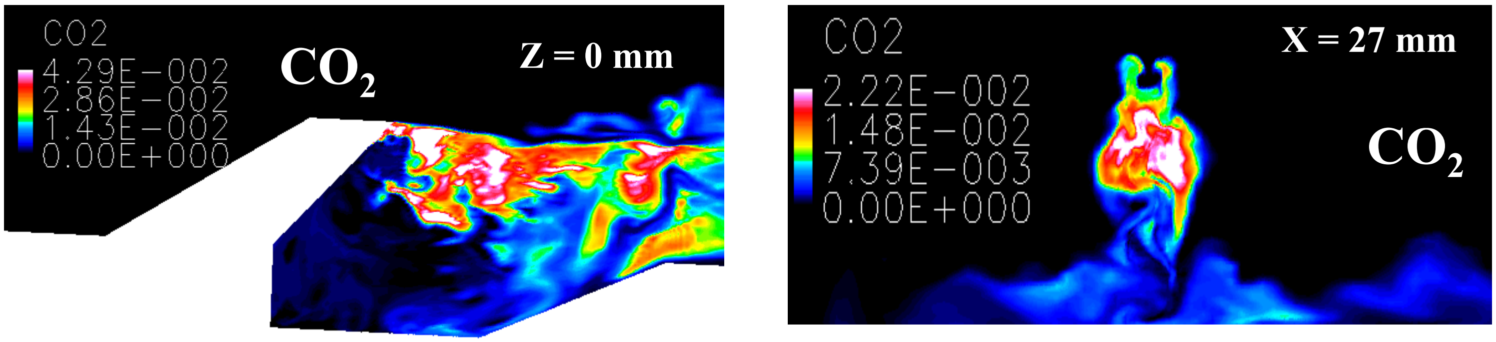

Contours of CO2 at (a) Z = 0 plane and (b) X = 27 mm span-wise plane

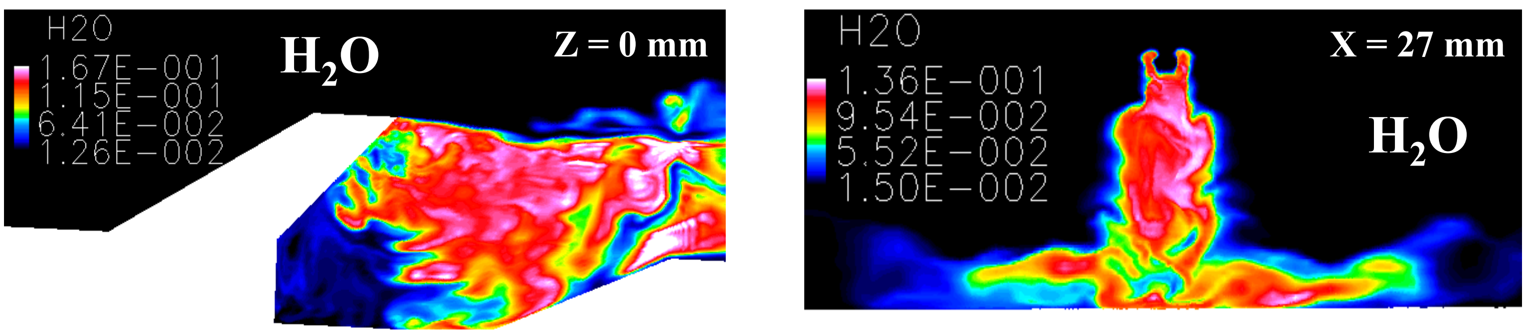

Contours of H2O at (a) Z = 0 plane and (b) X = 27 mm span-wise plane

Streamlines

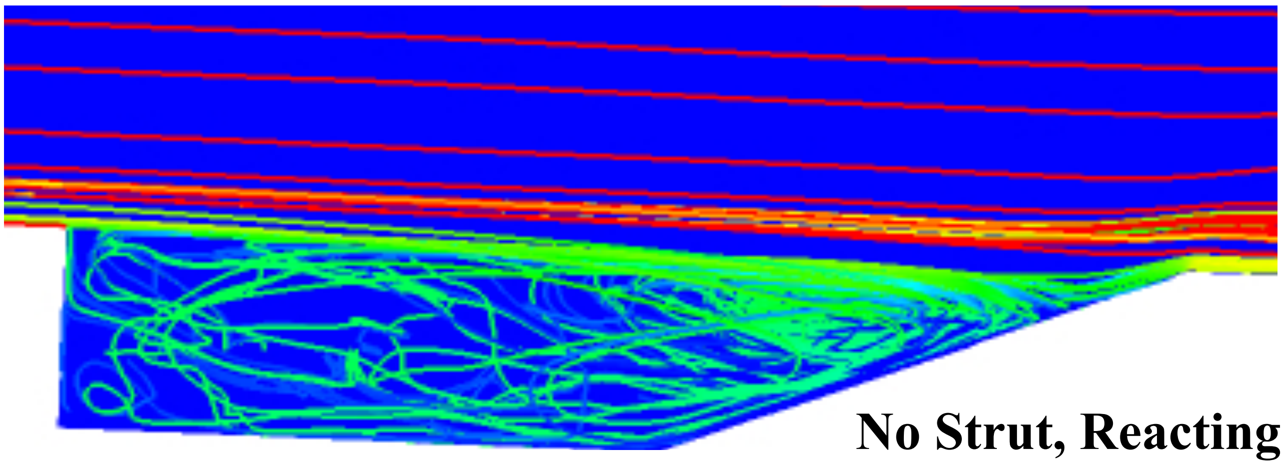

No Strut, Reacting

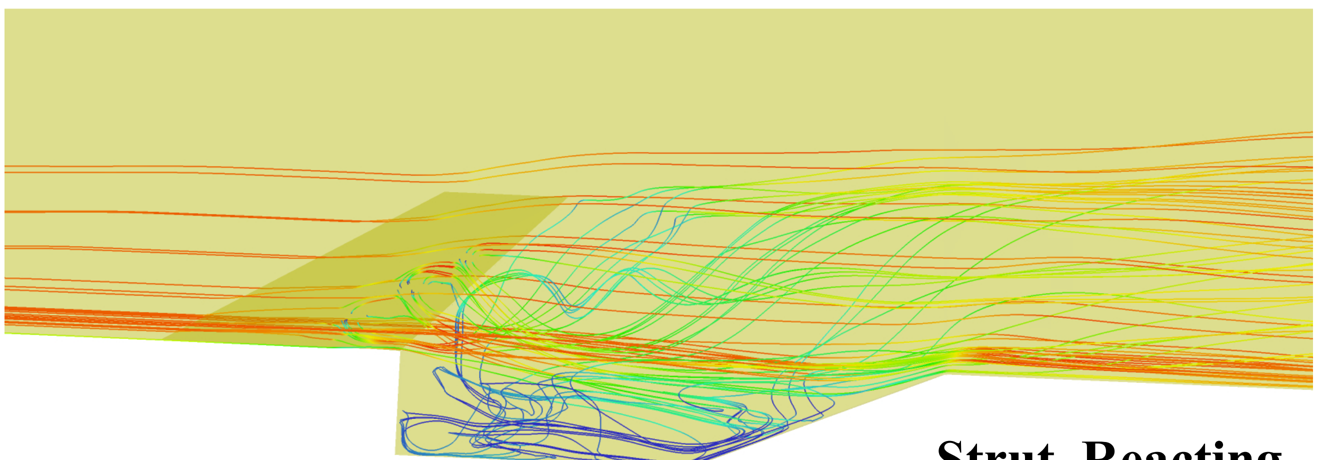

Strut, Reacting

Strut and No-Strut Comparison

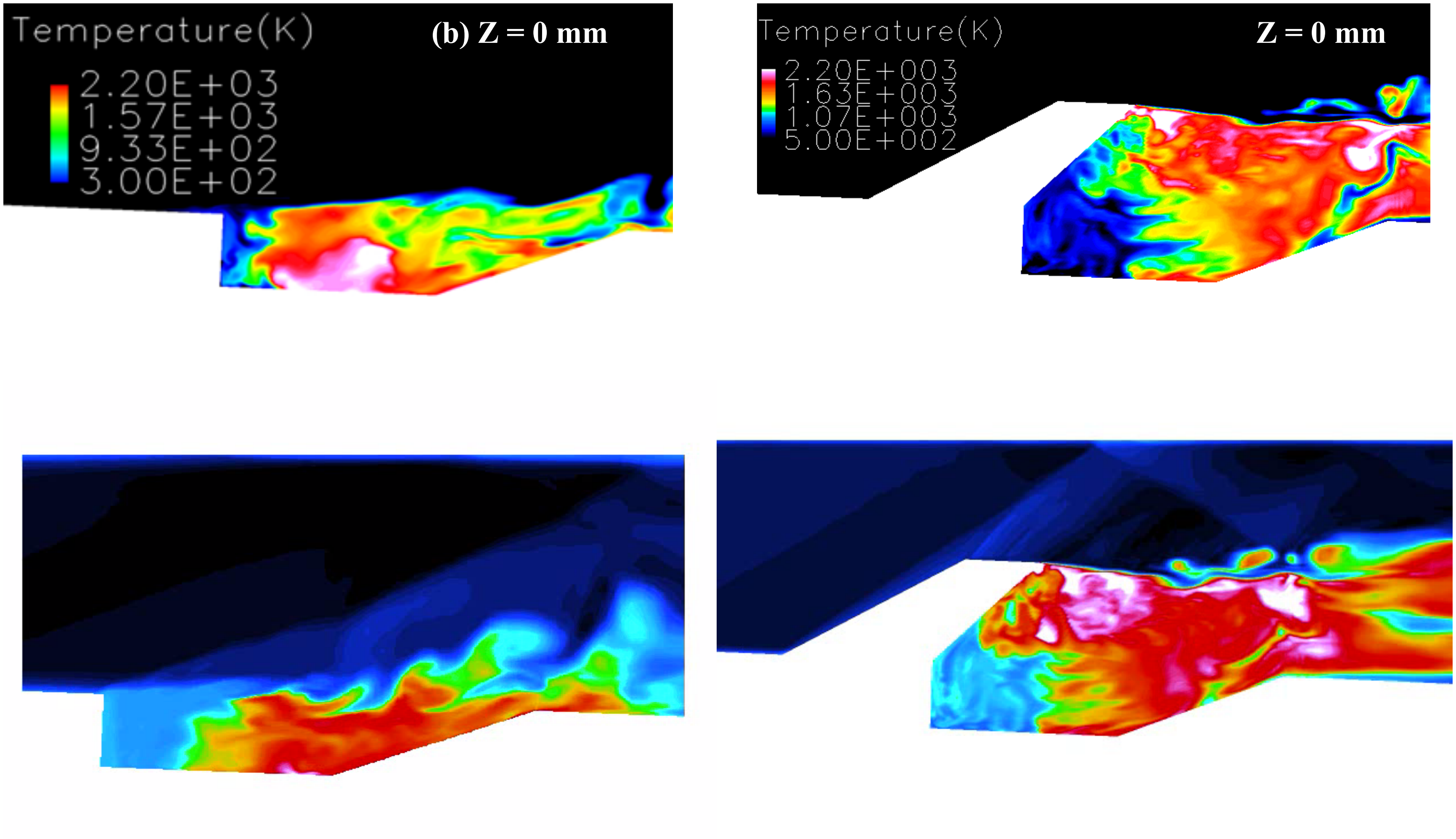

$$\textit{Flame Index} = \text{normalized } \nabla Y_F \cdot \nabla Y_O$$

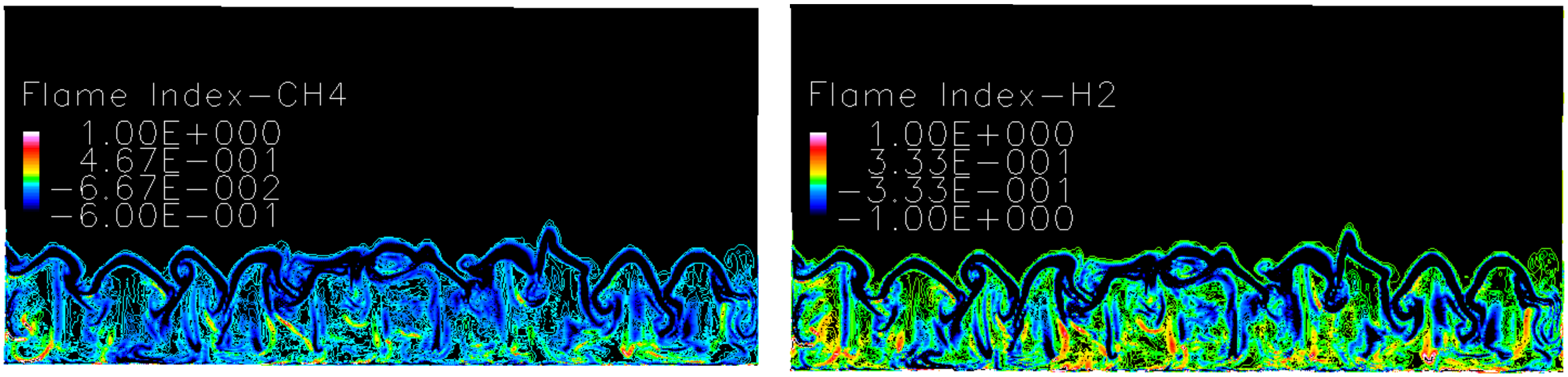

No Strut – Cavity

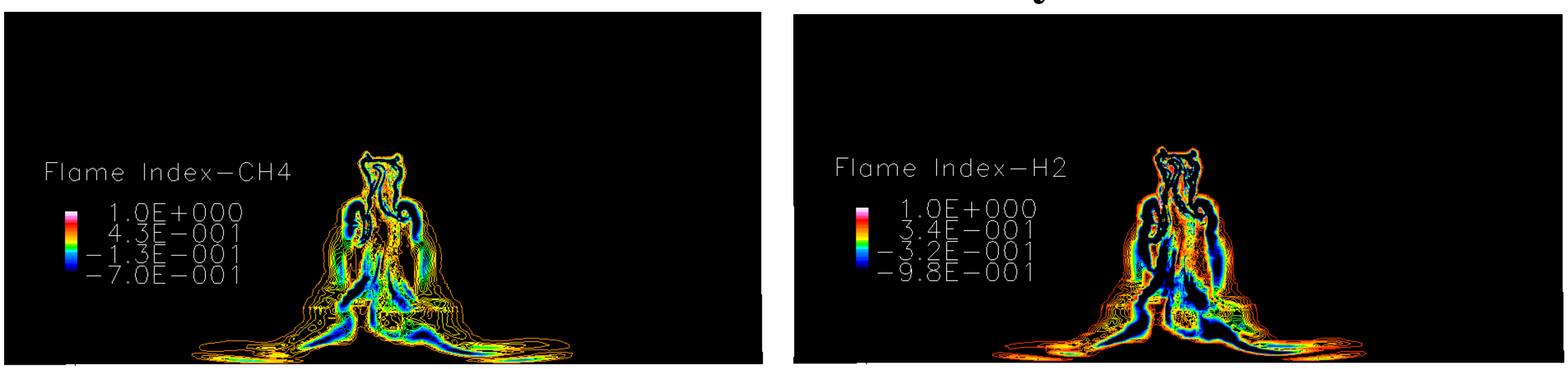

CH_4 Strut Wake H_2

- ***Flame Index*** **> 0 for premixed flame and < 0 for diffusion flame**

Reacting Flow – Flame Regimes for LES

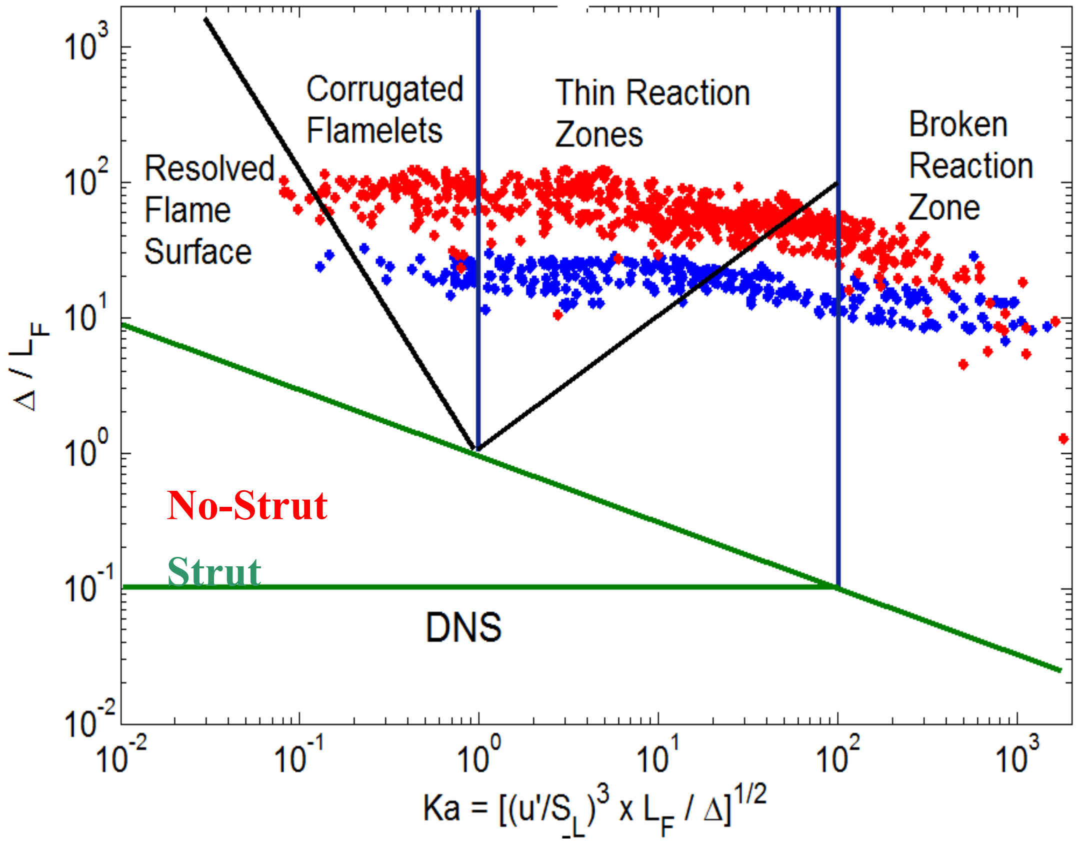

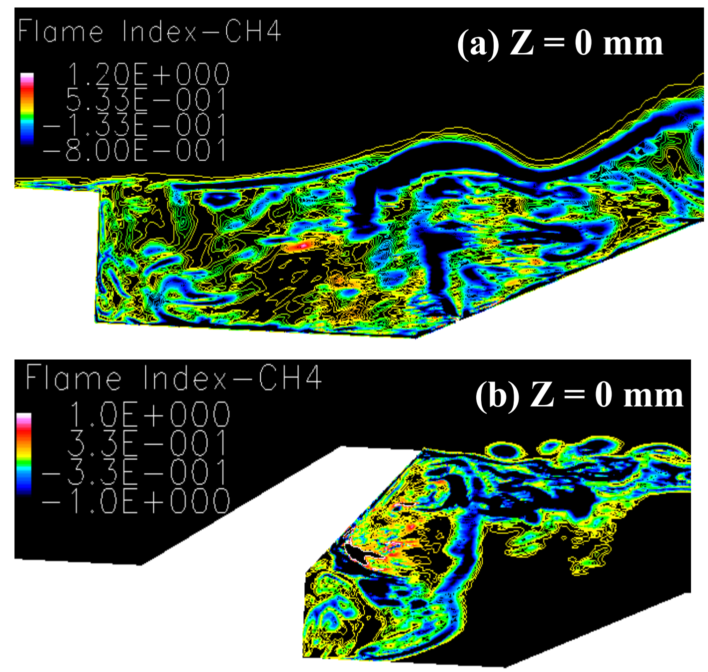

Flame Index for CH_4

- Strong variation of Ka from flamelet to broken reaction zone
- LEMLES captures all regimes without model change

Chemical Kinetics Modeling

The description of the chemical kinetics is very important as its time-scales (τ_c) are on the same order-of-magnitude as those of the flow (τ_I, τ_Δ, τ_T).

Parameters for the 9 species, 19-step Jachimowski mech.

Reaction	*A [mol-cm-s]*	*n*	*T_a [K]*
$H_2+O_2 \Leftrightarrow HO_2+H$	1.0×10^{14}	0	28000
$H+O_2 \Leftrightarrow OH+O$	2.6×10^{14}	0	8400
$O+H_2 \Leftrightarrow OH+H$	1.8×10^{10}	1.0	4450
$OH+H_2 \Leftrightarrow H_2O+H$	2.2×10^{13}	0	2575
$OH+OH \Leftrightarrow H_2O+O$	6.3×10^{12}	0	545
$H+OH+M \Leftrightarrow H_2O+M$	2.2×10^{22}	-2.0	0
$2H+M \Leftrightarrow H_2+M$	6.4×10^{17}	-1.0	0
$H+O+M \Leftrightarrow OH+M$	6.0×10^{16}	-0.6	0
$H+O_2+M \Leftrightarrow HO_2+M$	2.1×10^{15}	0	-500
$HO_2+H \Leftrightarrow OH+OH$	1.4×10^{14}	0	540
$HO_2+H \Leftrightarrow H_2O+O$	1.0×10^{13}	0	540
$HO_2+O \Leftrightarrow O_2+OH$	1.5×10^{13}	0	475
$HO_2+OH \Leftrightarrow H_2O+O_2$	8.0×10^{12}	0	0
$HO_2+HO_2 \Leftrightarrow H_2O_2+O_2$	2.0×10^{12}	0	0
$H+H_2O_2 \Leftrightarrow OH+HO_2$	1.4×10^{12}	0	1800
$O+H_2O_2 \Leftrightarrow H_2+HO_2$	1.4×10^{14}	0	3200
$OH+H_2O_2 \Leftrightarrow H_2O+HO_2$	6.1×10^{12}	0	715
$H_2O_2+M \Leftrightarrow 2OH+M$	1.2×10^{17}	0	22750
$O+O+M \Leftrightarrow O_2+M$	6.0×10^{13}	0	-900

Parameters for the 6 species, 7-step Davidenko mech.

Reaction	*A [mol-cm-s]*	*n*	*T_a [K]*
$H_2+O_2 \Leftrightarrow OH+OH$	1.700×10^{13}	0	24044
$H+O_2 \Leftrightarrow OH+O$	1.987×10^{14}	0	8456
$OH+H_2 \Leftrightarrow H_2O+H$	1.024×10^{8}	1.60	1660
$O+H_2 \Leftrightarrow OH+H$	5.119×10^{4}	2.67	3163
$OH+OH \Leftrightarrow H_2O+O$	1.506×10^{9}	1.14	50
$H+OH+M \Leftrightarrow H_2O+M$	2.212×10^{22}	-2.00	0
$H+H+M \Leftrightarrow H_2+M$	9.791×10^{16}	-0.60	0

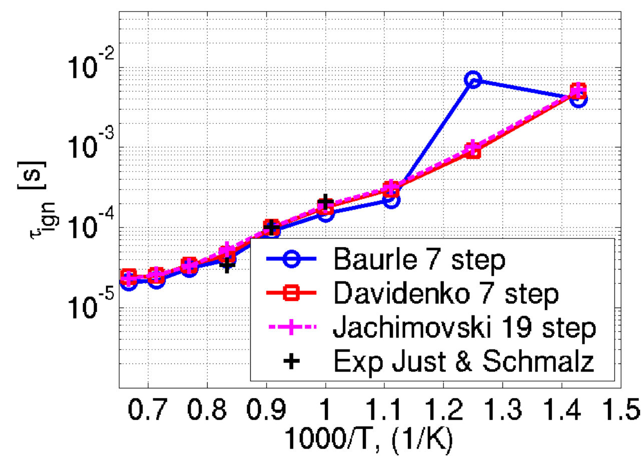

1 step Marinov *et al*
2 step Rogers & Chintz
7 step Davidenko *et al*
7 step Baurle & Girimaji
14 step Zhukov?

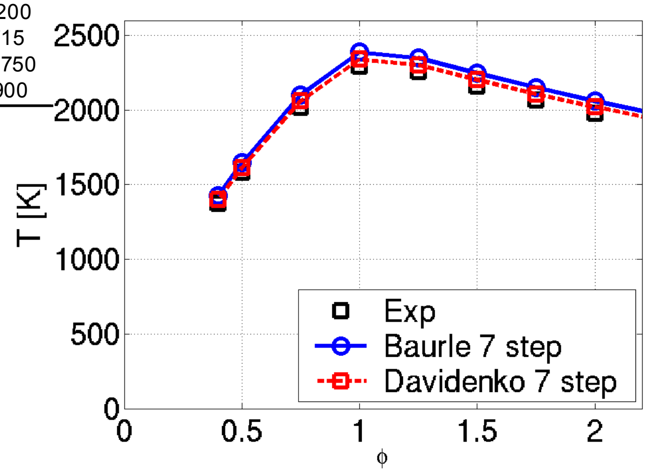

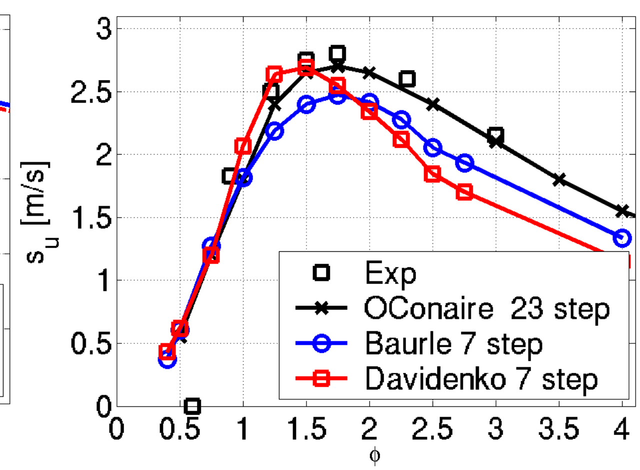

The Waidmann *et al* Combustor

DLR experimental investigation

Waidmann W., Brummund U. & Nuding J.; 1995, 8th Int. Symp. on Transp. Phenom. In Comb., p 1473.
Waidmann W., Alff F., Brummund U., Böhm M., Clauss W. & Oschwald M.; 1995, Space Tech. ***15****, p 421.*

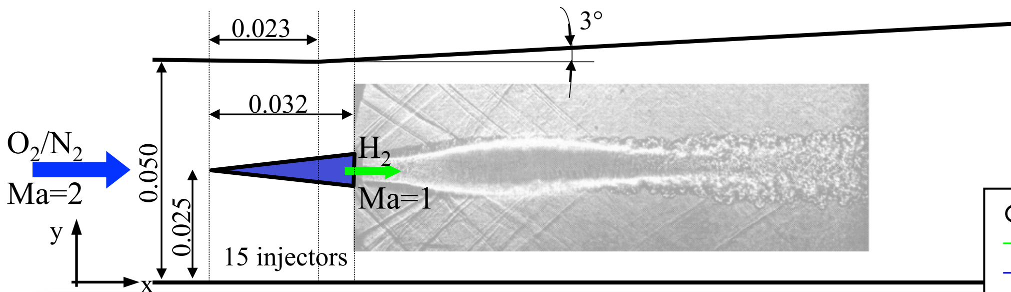

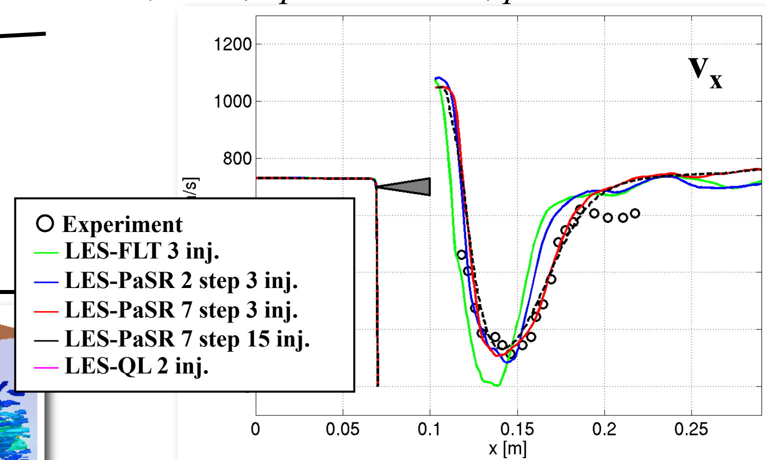

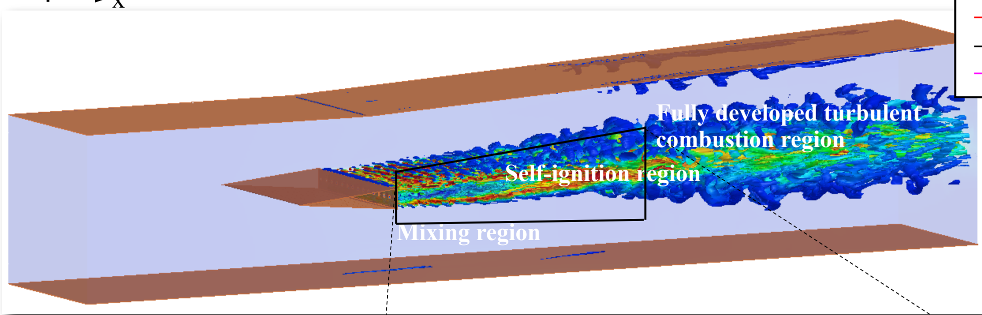

Fureby *et al*

3 injectors, 5 Mcells

15 injectors, 25 Mcells

Génin & Menon

2 injectors, 2.5 Mcells

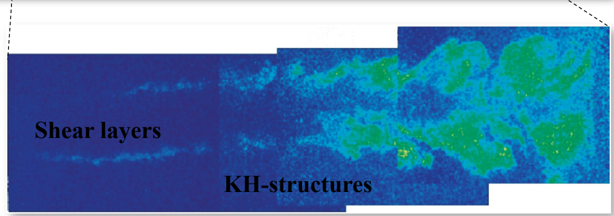

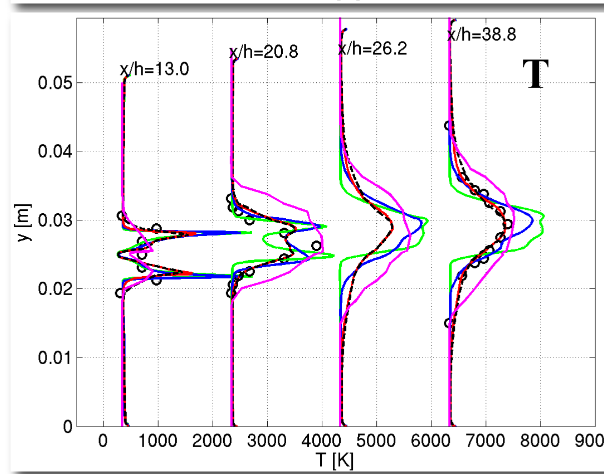

Berglund & Fureby, 2006, 31st Int. Symp. On Comb.
Génin & Menon, 2009, AIAA 2009-0132
Fureby et al., 2011, 28th ISSSW, Manchester

Sunami-Magré Combustor

Joint ONERA / JAXA experimental (scramjet) combustor study

Sunami T., Murakami A., Kudo K., Kodera M. & Nishioka M., AIAA 2002-5116,
Sunami T., Magré P., Bresson A., Grisch F., Orain M., & Kodera M., AIAA 2005-3304

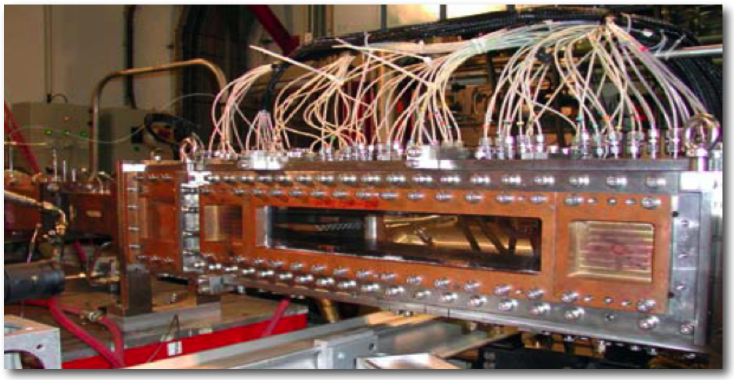

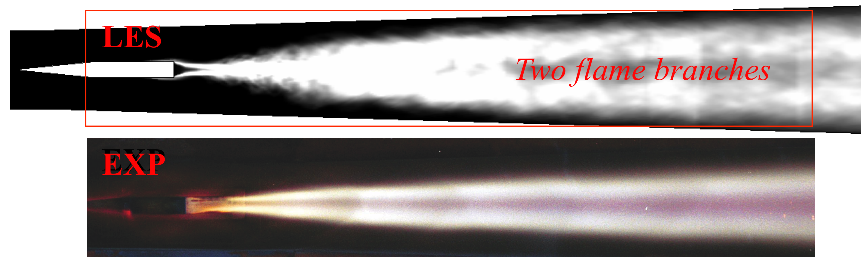

Spontaneous flame images

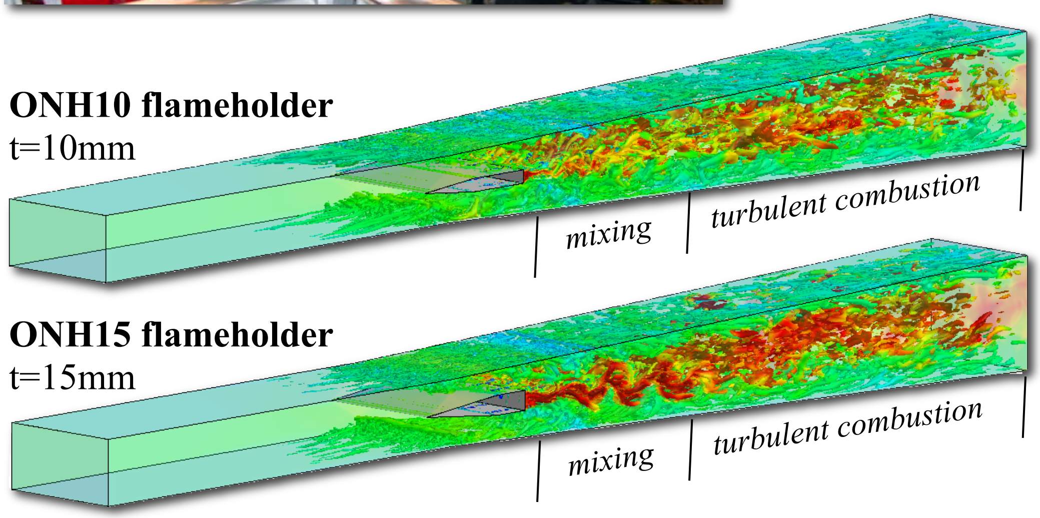

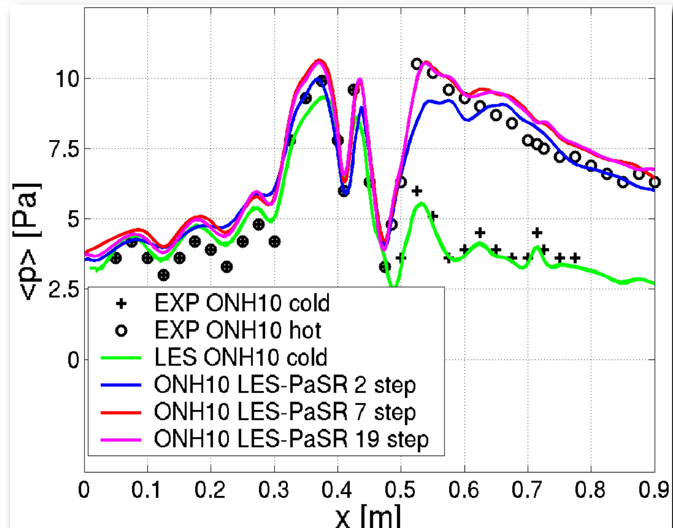

Berglund *et al*, 2009, AIAA J.
Sabelnikov & Fureby In Preparation 2011

ONERA

Sunami-Magré Combustor cont'd

Supersonic flame structure investigation (ONH10) and OH comparison

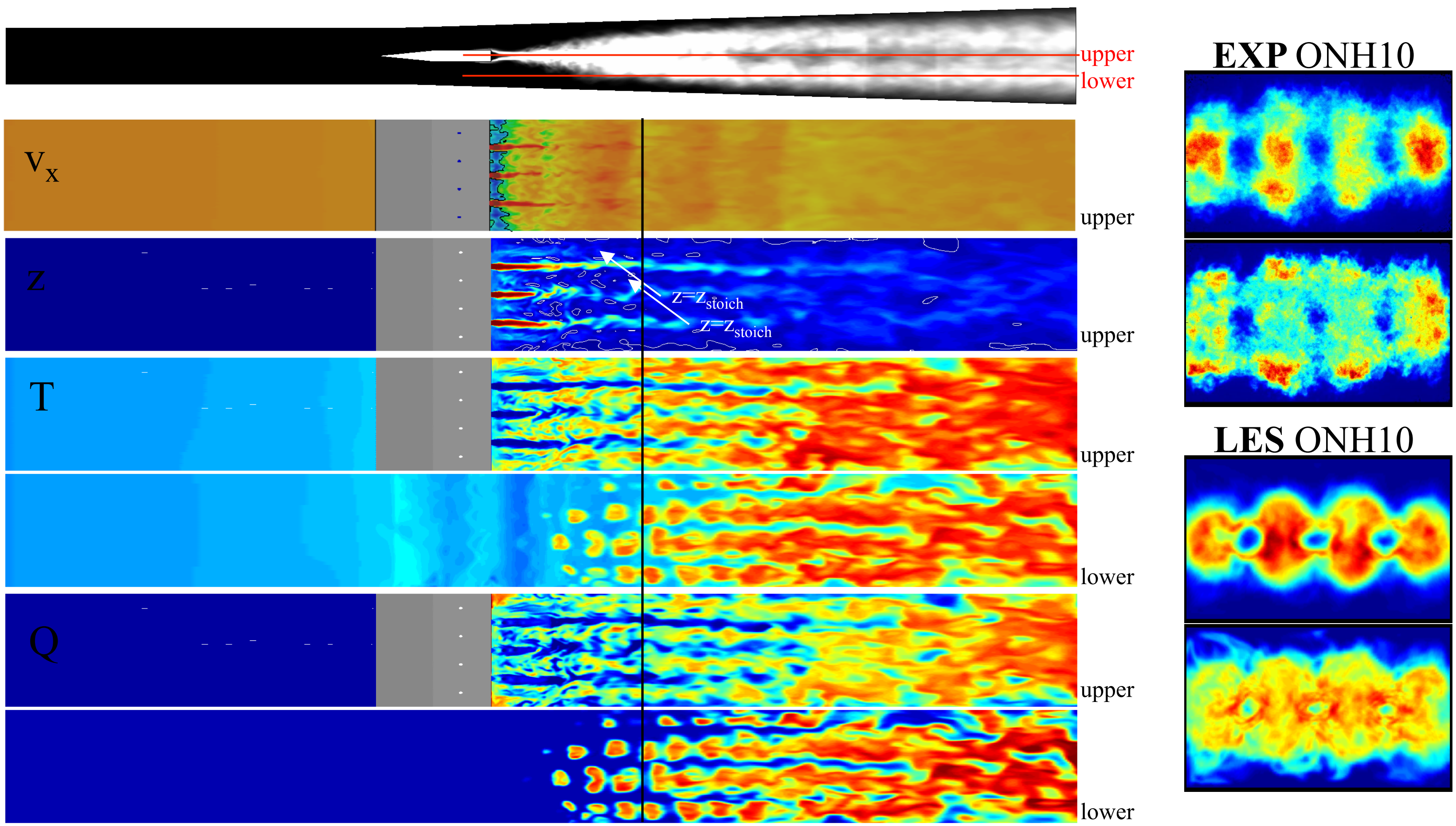

Berglund *et al*, 2009, AIAA J.
Sabelnikov & Fureby In Preparation 2011

ONERA

Real Gas: Basic thermodynamics

- Under atmospheric conditions, most fluids require a phase change to go from liquid to gas
  - Multiphase field: breakup, atomization, evaporation…
- Not necessary if T > T_c OR p > p
  - Smooth interface
  - No surface tension
  - No latent heat of vaporizatior
- If T > Tc AND p > pc, fluid is supercritical

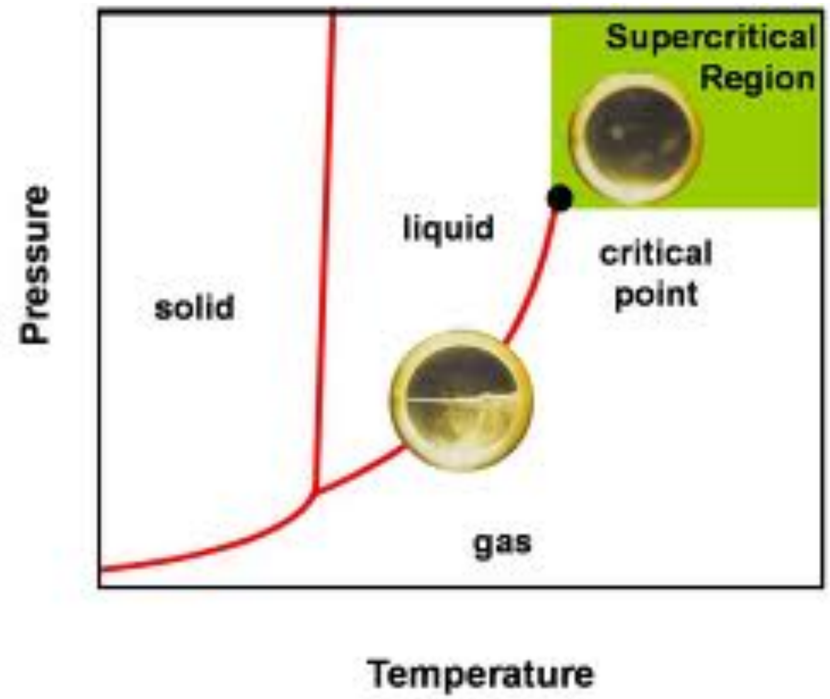

Basic thermodynamics

- A supercritical fluid may or may not follow the Ideal Gas Equation of State (IG EoS) $pV = R_u T$
- Departure from IG EoS caused by inter-molecular effects:
  - Molecules cannot be assumed to be points
  - Inter-molecular forces on top of simple collisions
- These real gas, i.e. non-ideal, effects occur when the density of the fluid is large enough
  - What is large enough?

Basic thermodynamics

$$Z = \frac{pV}{R_u T}$$

- Introduce compressibility
  - Z=1 => ideal gas
  - Z\=1 => real gas
- Hint at a universal behavior
  - Z is equivalent for simple species when normalizing T and p by T_c and p_c
- Mathematical translation into new EoS

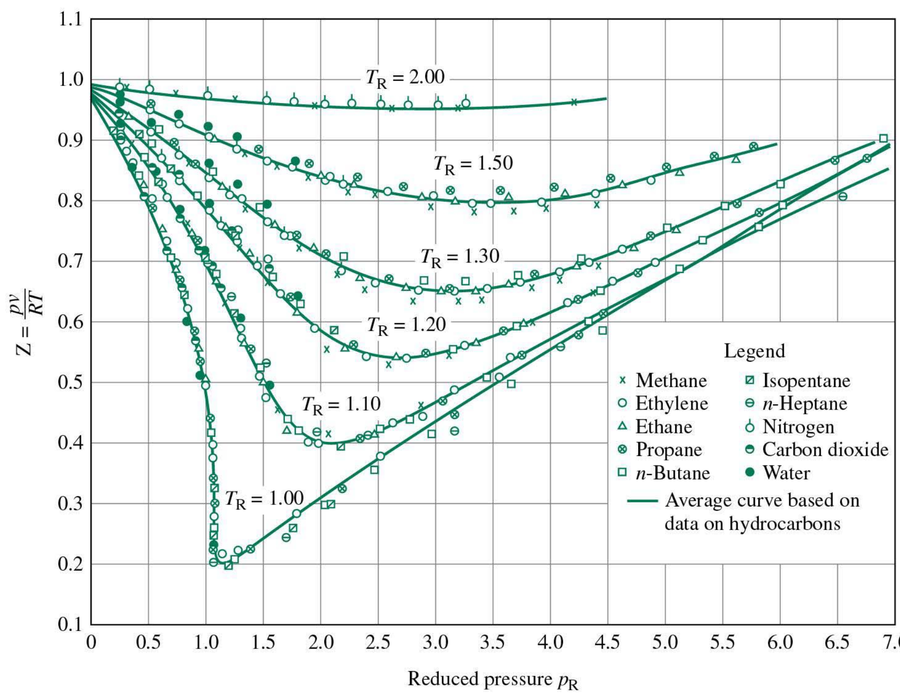

Relevance to combustion

- Overall trend is to increase pressure (GT,ICE,rockets)
- Three flows where real gas effects are important:
  - Sub-critical flows
    - All species gaseous, mild departures from Z = 1
  - Super-critical flows
    - Some species supercritical, Z = 0.3 to 1
  - Trans-critical flows
    - Some species are compressed liquids, Z can vary from 0.3 to 1 and pseudo-phase change phenomena

Relevance to combustion

- Concrete example: surrogate aircraft fuel
  - 82.6 % n-decane and 17.4% trimethylbenzene (Pitsch_2008a)
- Corresponding states principle (CSP)
  - Mixture behaves like a pure pseudo-fluid with pseudo critical propertie

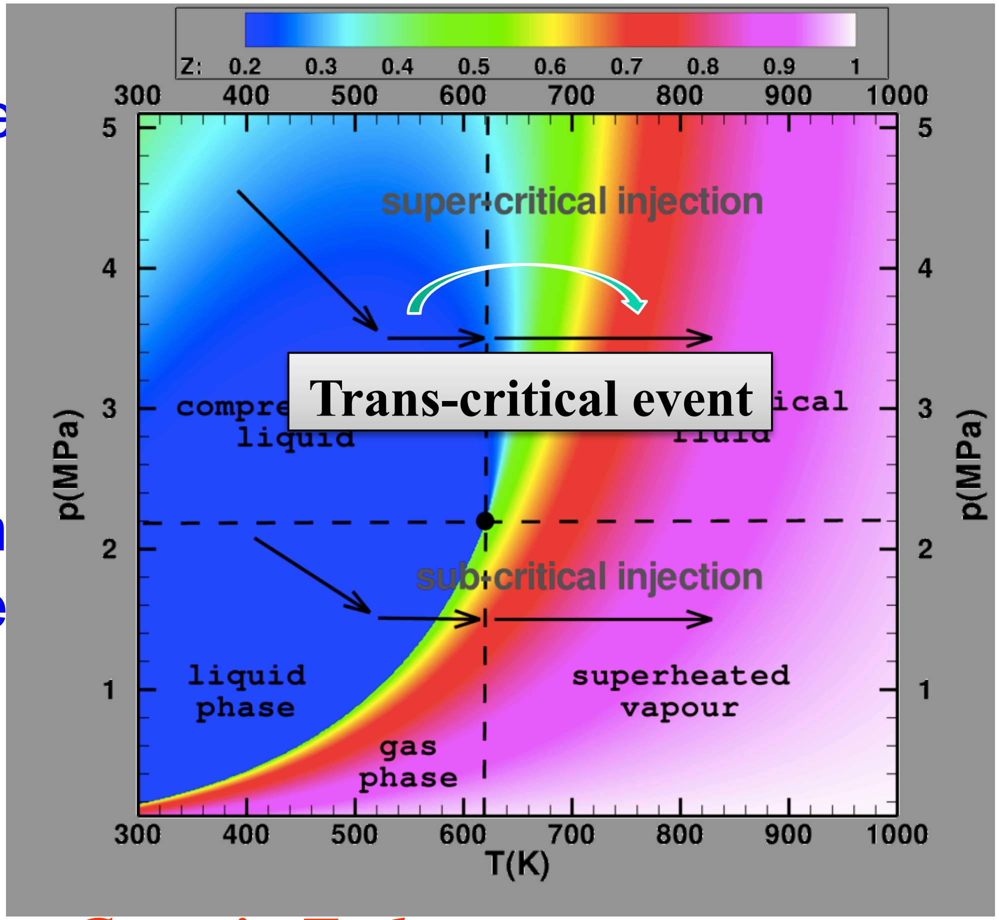

Issues for combustion modeling

- Large density gradients
- Computational cost
- Additional unclosed terms
- Pressure dependence in reaction mechanisms
- EoS validity for a wide range of flow conditions and species must be understood and established
  - Cubic EoS such as Peng-Robinson (PR), Soave-Redlich-Kwong (SRK)
  - Higher order empirical EoS such as Benedict-Webb-Rubin (BWR)

Dealing with density gradients

- Need to capture both large density gradients & turbulence at the same time
- Implement within the real gas EoS:
  - TVD MUSCL scheme using approximate Riemann solver for 3rd order accuracy
  - Dynamic switch based on local density gradients
- Pure central schemes cannot handle these gradients without huge resolution requirements
- Pure upwind schemes are too dissipative

Dealing with density gradients

- Shu-Osher test

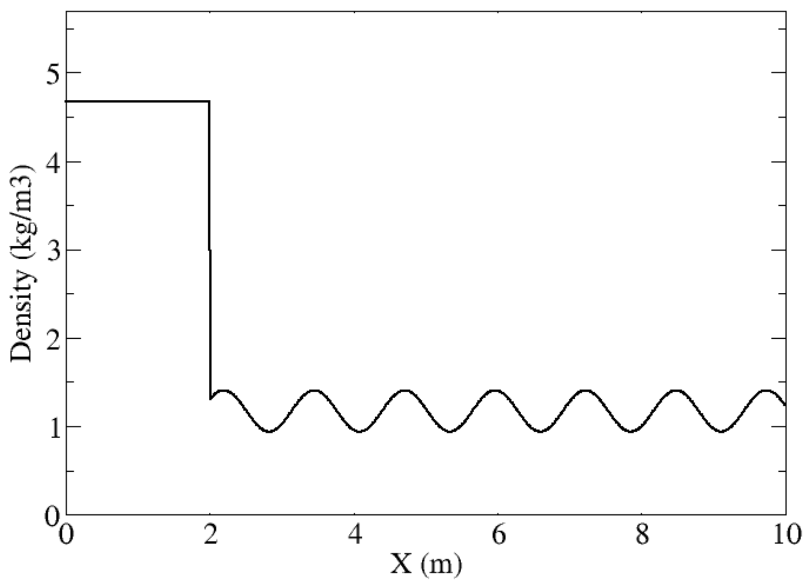

Standard air Z = 1

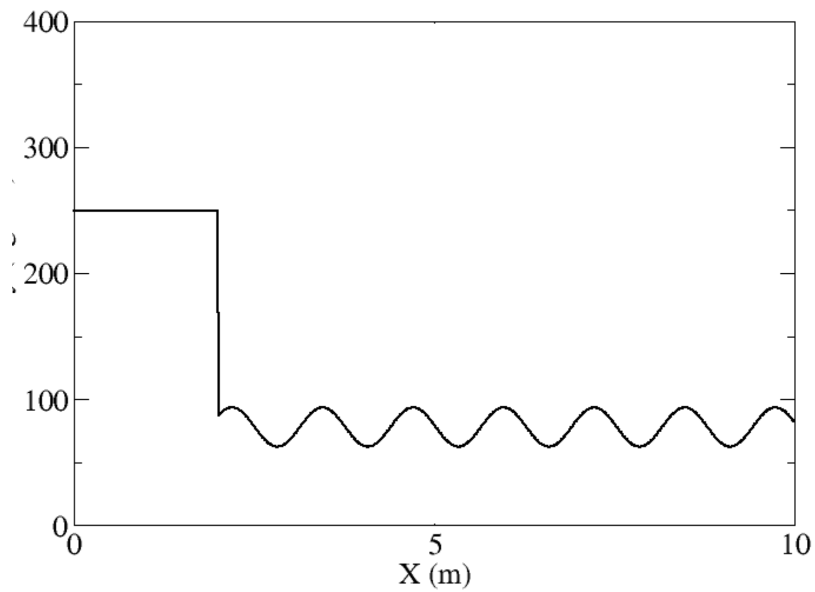

Compressed air,
Z = 0.85 pre-shock, Z = 1.15 post-shock

PSU RCM1

- Super-critical combustion without trans-critical event
  - Injection temperatures are high enough that real gas effects are negligible
  - Still large density gradients
  - Importance of pressure on reaction mechanism
- Simplest configuration relevant to staged combustion
  - Gas-gas H_2-O_2 shear coaxial injector
  - Cylindrical chamber instrumented for heat flux measurement

PSU-RCM1 - Geometry

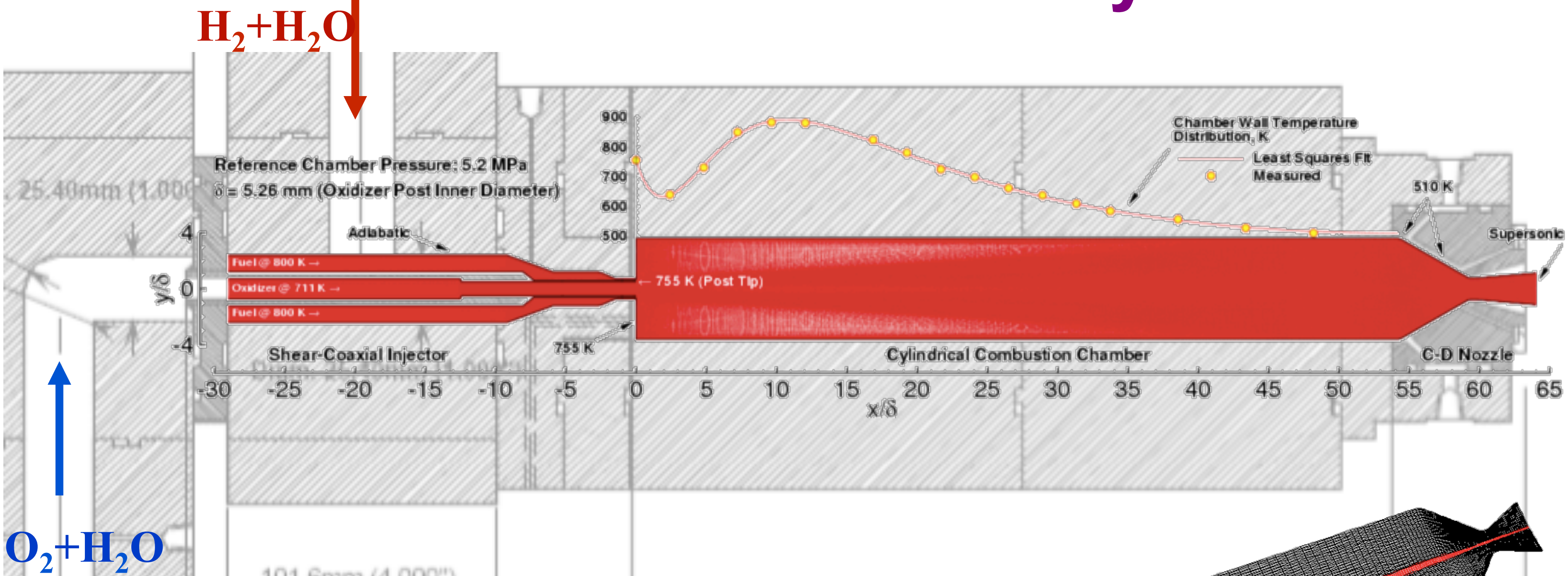

- Butterfly grid with 3.2M grid points

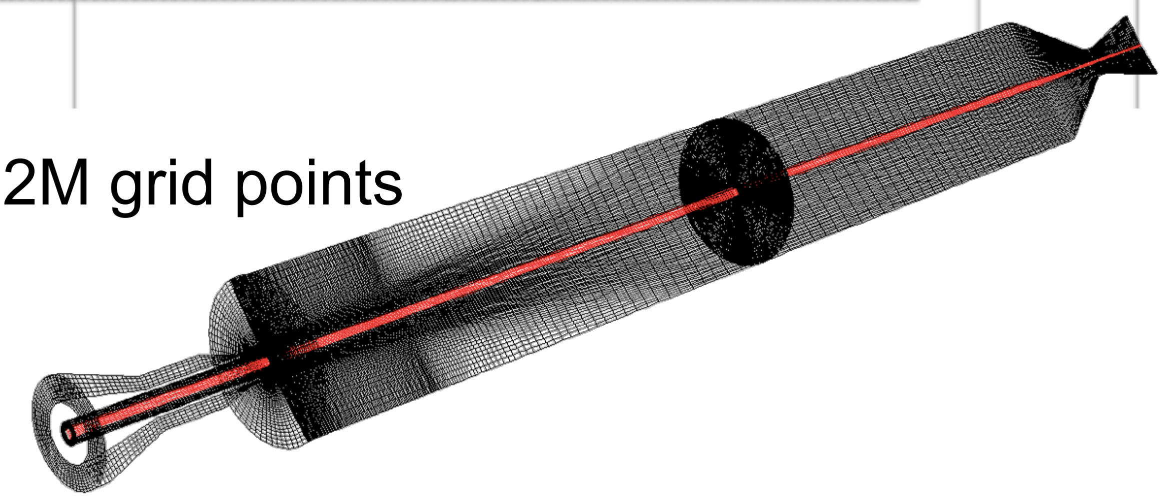

PSU RCM1 - Combustion modeling

- Characteristics of the PSU simulation
  - Good resolution in near-field and slow secondary combustion
  - Eddy Break-Up not adapted
- Detailed 21-step, 8-species mechanism (Conaire_2004)
  - Very stiff to integrate
- Simplest closure: sub-iteration scheme
- Future strategies
  - Reduced mechanism
  - LEM with ANN

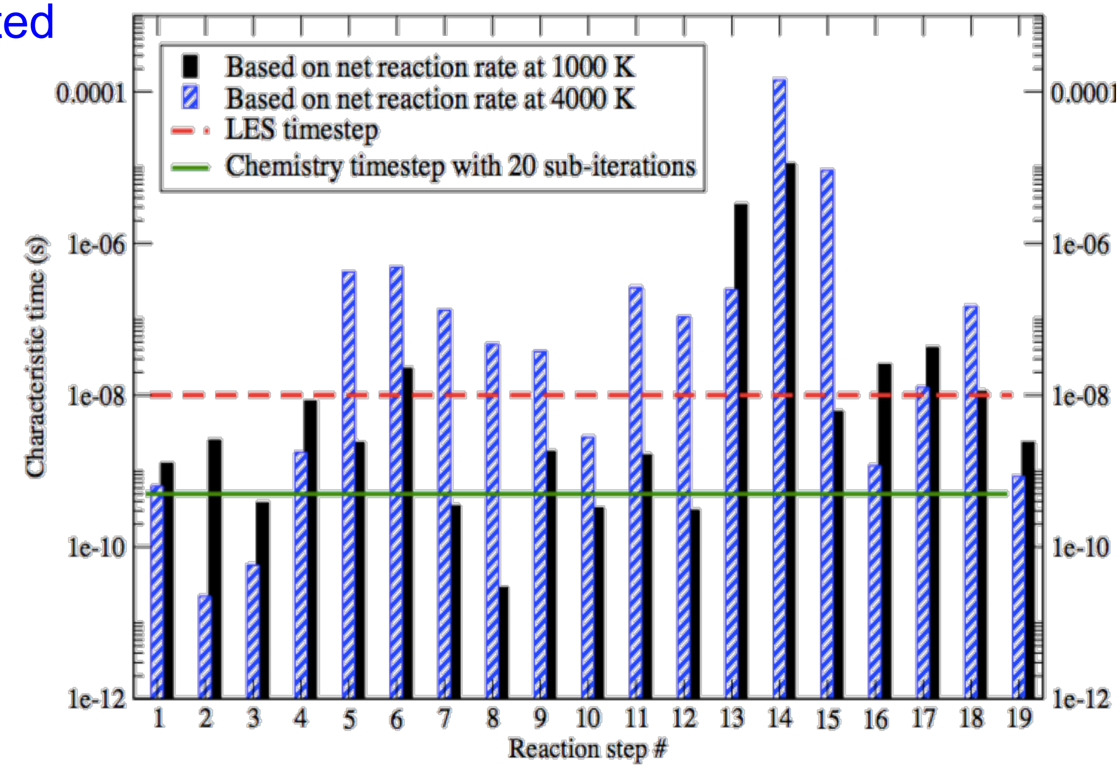

PSU RCM1 - Flowfield description

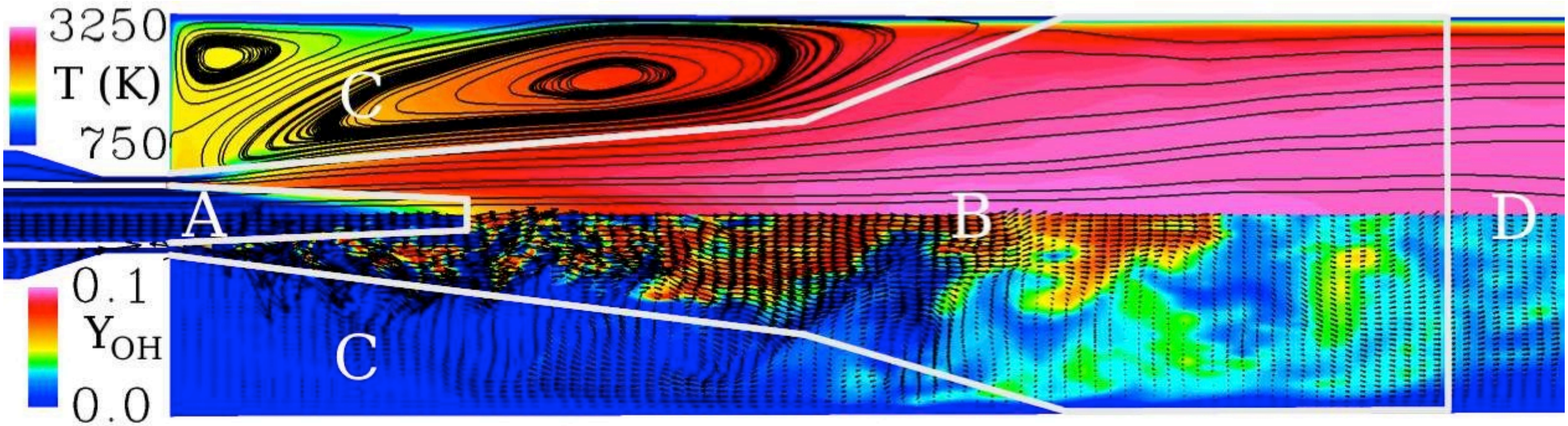

- Distinguishing 4 different zones:
  - A: oxygen jet core >>> primary diffusion flame
  - B: accelerating then decelerating flow >>> secondary combustion
  - C: recirculation zone >>> very little combustion
  - D: homogeneous flow >>> no more reaction

1 frame = 1 μs **movie = 0.3 ms**

Oxygen jet break-up

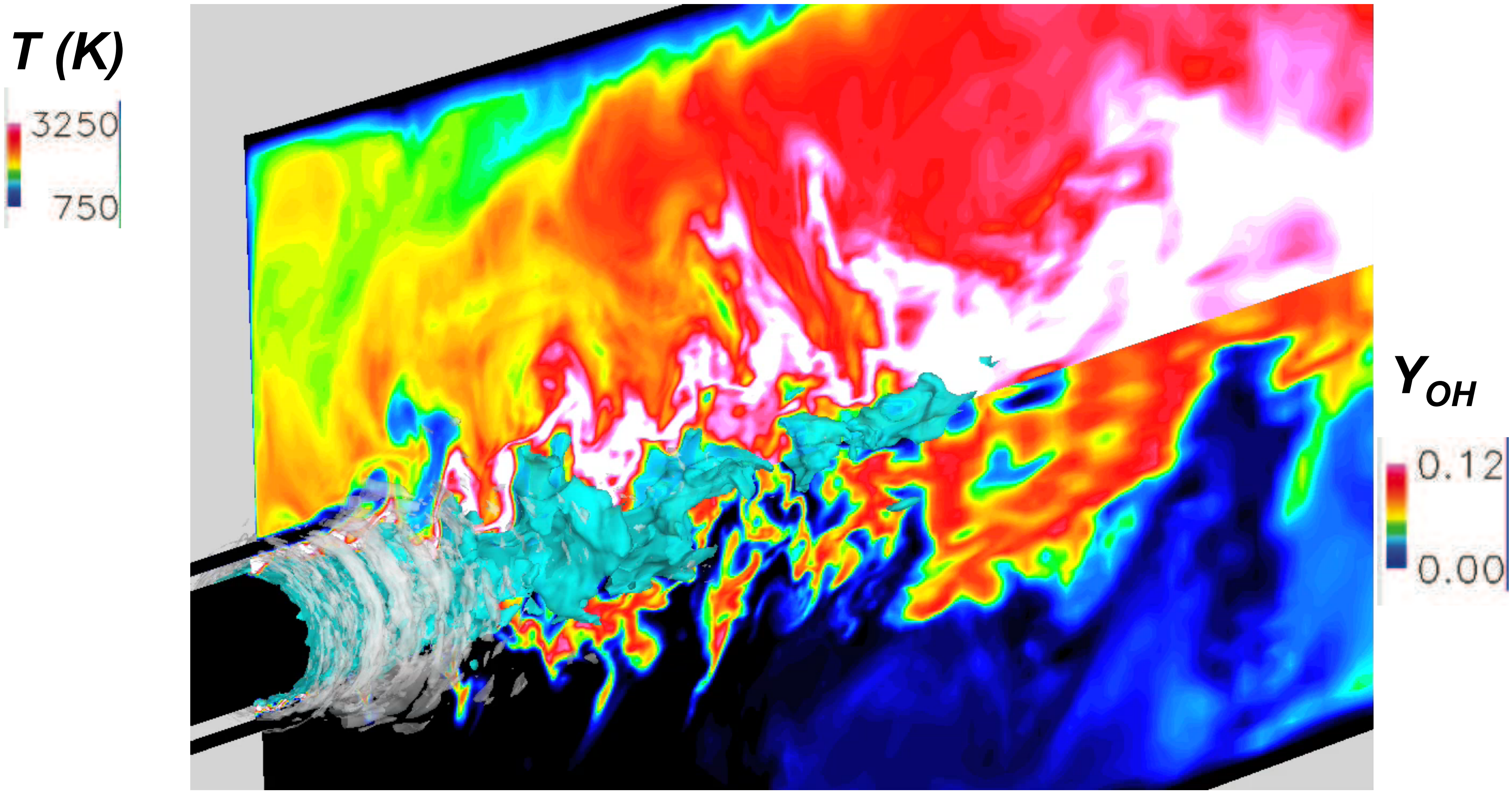

PSU RCM1 – Comparison CFD solvers

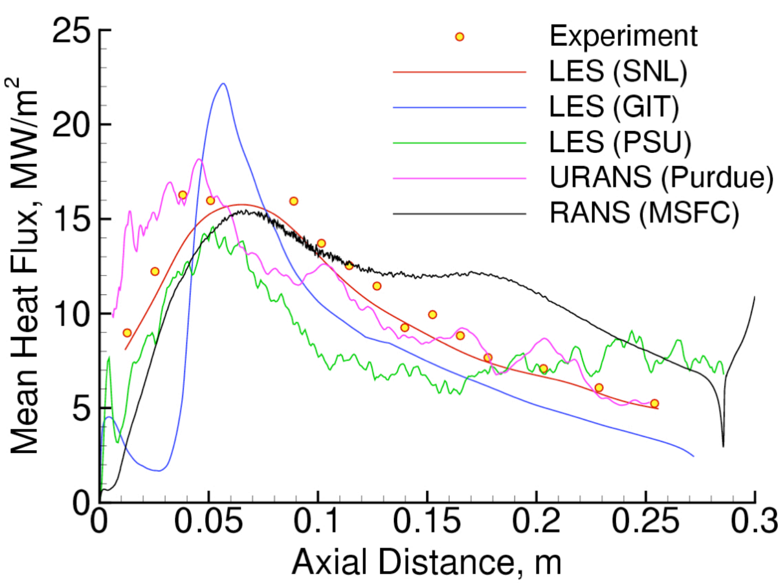

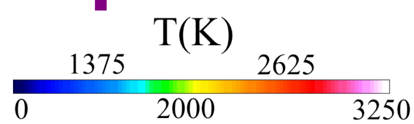

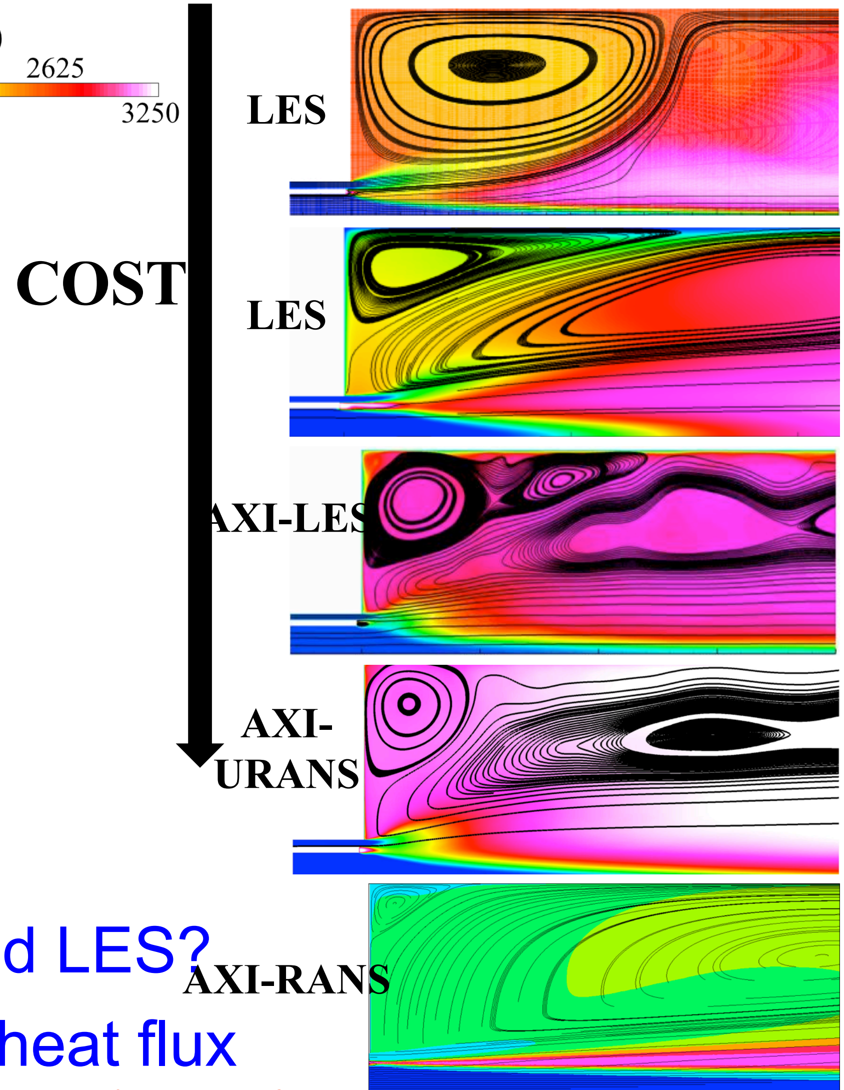

- Wide range of CFD tools
  - Similar heat flux
  - Different flow structure
  - Best prediction: wall-resolved LES?
  - Many parameters influence heat flux

PSU RCM1 – Comparison CFD solvers

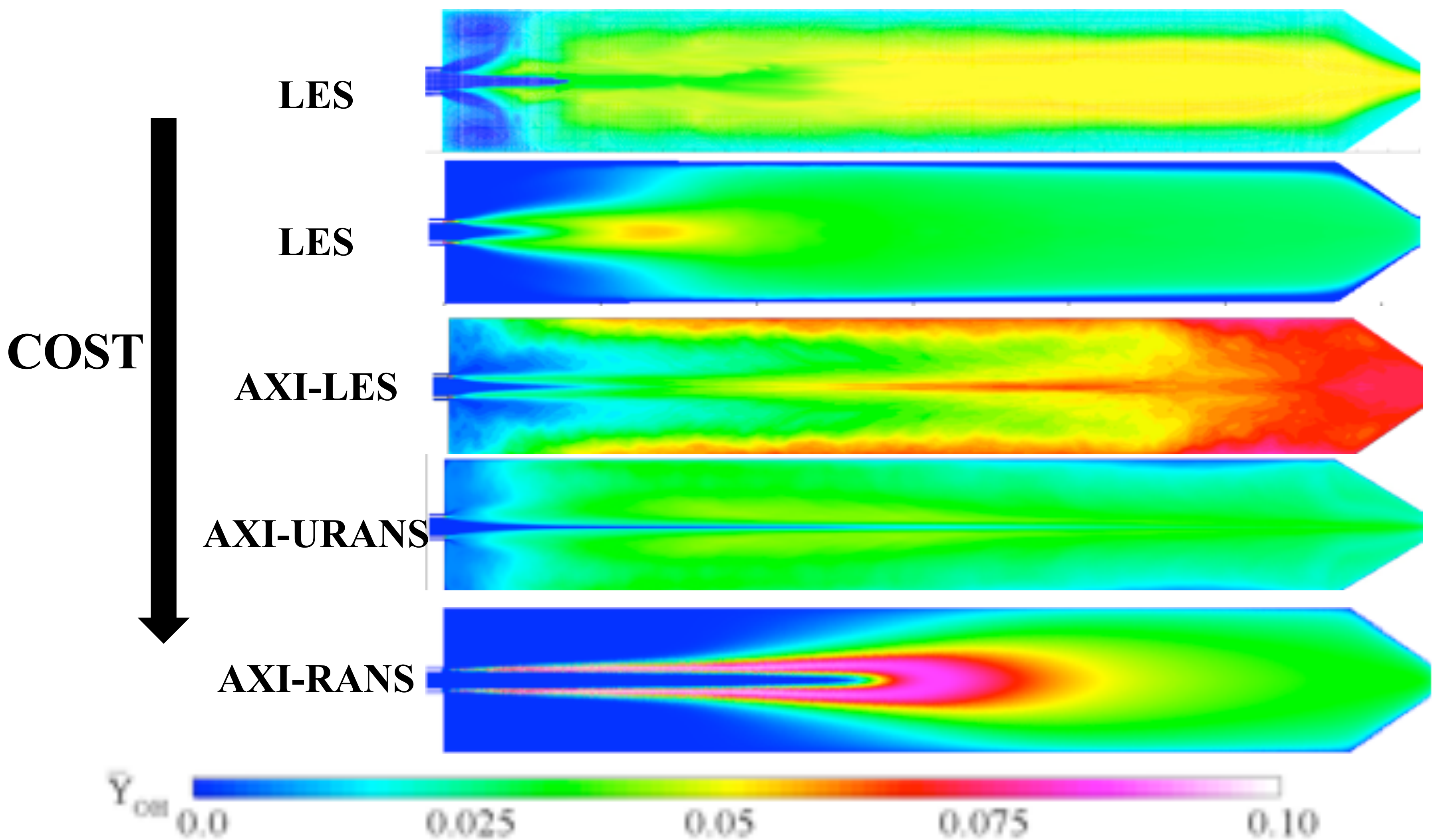

PSU RCM1 - Comparison 3D - 2D-axi LES

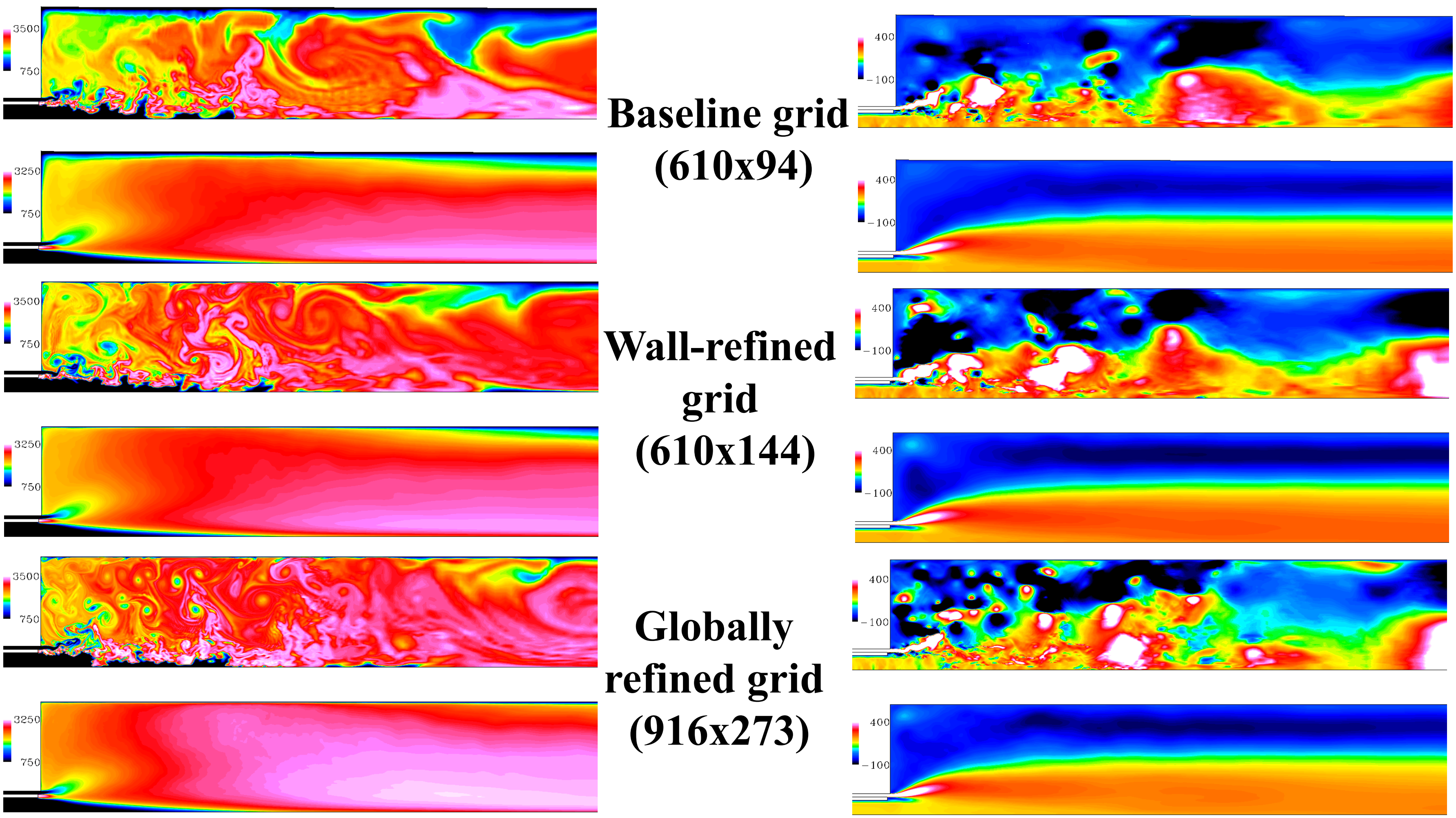

LOXGOX Experiment (PSU)

- Work on previous configuration has helped design new experimental facility
  - Square chamber for easy optical access
  - Coflow to eliminate recirculation zones
    - Perforated plate approximated as uniform flow for now

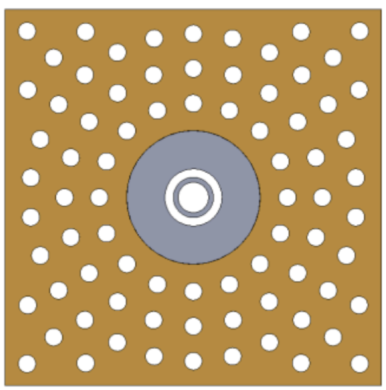

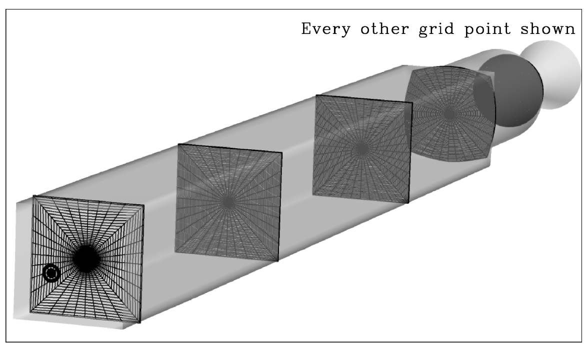

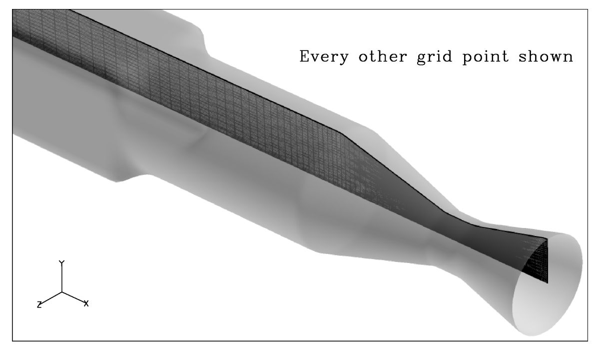

LOXGOX – Operating conditions

- Focus on the case with trans-critical injection
  - P > Pc AND Tinj < Tc for pure oxygen
- Hybrid scheme can capture trans-critical layer

Description	Units	Value
Main chamber		
Chamber pressure	Pa	5.750×10^{6}
Average density	$kg.m^{-3}$	138
Average velocity	m.s−1	4.57
Preburner background flow		
Mass flowrate	$kg.s^{-1}$	0.268
Inflow density	$kg.m^{-3}$	84.6
Inflow temperature	K	262
Compressibility		0.998
Inflow velocity	m.s−1	5.95
Injector inner post flow		
Mass flowrate	$kg.s^{-1}$	0.0836
Inflow density	$kg.m^{-3}$	1080
Inflow temperature	K	105
Compressibility		0.195
Inflow velocity	m.s−1	23.3
Injector annular flow		
Mass flowrate	$kg.s^{-1}$	0.0557
Inflow density	$kg.m^{-3}$	82.3
Inflow temperature	K	269
Compressibility		0.999
Inflow velocity	m.s−1	101

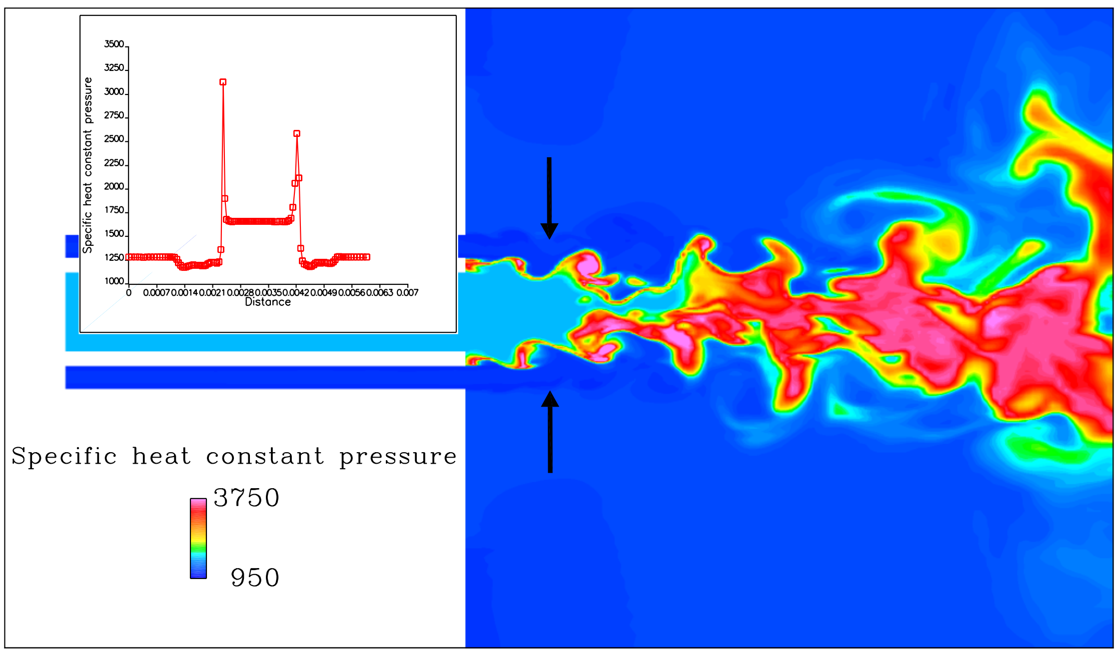

LOXGOX – Qualitative validation

- Trying to reproduce backlit images
- Good qualitative agreement

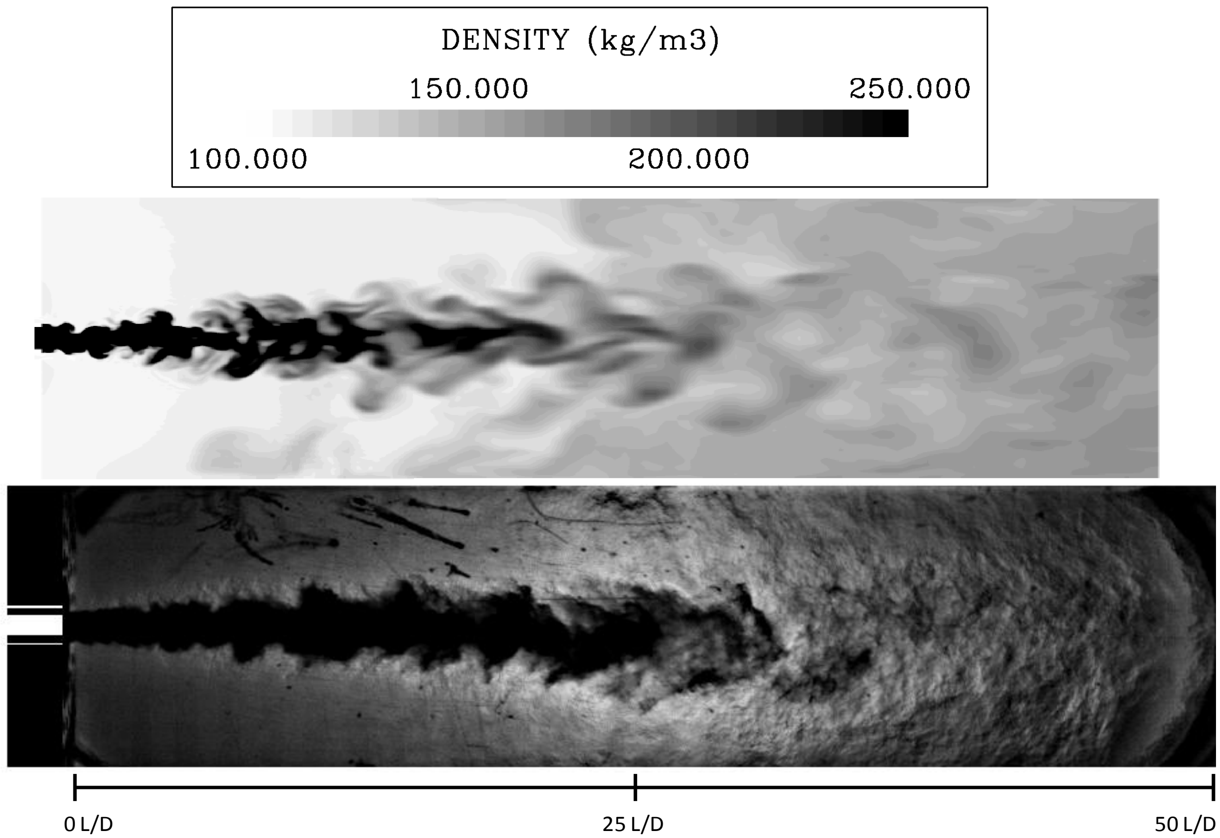

LOXGOX – Quantitative validation

- Measuring dark-core length
- Flow physics is captured with reasonable accuracy

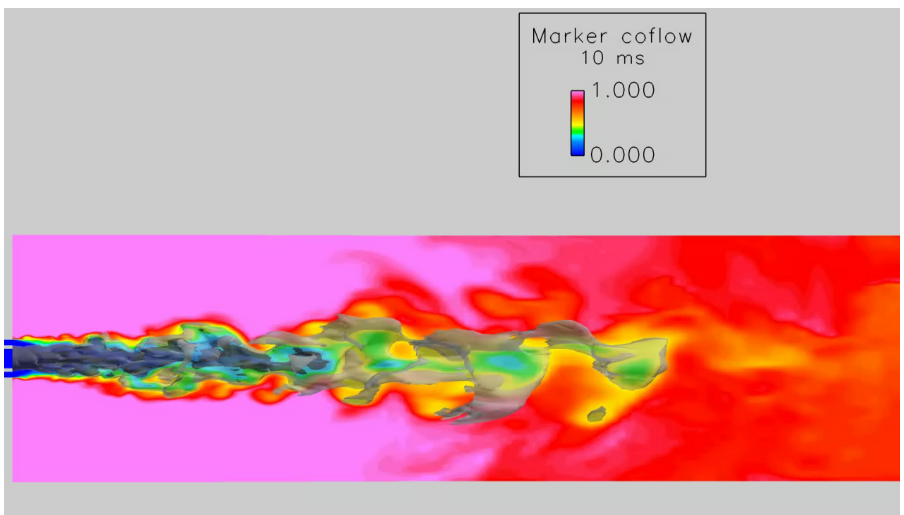

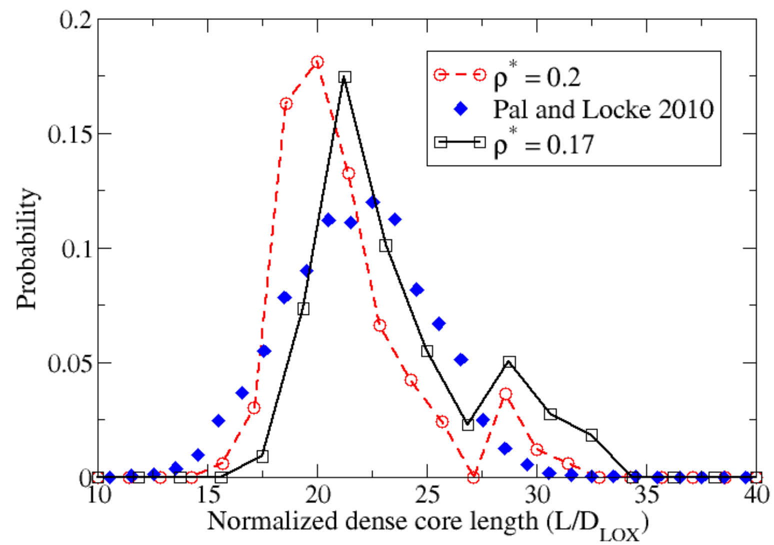

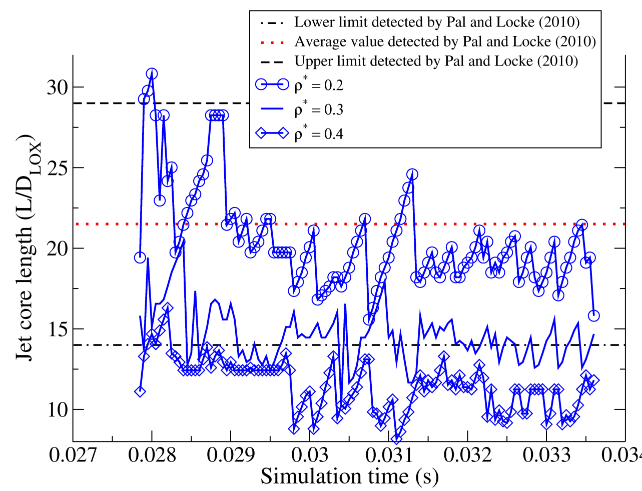

Observations from Rocket LES

- 3D simulations are required
  - Axisymmetric cannot capture flow physics
- Complex turbulent features require LES
  - But proper subgrid closures are still needed
- Validation of single-injector flow is still difficult
  - Good experimental data is rare
- Focus should move to multi-injector flows
  - More realistic configuration

Final Summary Comments

- CFD is a tool that can be exploited with various levels of confidence and reliability for a range of problems
- Sometimes asking too much of a simple and reliable model may not be the proper thing to do….
- Key areas to be aware of
  - Numerical scheme's strengths and limitations
  - Choice of grid and boundary conditions
  - Turbulence closures (RANS, URANS, DES or LES)
  - Scalar mixing closure (turbulent and molecular)
  - Reaction kinetics closure (finite-rate, mixture fraction)
  - Parallel optimization and scalability is essential

Further Reading

- All models and results discussed are in published papers
  - Cited work papers are available upon request
- Many excellent reviews and books are also available
  - Poinsot & Veynante: Theoretical and Numerical Combustion, Edwards, 2nd
  - Reviews by Pitsch (Ann. Rev. 2006), Janicka (Symp 2006), Peters (2008), Candel etc…
- Other papers are available
- LEM stand-alone codes can be used to learn and in needed implemented into in-house codes